2015

# Burst Strength of NPS30 Steel Pipes with Dent-Crack Defect

Hossein Ghaednia
*University of Windsor*

# Burst Strength of NPS30 Steel Pipes with Dent-Crack Defect

By

**Hossein Ghaednia**

A Dissertation
Submitted to the Faculty of Graduate Studies
through the Department of **Civil and Environmental Engineering**
in Partial Fulfillment of the Requirements for
the Degree of **Doctor of Philosophy**
at the University of Windsor

Windsor, Ontario, Canada

2015

# Burst Strength of NPS30 Steel Pipes with Dent-Crack Defect

By

Hossein Ghaednia

APPROVED BY:

_____

R. Cheng, External Examiner
University of Alberta, Edmonton, Alberta

_____

N. Zamani
Mechanical, Automotive & Materials Engineering

_____

B. Budkowska
Civil and Environmental Engineering

_____

M. Madugula
Civil and Environmental Engineering

_____

S. Das, Advisor
Civil and Environmental Engineering

16 April, 2015

# Declaration of Previous Publication

## I.    Co-Authorship Declaration

I hereby declare that this dissertation incorporates material that is the result of joint research undertaken with Mr. Jamshid Zohrehheydariha, of the University of Windsor, Mr. Rick Wang and Mr. Richard Kania, of TransCanada Pipelines Limited, and my supervisor, Dr. Sreekanta Das, of the University of Windsor. In all cases, the key ideas, the primary contributions, and data analysis and interpretation were performed by the author of this dissertation. The contributions of the co-authors were primarily focused on the provision of the study and suggesting possible directions. Results related to this research are reported in Chapters 2 through 7, inclusive.

I am aware of the University of Windsor's Senate Policy on Authorship and I certify that I have properly acknowledged the contributions of the other researchers to my dissertation, and I have obtained written permission from my co-authors to include the above materials in my dissertation.

I certify that, with the above qualification, this dissertation, and the research to which it refers to, is the product of my own work.

## II. Declaration of Previous Publication

This dissertation includes 6 original papers that have been previously published/submitted for publication in peer reviewed journals, as follows:

| Dissertation Chapter | Publication title/full citation | Publication status* |
|---|---|---|
| *Chapter 2* | *Structural evaluation of pipeline with dent defect* | *Submitted, Engineering Structures* |
| *Chapter 3* | *Effect of concentrated load on ovalization in buried oil and gas pipeline* | *Submitted, Journal of Pipeline Systems Engineering and Practice* |
| *Chapter 4* | *Pressure tests on 30 in diameter X70 grade pipes with dent-crack defect* | *Published, Journal of pipeline engineering* |
| *Chapter 5* | *Effect of operating pressure and dent depth on burst strength of NPS30 linepipe with dent-crack defect* | *Published, Journal of Offshore Mechanics and Arctic Engineering* |
| *Chapter 6* | *Dependence of burst strength on crack length and crack depth of a pipe with dent-crack defect* | *To be submitted, Structural Safety* |
| *Chapter 7* | *Burst strength of NPS30 pipes with various crack locations and dent depths* | *To be submitted, International Journal of Pressure Vessels and Piping* |

I certify that I have obtained a written permission from the copyright owners to include the above published materials in my dissertation. I certify that the above material

describes work completed during my registration as graduate student at the University of Windsor.

I declare that, to the best of my knowledge, my dissertation does not infringe upon anyone's copyright nor violate any proprietary rights and that any ideas, techniques, quotations, or any other material from the work of other people included in my dissertation, published or otherwise, are fully acknowledged in accordance with the standard referencing practices. Furthermore, to the extent that I have included copyrighted material that surpasses the bounds of fair dealing within the meaning of the Canada Copyright Act, I certify that I have obtained a written permission from the copyright owners to include such materials in my dissertation.

I declare that this is a true copy of my dissertation, including any final revisions, as approved by my dissertation committee and the Graduate Studies office, and that this dissertation has not been submitted for a higher degree to any other University or Institution.

# ABSTRACT

Pipeline is the common mode for transporting oil, gas, and various petroleum products. Structural integrity of oil and gas transmission pipelines is often threatened by damages such as dent, corrosion, crack, gouge, or any combination of these damages. Such a damage may lead to structural failure in a field pipeline. One of combined defects is *dent-crack* defect which is a dent defect that contains a crack defect within the dent. Hence, the pipeline operator becomes concerned about the performance and safety of the linepipe if a pipe wall is subject to a dent-crack defect. Research work using full-scale tests and finite element method was undertaken at the Centre for Engineering Research in Pipelines, University of Windsor to study the influence of various internal pressures, diameter-to-thickness ratios, dent depths, crack lengths, crack depths, crack locations, and pipe steel grade on the structural behaviour and the burst strength of NPS30 (30 in diameter) and X70 and X55 grade pipes when a dent-crack defect is developed. This dissertation discusses the experimental and numerical results obtained from this study with the conclusions drawn.

# DEDICATION

I dedicate this work to my lovely wife, Aida and my parents.

# ACKNOWLEDGEMENTS

# TABLE OF CONTENTS

# LIST OF TABLES

# LIST OF FIGURES

# LIST OF APPENDICES

# CHAPTER 1

# GENERAL INTRODUCTION

Like any other structures, failure occurs in oil and gas pipeline in service. However, due to good design guidelines, materials, and operating practice, transmission pipelines have a good record of safety. Research in North America and western Europe has found external interference and corrosion are the most common causes of damage and failures in onshore and offshore oil and gas transmission pipelines [1]. In oil and gas industry the damages as result of contact with foreign objects are often referred to as mechanical damages. Defects in field pipeline can occur in the form of dent, corrosion, gouge, crack, or wrinkle. A combination of two or more defects is also common in the field pipelines. In Canada alone, more than 700,000 km of energy pipelines are in operation and these defects pose serious threats to the structural and/or operational integrity of these pipelines. As an example, according to the Alberta Energy Regulator (AER) mechanical damages has been responsible for more than 53% of crude oil pipeline failure from 1990 to 2012 [2]. At the end of 2012, the total length of pipeline recorded in AER database was 415 152 km. Figure 1.1 shows the number and the percentage of incidents in crude oil pipelines in this time period. Further, it has been reported that the failure of oil and gas transmission pipelines resulting from mechanical damages ranges from 55% in the USA to around 70% in Europe [3-6]. It is worth noting that according to AER report in January 2013 most common crude oil pipeline diameter were 12 in. (305 mm), 16 in., 20 in., and 30 in. (762 mm) (Figure 1.2) [2].
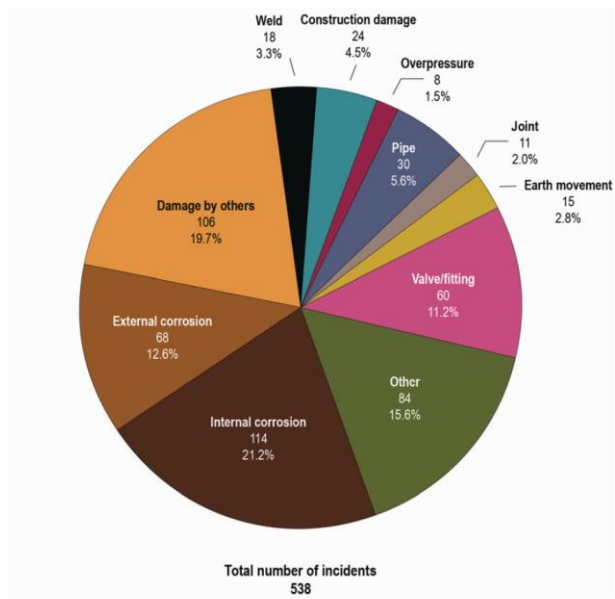
**Figure 1.1: Crude oil pipeline incidents (hits, leaks, and ruptures) from 1990 to 2012 [2]**
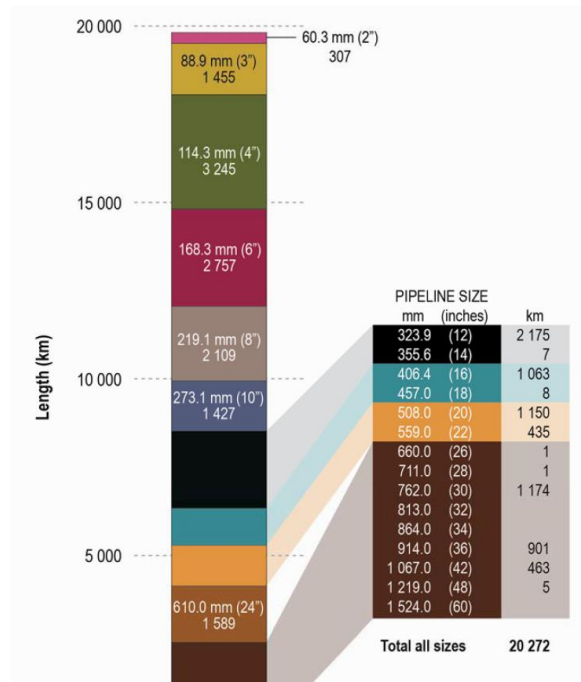


**Figure 1.2: Crude oil pipeline diameter according to AER [2]**

## 1.1 SUMMARY OF LITERATURE REVIEW

Accidental impact from excavating and construction equipment is not uncommon for onshore pipelines. On the other hand, offshore pipelines may suffer similar impact from anchors or trawling gear. These impacts cause damages in the form of dents and/or gouges with or without crack in the pipe wall. A dent in an oil or gas pipeline refers to a permanent inward deformation of the circular cross-section of the pipe. A dent can lead to stress and strain concentrations and a local reduction in the pipe diameter (ovalization or out-of-roundness). A gouge is a metal loss defect that occurs in the pipeline due to the scraping action of the excavating equipment or due to the rubbing action of the pipeline with a foreign object such as a rock. A gouge and dent both can form at the same time. A crack in the dent can also form during the formation of the dent or later in its service life if the corrosion protection coating of the pipeline is damaged locally in and around the dent and as a result, it becomes exposed to a corrosive environment. The crack can also occur in the dent if the dented area of the pipeline is subjected to fatigue or cyclic loads, primarily from pressure fluctuations [5, 7-13].

### 1.1.1 Dent Defect

Dent defects in energy pipelines have been the major concern for pipeline operators. As a result, numerous research works were completed to understand the behaviour of a dent. Balonos and Ryan (1958), Eiber et al. (1981), Wang and Smith (1982), Hopkins (1989), Alexander and Keifner (1997 and 1999), and Bjornoy et al. (2000) studied the effect of plain-smooth dents on the static pressure strength of line pipes [7, 14-19]. The burst strength of pipe with plain-kinked dent, and confined or unconfined dent has never

been the objective of any research. However, Cosham and Hopkins (2003) presumed that the kinked dent would have lower burst strength than the plain dent of the same depth [1]

The fatigue behaviour of pipe with a wide range of diameter, wall thickness, and dent with different depth was studied by Fowler et al. (1995) and Rinehart and Keating (2002) [20, 21]. Further, a significant number of researches were completed to understand the effect of dent with various shapes and sizes on the behaviour of energy pipes under monotonic and cyclic pressures. It was found and it is now generally accepted that the dent defect alone is not a threat to the integrity of pipe structure under monotonic pressure load [22-24].

**1.1.2 Dent-gouge defect**

Numerous studies were also undertaken by various research groups and individuals to determine the burst pressure capacity of pipes that have developed a gouge in the dent (often known as dent-gouge defect). Bachut and Iflefel (2011) and Alouti et al. (2014) studied behaviour of pipes containing dent-gouge defect [13, 25].

Wang and Smith (1985) and Corder and Chatain (1995) proposed design guidelines and equations for calculating the burst strength of such pipes [26-28]. However, the two most popular models are (i) EPRG dent-gouge equation and (ii) PRCI Q-factor equation. These two equations (models) are currently used by many oil and gas transporting pipeline industries for estimating the burst pressure capacity of field pipelines that have developed a dent-gouge defect. The EPRG dent-gouge equation was developed jointly by British Gas in the UK and Gaz de France in France with the financial assistance of the European Pipeline Research Group (EPRG) and the Q-factor equation was developed by Battelle Memorial Institute in USA with the financial support from the Pipeline Research Council

International (PRCI). A detailed discussion on how these equations were developed and how to use these models are available in various studies and reports. It is generally believed that the EPRG dent-gouge equation correlates better with the test data available in the public domain [29].

### 1.1.3 Crack defect

Extensive research was completed to understand how the burst strength of pipelines with part-wall defects (such as corrosion alone and crack alone) is affected as the shape of the corrosion and as the crack dimensions change. Ruggieri and Dotta (2011) and Staat and Duc Khoi (2013) developed numerical modeling on predicting the burst strength of such pipes [30, 31].

The weakening or breakdown of a material due to a variation in the loads or temperature resulting in cyclic stresses are mostly known as fatigue crack growth [32]. Crack growth occurs as a result of slip and crack tip blunting. Due to stress concentration at crack tips there will be plastic deformation even at very small loads that will blunt the crack tip. Several researches by Cottam (1973), Singh et al. (2003 and 2008), Luo et al. (2004), and Saxena et al. (2009) were completed using full-scale tests on pipe specimens to investigate fatigue crack growth [33-37]. Singh et al. (2003 and 2008), and Saxena et al. (2009) employed pipes subjected to four-point constant amplitude fatigue bending load having an initial circumferential notch [33-35] while, Luo et al. (2004) undertook a study with a longitudinal notch under constant amplitude loading [37]. Accordingly, various methods are available to estimate remaining fatigue life of pipes. Many of these method used the Paris equation to develop a model to estimate fatigue life of a full scale pipe (as an example Cottam (1973), Luo et al. (2004), and Silva et al.) [36-38].

### 1.1.4 Recommendations in Codes and standards

The current codes, standards, and design manuals provide recommendations on the assessment of dent severity considering the fact that a dent may form in conjunction with other stress raisers such as cracks, gouges, corrosion, seam or girth weld and it may also form alone. Most of these guidelines consider dent depth as a percentage of the outer diameter of the pipe as the most critical parameter for judging its severity. Severity assessment criteria when a dent contains other mechanical damages or when it contains no other damages based on its depth as outlined in different codes, standards, and design manuals are summarized in the following sections.

*Oil and Gas pipeline Systems (CSA Z662-2011)*

In accordance with CSA Z662-2011 [39], dents with following characteristics should be considered as defects:

- Dents that are located on the pipe with outer diameter of 101.6 mm or smaller should not be larger than 6 mm. However, for pipes with outside diameter larger than 101.6 mm it should not be larger than 6% of outside diameter.

- Dents containing stress concentrators or stress raisers (gouges, grooves, arc burns, or cracks).

- Dents located on a mill or field weld and exceed a depth of 6 mm in pipe with outer diameter 323.9 mm or smaller or 2% of outside diameter in pipe with outer diameter larger than 323.9 mm.

- Dents those contain corroded areas with a corrosion depth greater than 40% of the nominal wall thickness of the pipe.

- Dents those contain corroded areas having a depth greater than 10%, up to and including 40%, of the nominal wall thickness of the pipe and a depth and length that exceed the maximum allowable longitudinal extent determined as specified in ASME B31G.

Also, crack on pipe surface should be considered to be a defect unless determined by an engineering assessment to be acceptable. This assessment includes consideration of service history and loading, anticipated service conditions (including the effects of corrosive and chemical attack), the mechanism of crack formation, crack dimensions, crack growth mechanisms, failure modes, and material properties (including fracture toughness properties).

This standard recommends that pipe containing such defects (cracks or dents) should be replaced or repaired using one or more of the acceptable repair methods. It is worth mentioning that this standard suggests that an external metal loss resulting from grinding may be of any length, provided that the maximum depth of such areas is 10% or less of the nominal wall thickness of the pipe.

***Pipeline Transportation Systems for Liquids and Slurries (ASME B 31.4-2012)***

ASME code B 31.4 [40] defines dent as a gross disturbance in the curvature of the pipe wall. This code recommends that if a dent contains a scratch, gouge, groove, arc burn, or crack, which can make stress concentration, it has to be repaired or removed by cutting out the damaged portion of the pipe. Also, a dent containing metal loss as result of corrosion or grinding where remained wall thickness is less than 87.5% of wall thickness is also recommended to be removed. Further, this code recommends removing the part of pipeline

containing cracks except shallow crater cracks or star cracks in girth welds should be considered defects and hence, they need to be removed or repaired.

This code sets a limitation on the depth of a dent containing no stress concentrator, such as a scratch, gouge, groove, arc burn, or crack and also do not interact with the girth or seam weld to be removed by cutting out the damaged portion of the pipe as a cylinder. It recommends that all linepipe with a dent which exceeds a maximum dent depth of ¼ in. or 6 mm in NPS 4 or smaller pipe (nominal diameter ≤ 4 in. or 100 mm) may be allowed to operate but at a hoop stress of 20% or less of the specified minimum yield strength (SMYS) of the pipe. This value in pipe larger than NPS 4 (nominal diameter ≥ 4 in. or 100 mm) is 6%.

*Gas Transmission and Distribution Piping Systems (ASME B31.8-2012):*

ASME B31.8 [41] defines dent as an inward permanent deformation of the circular cross-section of the pipe that produces a decrease in the diameter. This code defines crack as a very narrow, elongated defect caused by mechanical splitting into parts. ASME B31.4 defines fracture toughness as the resistance of a material to fail from the extension of a crack.

This ASME code recommends a limiting dent depth of 6% of the nominal pipe diameter to consider a plain dent on the pipe surface is harmful. According to this code, a dent is considered to be a plain dent when the curvature in the dent varies smoothly and does not contain creases or other mechanical damages or corrosion or arc burns or girth or seam welds. It recommends that the depth of dent should be measured as the gap between the lowest point of the dent and a prolongation of the original contour of the pipe in any direction (Figure 1.3). The code requires that a dent which contains any mechanical

damages or stress raisers such as a scratch or gouge or groove or arch burn should be removed by cutting out the damaged portion of the pipe.
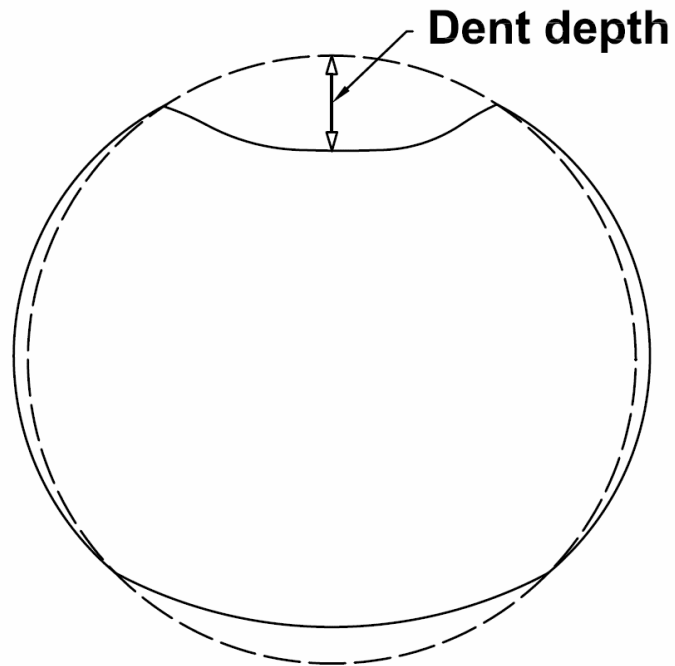


**Figure 1.3: Dent depth according to the definition of ASME**

Also, this code says external mechanical damage, including cracks, may be repaired by grinding out the damage, provided any associated indentation of the pipe does not exceed a depth of 4% of the nominal pipe diameter. Grinding is permitted to a depth of 10% of the nominal pipe wall with no limit on its length

However, the other ASME code, ASME B 31.8-2012 [41] provides dent acceptance criterion which is based on strain values rather than the dent depth. It recommends that a plain dent of any depth is acceptable provided strain levels associated with the deformation do not exceed 6% strain. Strain levels may be calculated in accordance with Non-mandatory Appendix R or other engineering methodology.

*Submarine Pipeline Systems (DNV-OS-F101-2012)*

According to DNV-OS-F101 [42], the maximum accepted ratio of permanent dent depth to the pipe diameter is given in the following criterion.

$$\frac{H_p}{D} \leq 0.05\eta \tag{1}$$

where,

$H_p$ = permanent plastic dent depth

$\eta$ = usage factor given ($\eta$ =0 if impact frequency >100, $\eta$ =0.3 if 1<impact frequency <100, $\eta$ =0.7 if Impact frequency <1)

Also this standard recommends, sharp defects like grooves, gouges, and notches should preferably be removed by grinding or other agreed repair methods according to DNV-RP-F113 [42].

*European Pipeline Research Group (EPRG)*

According to EPRG, severity assessment of a plain dent (a dent without any other mechanical damages) can be undertaken by considering its depth and radius of curvature [43]. This guideline provides recommendation by considering the difference between the dent depths measured at pressurized (H) and unpressurised ($H_0$) conditions of the pipe. The recommendations made by them are based on experimental studies competed by them. A total of 76 tests were completed on different sizes of pipe with outside diameter ranges from 168.3 mm to 914.4 mm. A few of these tests included dent along with seam weld. However, due to insufficient data to determine the interaction between a weld and a dent, EPRG limited their recommendation for a plain dent only.

For plain-smooth dents, EPRG concluded that dents up to 10% of the pipeline outer diameter (in unpressurised condition) will not fail at stress levels below 72% of SMYS. This is shown by the following equation.

$$\frac{H_0}{2R} \leq 10\% \tag{2}$$

Where:

$H_0$ = the depth of the dent measured at unpressurised condition

$R$ = the radius of the pipe

It is worth mentioning that EPRG considers that this criterion applies to dents with a radius of curvature being more than five times the wall thickness.

Since the internal pressure tends to push out the dent, thus, reducing the dent depth (spring back phenomenon), the measured depth on an operational pipeline has, therefore, to be corrected in order to use the EPRG method in a conservative manner. It is worth mentioning that EPRG considers that this criterion applies to dents with a radius of curvature of more than five times the wall thickness. The relationship between the dent depth on an unpressurised pipeline ($H_0$) and a pressurized pipeline (H) proposed by EPRG is as follows.

$$H_0 = 1.43H \tag{3}$$

Therefore EPRG's limit on the acceptance of a plain dent in an operational pipeline (when there is pressure) can be written as follows.

$$\frac{H}{2R} \leq 7\% \tag{4}$$

The acceptable limit of dent depth is relaxed in operating field pipelines. This is because the dent rebounds as internal pressure is applied.

In summary, the literature review reveals that extensive research has been completed to determine the burst strength of pipes with single part-wall defect (corrosion or crack alone), dent alone, and combined dent-gouge defect. However, no experimental studies were completed to determine the burst strength of dented pipe that has developed crack in the dent. Also, these studies did not investigate the effect of parameters such as dent depth, dent shape, and internal pressure during indentation on the strain distributions of the dent. It was found that a dent evaluation criterion using dent depth alone is not universally accepted and it may be realistic to include strain values for the assessment of the dent severity.

## 1.2 OBJECTIVES

The primary objective of this research is to determine the burst strength of NPS30 pipe with dent-crack defect with various dent depths, crack depth, crack length, crack location, steel grade, and operating pressure. The other objectives of this research project are to study the overall structural behaviour of the oil and gas pipe while subjected to concentrated lateral (denting) loading, to investigate the effect of various parameters (internal pressure, dent depth, and dent shape and size) on the strain distribution in and around dented area, and to study the validity of dent depth as criterion for determining the severity of a dent.

## 1.3 METHODOLOGY

Full scale tests, Material tests, and numerical study have been done in following sequence to study how burst strength of linepipe with dent-crack defect is affected by different parameters such as dent depth, crack depth, crack length, operating or internal

pressure, material property, dent geometry, and crack location. All pipe specimens were subjected to the same loading procedure and same loading sequence as full scale test. First fatigue load applied, followed by denting load to make a combination of crack defect and dent defect on all these pipe specimens. Then pipes were subjected to monotonically increasing water pressure until rupture occurred .The purpose of the fatigue load was to create a crack at the tip of the V-notch through the thickness of the pipe wall. Hence, pipe specimens send to a shop and a V shaped notch was created using electro-discharging machine (EDM) technique. Then, the notched pipe was subjected to fatigue load cycles with stress ratio of 0.5 and the fatigue loading continued until a crack at the tip of the V-notch of about 0.3 mm deep was obtained.  As a result, the notch tip was associated with a true crack at the tip of the V-notch.

Before next loading step (denting), pipe specimens were send out to weld two caps at the end of them to maintain operating pressure during indentation process. Then a dent of required depth was created on the pipe wall at the crack defect location by applying a load through the steel indenter using displacement control method to have a combination of dent defect and crack defect.

The pipe specimen in the last loading step was placed on semi-circular bed trolley. The pipe specimen with dent-crack defect was then subjected to monotonically increasing water pressure until a leak or a rupture occurred in the dent-crack defect.

Several material tests have been done with different purposes. Tensile tests, charpy impact test, and fracture toughness test have been carry out to determine the mechanical properties and critical J-integral of pipe material. Numerical model was developed using results of these two tests to study the effect of each parameter in the wider range. Also ten

small samples collected from the crack area to complete fractography. Fractographic method are used to confirm the existence of fatigue crack at the end of V-notch.

Numerical model was developed and validated using experimental data. Also comprehensive parametric study carry out to determine the effect of each parameter on the burst strength of pipe specimens with dent-crack defect.

Finally by using parametric study results, an empirical equation developed using the symbolic regression, or symbolic function identification to calculate the burst strength of linepipe with a combination of dent defect and crack defect.

## 1.4 ORGANIZATION OF THE DISSERTATION

This dissertation consist of eight chapters. The first chapter provides a general introduction and the very last chapter, Chapter 8 discusses general discussions and conclusions.

The second chapter provides a detailed account of results on the strain distribution in the pipe wall due to the formation of dent. Also, this chapter discusses the effect of different parameters on the strain concentration and distributions.

The third chapter discusses the effect of internal (operating) pressure, shape of the rock tip (dent shape), and diameter-to-thickness ratio of pipe on the ovalization (out-of-roundness) of pipe specimens when subjected to a concentrated (denting) load.

The forth chapter describes a pipe with dent-crack when the crack depth is less than 2 mm. This chapter also discusses how the burst pressure of this pipe is affected by its internal (operating) pressure.

The fifth chapter discusses the effect of the dent depth and operating line pressure on the pressure capacity of NPS30 X70 grade linepipes.

The sixth chapter talks about the effect of crack length and crack depth on burst strength of a pipe with dent-crack defect.

The seventh chapter discusses the effect of dent depth on X55 grade steel pipe and crack location on burst strength of a pipe with dent-crack defect.

## 1.4 REFERENCES

[1] Cosham, A., and Hopkins, P., 2004, "The effect of dents in pipelines-guidance in the pipeline defect assessment manual," International Journal of Pressure Vessels and Piping, 81(2), pp. 127-139.

[2] AER, 2013, "Report 2013-B: Pipeline Performance in Alberta, 1990–2012," Alberta Energy Regulator, Calgary, Alberta, Canada.

[3] Smith, R. B., and Gideon, D. N., 1979, "STATISTICAL ANALYSIS OF DOT-OPSO DATA," Proceedings, Annual Symposium - Society of Flight Test Engineers, pp. D. 1-D. 9.

[4] Wang, K., and Smith, E., 1982, The Effect of Mechanical Damage on Fracture Initiation in Line Pipe, Part I: Dents, Energy, Mines and Resources Canada, Canada Centre for Mineral and Energy Technology.

[5] Zarea, M. F., Toumbas, D. N., Philibert, C. E., and Deo, I., "Numerical models for static denting and dynamic puncture of gas transmission linepipe and their validation," Proc. Proceedings of the 1996 1st International Pipeline Conference, IPC. Part 2 (of 2), June 9, 1996 - June 13, 1996, ASME, pp. 777-784.

[6] Lancaster, E. R., 1996, "Burst pressures of pipes containing dents and gouges," Proceedings of the Institution of Mechanical Engineers, Part E: Journal of Process Mechanical Engineering, 210(1), pp. 19-27.

[7] Belonos, S. P., and Ryan, R. S., 1958, "How dents in pipe can affect service performance of lines," Oil and Gas Journal, 56(46), pp. 155-156.

[8] Maxey, W. A., and Committee, A. G. A. P. R. C. L. P. R. S., 1986, Topical Report on Outside Force Defect Behaviour: To Line Pipe Research Supervisory Committee of the Pipeline Research Committee of the American Gas Association, Batelle.

[9] Lancaster, E. R., and Palmer, S. C., 1996, "Strain concentrations in pressurized dented pipes," Proceedings of the Institution of Mechanical Engineers, Part E: Journal of Process Mechanical Engineering, 210(E1), pp. 29-38.

[10] Moffat, D. G., Iflefel, I. B., and Mistry, J., 2005, "The interaction of pressure and bending on a dented pipe," International Journal of Pressure Vessels and Piping, 82(10), pp. 761-769.

[11] Karamanos, S. A., and Andreadakis, K. P., 2006, "Denting of internally pressurized tubes under lateral loads," International Journal of Mechanical Sciences, 48(10), pp. 1080-1094.

[12] Bachut, J., and Iflefel, I. B., "Experimental and numerical investigation of plain and gouged dents in steel pipes subjected to pressure and moment loading," American Society of Mechanical Engineers, pp. 0212031-0212039.

[13] Allouti, M., Schmitt, C., and Pluvinage, G., 2014, "Assessment of a gouge and dent defect in a pipeline by a combined criterion," Engineering Failure Analysis, 36, pp. 1-13.

[14] Eiber, R. J., Maxey, W. A., Bert, C. W., McClure, G. M., Committee, A. G. A. N.-., and Laboratories, B. C., 1981, Effects of Dents on the Failure Characteristics of Line Pipe: Final Report to NG-18 Committee AGA : NG-18 Report No. 125 : May 8 1981, American Gas Association.

[15] Wang, K. C., Smith, E. D., Mineral, C. C. f., and Program, E. T. E. R., 1982, The Effect of Mechanical Damage on Fracture Initiation in Line Pipe: Dents, Energy, Mines and Resources Canada, CANMET, Energy Research Program.

[16] Hopkins, P., 1989, "The significance of dents and defects in transmission pipelines," pp. IMechE 1989-1981.

[17] Alexander, C. R., Kiefner, J. F., Institute, A. P., Services, S. E., Kiefner, and Associates, 1997, Final Report on Effects of Smooth and Rock Dents on Liquid Petroleum Pipelines: To the American Petroleum Institute, October 10, 1997, American Petroleum Institute.

[18] Kiefner, J. F., and Alexander, C. R., 1999, Repair of Pipeline Dents Containing Minor Scratches: Final Report on Contract No. PR 218-9508 to Line Pipe Research Supervisory Committee PRC/International, Kiefner & Associates.

[19] Bjornoy, O. H., Rengard, O., Fredheim, S., and Bruce, P., "Residual strength of dented pipelines, DNV test results," Proc. Proceeedings of the 10th International Offshore and Polar Engineering Conference, May 28, 2000 - June 2, 2000, ISOPE, pp. 182-188.

[20] Fowler, J. R., Alexander, C. R., Kovach, P. J., and Connelly, L. M., "Fatigue life of pipelines with dents and gouges subjected to cyclic internal pressure," Proc. Proceedings of the Energy-Sources Technology Conference and Exhibition, January 29, 1995 - February 1, 1995, ASME, pp. 17-35.

[21] Rinehart, A. J., and Keating, P. B., "Fatigue life prediction for short dents in petroleum pipelines," Proc. Design and Analysis of Piping, Vessels and Components (2002 ASME Prssure Vessels and Piping Conference), August 5, 2002 - August 9, 2002, American Society of Mechanical Engineers, pp. 103-111.

[22] Dama, E., Karamanos, S. A., and Gresnigt, A. M., 2007, "Failure of locally buckled pipelines," Transactions of the ASME. Journal of Pressure Vessel Technology, 129(2), pp. 272-279.

[23] Gresnigt, A. M., Karamanos, S. A., and Andreadakis, K. P., 2007, "Lateral loading of internally pressurized steel pipes," Transactions of the ASME.Journal of Pressure Vessel Technology, 129(4), pp. 630-638.

[24] de C. Pinheiro, B., and Pasqualino, I. P., 2009, "Fatigue analysis of damaged steel pipelines under cyclic internal pressure," International Journal of Fatigue, 31(5), pp. 962-973.

[25] Bachut, J., and Iflefel, I. B., 2011, "Analysis of pipes containing plain and gouged dents," Strain, 47(SUPPL. 1), pp. e34-e51.

[26] Wang, K. C., and Smith, E. D., 1985, "The effect of mechanical damage on fracture initiation in linepipes: Part III-gouge in a dent," No. PMRL 85-69(TR), An internal report submitted to Physical Metallurgical Research Laboratories of CANMET, Ottawa, ON, Canada.
[27] Corder, I., and Chatain, P., 1995, "Towards recommendations for the assessment of the tolerance and resistance of pipelines to external damage," No. 13, EPRG/PRC 10th joint Technical Meeting on Pipeline Research, Cambridge, UK.
[28] Corder, I., and Chatain, P., 1995, "EPRG recommendations for the assessment of the resistance of pipelines to external damage," No. 12, EPRG/PRC 10th joint Technical Meeting on Pipeline Research, Cambridge, UK.

[29] Macdonald, K., and Cosham, A., 2005, "Best practice for the assessment of defects in pipelines–gouges and dents," Engineering Failure Analysis, 12(5), pp. 720-745.

[30] Staat, M., and Duc Khoi, V., 2013, "Limit analysis of flaws in pressurized pipes and cylindrical vessels. Part II: Circumferential defects," Engineering Fracture Mechanics, 97, pp. 314-333.

[31] Ruggieri, C., and Dotta, F., 2011, "Numerical modeling of ductile crack extension in high pressure pipelines with longitudinal flaws," Engineering Structures, 33(5), pp. 1423-1438.

[32] Broek, D., 1989, The practical use of fracture mechanics, Springer Science & Business Media.

[33] Singh, P. K., Vaze, K. K., Bhasin, V., Kushwaha, H. S., Gandhi, P., and Ramachandra Murthy, D. S., 2003, "Crack initiation and growth behaviour of circumferentially cracked pipes under cyclic and monotonic loading," International Journal of Pressure Vessels and Piping, 80(9), pp. 629-640.

[34] Singh, P. K., Bhasin, V., Vaze, K. K., Ghosh, A. K., Kushwaha, H. S., Murthy, D. S. R., Gandhi, P., and Sivaprasad, S., 2008, "Fatigue studies on carbon steel piping materials and components: Indian PHWRs," Nuclear Engineering and Design, 238(4), pp. 801-813.

[35] Saxena, S., Ramakrishnan, N., and Chouhan, J. S., 2009, "Fatigue life prediction analysis of surface cracked straight pipes," Transactions of the Indian Institute of Metals, 62(3), pp. 191-195.

[36] Cottam, W. J., 1973, "Application of Fracture Mechanics  Concepts to Pipeline Design," Conference on Stress and Straing in EngineeringBrisbane, Australia, pp. 135-142.

[37] Luo, J., Zhao, X., Xiong, Q., and Huo, C., "Defective pipeline fatigue-life prediction using failure assessment diagram technique," Proc. Proceedings of the Biennial International Pipeline Conference, pp. 1277-1280.

[38] Silva, J., Ghaednia, H., and Das, S., "Fatigue life assessment for nps30 steel pipe," Proc. 2012 9th International Pipeline Conference, IPC 2012, September 24, 2012 - September 28, 2012, American Society of Mechanical Engineers, pp. 619-624.

[39] CSA, 20011, "Z662-11: Oil and Gas Pipeline Systems," Canadian Standard Association, Mississauga, ON, Canada.

[40] ASME, 2012, "B31.4: Pipeline Transportation Systems for Liquids and Slurries," ASME International, New York, NY, USA.

[41] ASME, 2012, "B31.8: Gas Transmission and Distribution Piping Systems," ASME International, New York, NY, USA.

[42] DNV, 2012, "OS-F101: Submarine Pipeline Systems," Det Norske Veritas.

[43] Roovers, P., Bood, R., Gali, M., Marewski, U., Steiner, M., and Zarea, M., 2000, "EPRG methods for assessing the tolerance and resistance of pipelines to external damage," Pipeline technology, 2, p. 21.

# CHAPTER 2

# STRUCTURAL EVALUATION OF PIPELINE WITH DENT DEFECT

## 2.1 INTRODUCTION

Various defects develop in field oil and gas pipeline and these defects significantly affect the performance and structural safety of oil and gas pipelines. Corrosion, crack, puncture, dent, gouge, and combination of such damages are some common examples of surface defects found in the field pipeline. Surface defects such as gouges, dents, cracks, and punctures that form in the pipe wall as a result of contact and/or impact from foreign objects are often referred to as mechanical damages. Mechanical damage of oil and gas pipeline is considered to be the major cause of failure of pipelines in service and this damage may result in loss of product, explosion, fire, human and/or animal casualties, and pollution. It has been reported that the failure of oil and gas transmission pipelines resulting from mechanical damages ranges from 55% in the USA to around 70% in Europe [1-4].

Accidental impacts are common in onshore and offshore pipeline. Construction and excavation activities can cause impact loads resulting in mechanical damages in onshore pipeline while anchors or trawling gear actions can cause mechanical damages in offshore pipelines. A concentrated lateral load resulting from rock tip or hard surface can also create a dent in the field buried pipeline. A dent is an inward plastic deformation in the pipe wall which causes a gross distortion of the pipe cross section and reduction in pipe's diameter locally [6]. The ability of the pipeline to sustain the concentrated loading and transform it into plastic deformation is of particular interest for safeguarding its structural integrity

against such loading [5, 6]. Formation of a dent results in localized strain concentrations in the pipe wall which can lead to a leak or rupture causing loss of containment, damage to environment, and threat to the safety of habitants living nearby, and also interruption in oil and gas supply, and a loss in the pipeline operator's revenue. A dent also causes local reduction in the pipe diameter and ovalization in the pipe's cross-section. Hence, the dent defect has been a major concern for the pipeline operators.

Several investigations in the past were completed to understand the effect of dent defect on the structural behaviour of energy pipes under monotonic and cyclic pressures. Based on these research works, it is generally accepted that dent defect is not a threat to the integrity of pipe structure under monotonic pressure load when the dent depth is up to 6% of the diameter of the pipe [7, 8]. However, it is also understood that the dent depth is not the most useful parameter for determining whether or not a dent defect is a threat to structural integrity and safety of pipeline. The use of dent depth alone for the assessment of structural integrity of pipeline can be misleading and can result in unnecessary excavations and repair activities for the dent defect which may not necessarily be harmful to the structural integrity of the pipeline. On the other hand, it is also possible that a dent with a small dent depth (dent depth less than 6% of the diameter of the pipe) could be a threat to the structural integrity of the pipeline if the strain value is high. Hence, the measures of strain values and their distributions is an appropriate and more relevant parameter for assessing the severity and acceptability of a dent defect [9, 10]. Therefore, the distribution of strains in the pipe wall due to the formation of dent is of particular interest in this study. This study was completed at the Centre of Engineering Research in Pipeline (CERP), University of Windsor for determining the structural behaviour of NPS30

X70 pipe with dent defect. This work was completed using a combined method of laboratory based experimental study and finite element method (FEM) based numerical study. This paper discusses the results obtained from this study.

## 2.2 EXPERIMENTAL WORK

### 2.2.1 Test specimen

The purpose of conducting full-scale tests was to determine experimentally the structural behaviour of steel pipes used in oil and gas transmission when subjected to denting load. The study also determined the critical strain values from the tests. NPS 30 X70 steel pipe [11] used in oil and gas onshore pipelines was used to prepare the test specimens. Six specimens were fabricated from pipe with nominal diameter of 762 mm, wall thickness of 8.5 mm, and conforming to grade, API 5L X70 steel pipes [11]. The diameter-to-thickness ratio (D/t) of the specimens used in this study was about 90. The length of each pipe specimen was 2000 mm. Two ends of the specimen were welded to semi-spherical steel caps of 8.5 mm thick for holding the water pressure. Three tensile specimens were cut from the virgin pipe section and the standard tensile tests were carried out to determine the mechanical properties of the pipe material in accordance with ASTM E8 [12]. The properties of the material which were obtained from the tensile test are: actual yield strength of 543 MPa at 5% total strain; tensile strength of 624 MPa; and modulus of elasticity of 204 GPa.

The main parameters of the study were: (i) the shape of the indenter, (ii) the operating (internal) pressure and (iii) the dent depth (Table 2.1). The permanent dent depth is the plastic deformation resulting from denting process and calculated after removal of

the indenter. The pressure was varied from 0 MPa (no internal pressure) to 7.6 MPa (1100 psi) and hence, the internal pressure was varied from $0.0p_y$ to $0.6p_y$ where $p_y$ is the pressure required to cause yielding of the pipe material. The yield pressure ($p_y$) for this pipe was calculated at 12.67 MPa (1837 psi). Indenters of two different shapes were used to create dent with two different shapes. These were: (i) short dent (rectangular shape) and (ii) long dent (canoe shape) as shown in Figure 2.1. The dent depth was varied from 2% to 6% of the outer diameter of the pipe (Table 2.1).



(a) Short or rectangular indenter    (b) Long or canoe shape indenter

**Figure 2.1: Two different indenters used in the experiments**

Table 2.1 shows the matrix of the test specimens used in this study. Specimens were named to reflect the primary attributes attached to each specimen. For example, for specimen S2-SI-D4-P30, the first letter and number combination (S2) indicates that it is specimen number 2, the next two letters (SI) indicate that the specimen was loaded with short indenter, the next letter and number combination (D4) indicates that the inward permanent dent depth in the pipe wall due to loading in this specimen was 4% (~30 mm) of the diameter of the pipe, and the last combination of letter and number (P30) indicates that the internal pressure was held constant at $0.3p_y$ or 30% of $p_y$ which is about 3.8 MPa

(550 psi).  Similarly, specimen S6-LI-D4-P30 was the sixth specimen and this specimen was identical to specimen S2-SI-D4-P30 except the earlier one was loaded with long indenter. The first specimen in Table 2.1, S1-SI-D4-P00 is considered as the reference specimen.

<div align="center">Table 2.1: Test matrix</div>

| Specimen name | Indenter Dimension | Indenter Type | Dent Depth (% of diameter) | Internal pressure (% of $p_y$)* | Parameter |
|---|---|---|---|---|---|
| S1-SI-D4-P00 | 100×50 mm | Short | 30 mm (4%) | 0 MPa (0%) | Reference specimen |
| S2-SI-D4-P30 | 100×50 mm | Short | 30 mm (4%) | 3.8 MPa (30%) | Internal pressure |
| S3-SI-D4-P60 | 100×50 mm | Short | 30 mm (4%) | 7.6 MPa (60%) | |
| S4-SI-D2-P00 | 100×50 mm | Short | 15 mm (2%) | 0 MPa (0%) | Dent depth |
| S5-SI-D6-P00 | 100×50 mm | Short | 46 mm (6%) | 0 MPa (0%) | |
| S6-LI-D4-P30 | 500×35 mm | Long | 30 mm (4%) | 3.8 MPa (30%) | Indenter shape and size |

<div align="center">* Pressure held constant during application of concentrated load</div>

## 2.2.2 Test setup

The experimental program was carried out in the Structural Engineering Laboratory of the University of Windsor by CERP. Figure 2.2 schematically shows the test setup. The pipe specimens were placed on three very thick and rigid T-shaped steel supports. Denting load was applied on the top surface of the pipe wall using a universal loading actuator.

The total and plastic deformation (dent depth) of the pipe due to application of denting load was measured using linear variable differential transformers (LVDTs). Two LVDTs were used. The LVDTs were located on the actuator to acquire downward displacement of the indenter. Hemispherical steel end caps were welded at the end of each specimen to be able to hold the water and pressurize the pipes using a hydrostatic pump. Specimens were instrumented with strain gauges to monitor and record the variations of strain around the dent. Two different lines of strain gages consisting of eight to ten strain gauges on each line were installed. The layout of the strain gauges is shown in Figure 2.3. No strain gauges were installed underneath the indenter since these gauges fail as soon as load is applied.
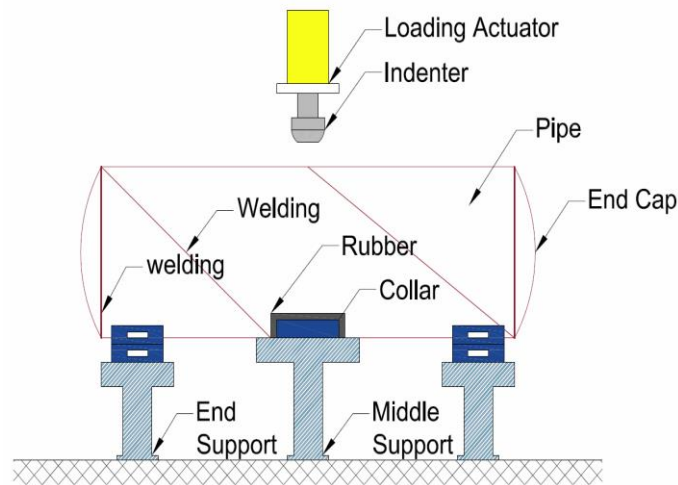


**Figure 2.2: Denting test setup**

### 2.2.3 Test procedure

For all the six specimens same loading procedure was used. First, the pipe specimen was filled with water and then pressurized using a hydrostatic pump. Next, a monotonically increasing quasi-static denting load was applied while keeping the level of internal pressure unchanged. Then the denting load was gradually removed. The internal pressure simulates

operating pressure of the pipeline. After complete removal of the denting load, the internal

pressure in the pipe specimen was reduced to zero. The objective was to obtain strain data

(distribution) when the pipe is completely unloaded at a certain dent depth. For all the

specimens, the test was carried out and controlled to produce a dent with permanent depth

of 0% to 6% of the outer diameter of the pipe (Table 2.1).
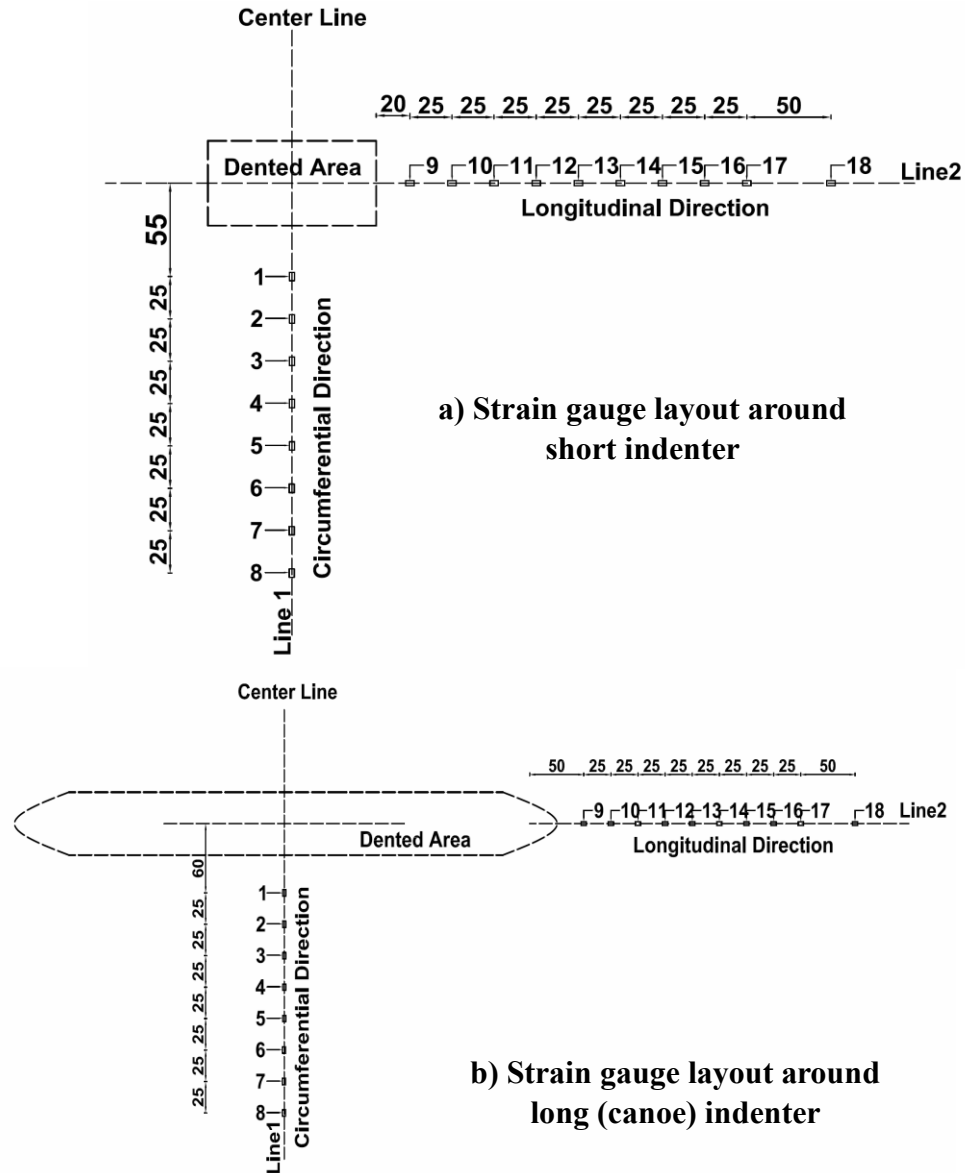


**Figure 2.3: Strain gauge layout**

## 2.3 TEST RESULTS

### 2.3.1 Load-deformation behaviour

For specimens S1-SI-D4-P00, S2-SI-D4-P30, S3-SI-D4-P60, S4-SI-D2-P00, and S5-SI-D6-P00, the denting load was applied using the short (rectangular) indenter while long (canoe) indenter was used for the application of denting load on specimen S6-LI-D4-P30 (Table 2.1). The load-deformation behaviour of these specimens are shown in Figures 2.4a to 2.4c.

Figure 2.4a shows the load-deformation for three specimens, S1-SI-D4-P00, S2-SI-D4-P30, and S3-SI-D4-P60. These three specimens were identical except the internal pressure during application of denting load was different and it ranged from no pressure to $0.6p_y$. This figure shows that as the operating (internal) pressure of pipeline increases the maximum load and total displacement required to produce same permanent deformation depth (4%) increase as well. The maximum load required for these three specimens were 812 kN, 497 kN, and 183 kN, respectively. The total deformation required in these three specimen were 49 mm, 64 mm, and 71 mm respectively. Hence, this figure shows that higher operating pressure is beneficial in delaying the dent growth.

Figure 2.4b shows load-deformation behaviour of specimens S4-SI-D2-P00, S1-SI-D4-P00, and S5-SI-D6-P00. These three specimens had no internal pressure during application of the denting load and they were loaded with same (short) indenter. The difference in these specimens was the permanent deformation depth (dent depth) due to application of the denting load which varied from 2% to 6%. From this figure it can be

found that as the dent depth reduces the maximum load and total deformation reduce as well.

Figure 2.4c shows load-deformation behaviour of specimens S2-SI-D4-P30 and S6-LI-D4-P30. The only difference between these two specimens is the length and shape of the indenter. For specimen S2-SI-D4-P30, the length was short and shape was rectangular whereas, the shape and length of indenter for specimen S6-LI-D4-P30 were canoe and relatively long. This figure shows that longer indenter required much higher load than the shorter indenter and the maximum load values for these two specimens were 755 kN and 497 kN, respectively. However, total deformation required during application of denting load was about 64 mm for both specimens. Hence, this figure shows that shape and length of rock tip that creates dent may be an important factor if the load applied on the buried pipeline is in load control mode. However, the shape and length of rock tip is irrelevant if the denting load is applied in displacement control mode.

## 2.3.2 Strain distributions

Strain data obtained from the strain gauges installed in the circumferential direction (Line 1 in Figure 2.3) is presented in Figure 2.5. From the strain gauge readings as shown in Figure 2.5a, it is observed that as the internal pressure increases the values of maximum circumferential strains increase as well. The highest circumferential strain for specimens S1-SI-D4-P00, S2-SI-D4-P30 and S3-SI-D4-P60 after unloading was 0.81%, 1.37%, and 2.17% respectively. The maximum values of tensile circumferential strain were obtained from the strain gauge 6 for specimens S1-SI-D4-P00 and strain gauge 4 for specimens S2-SI-D4-P30 and S3-SI-D4-P60. These strain gauges were located at 180 and 130 mm away from the center of the indenter along the perimeter of the pipe (Figure 2.3), respectively.
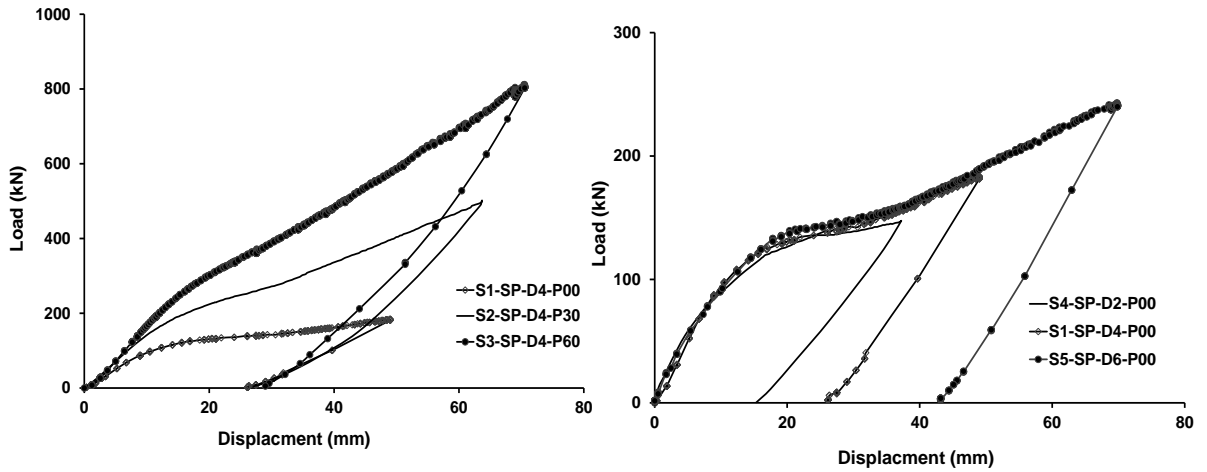
**(a): Specimens S1, S2, and S3**

**(b): Specimens S1, S4, and S5**
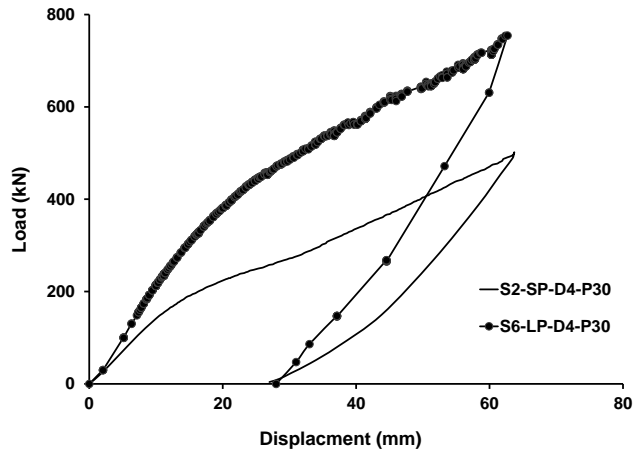
**(c): Specimens S2 and S6**

**Figure 2.4: Load-deformation behaviours**

Figure 2.5b shows strain distribution of specimens S4-SI-D2-P00, S1-SI-D4-P00, and S5-SI-D6-P00. These three specimens had no internal pressure during application of the denting load and they were dented with same (short) indenter. The difference in these specimens was the permanent deformation depth due to application of the dent load which varied from 2% to 6%. From this figure it can be found that as the permanent depth reduces the maximum strain reduces as well. However, pattern of strain distribution remains almost

28

same. The maximum circumferential strain for specimens S4-SI-D2-P00, S1-SI-D4-P00, and S5-SI-D6-P00 after removing the dent load was 0.39%, 0.81%, and 1.29% respectively. The location of the maximum strain reduces from 180 mm in specimen S4-SI-D2-P00 which had dent depth of 2% to 155 mm in specimen S5-SI-D6-P00 which had dent depth of 6%. Hence, this study shows that location of critical strain also changes as dent depth changes.

Figure 2.5c compares strain distributions in the circumferential direction for specimens, S2-SI-D4-P30 and S6-LI-D4-P30, both had same operating (internal) pressure but two different indenters. For the long (canoe shaped) indenter (for specimen S6-LI-D4-P30), maximum tensile circumferential strain was 0.63% obtained from strain gauge 6, which was located 185 mm away from the center of the dent along the perimeter of the pipe. However, for the short (rectangular shaped) indenter (for specimen S2-SI-D4-P30), maximum tensile strain was 1.37% at strain gauge 4, which was located 130 mm away from the dent center (Figure 2.3). Hence, the specimen with the smaller dent (S2-SI-D4-P30) experienced a higher strain. This strain occurred at a closer distance than the specimen with the long indenter (specimen S6-LI-D4-P30).
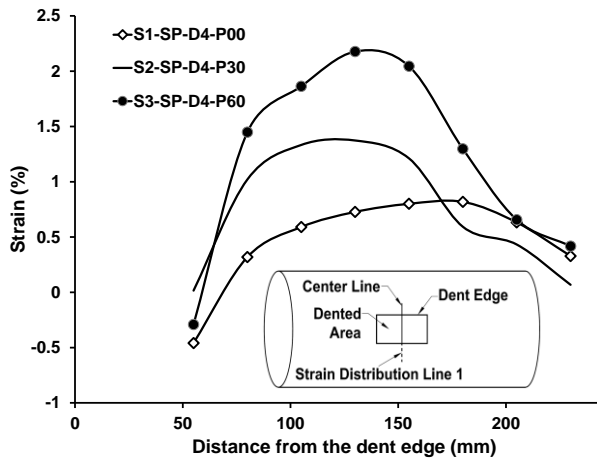
(a): Specimens S1, S2, and S3
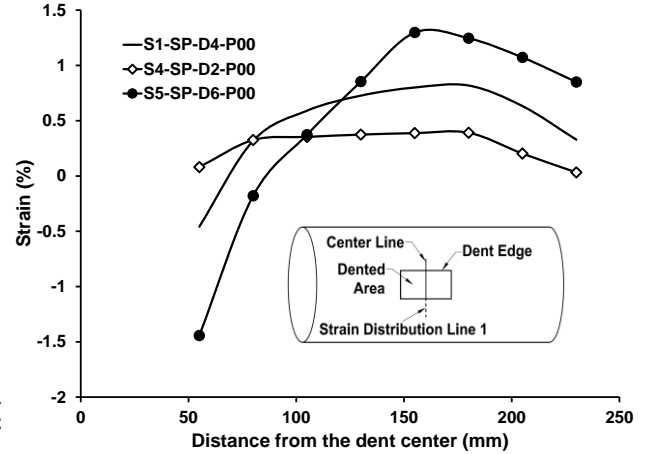


(b): Specimens S1, S4, and S5
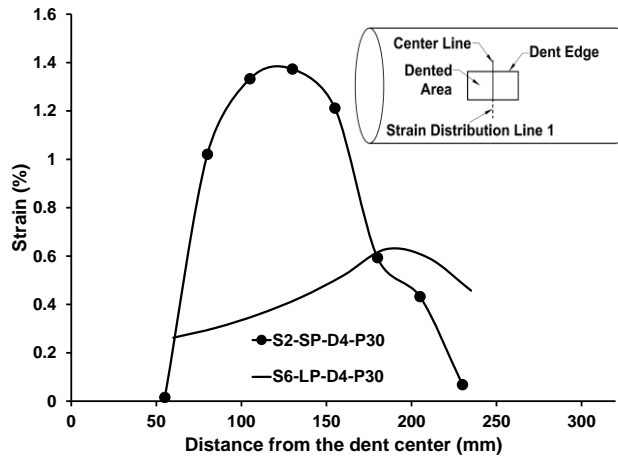


(c): Specimens S2 and S6

**Figure 2.5: Strain distributions in circumferential direction**

Figure 2.6 shows the distributions of strains in the longitudinal direction and it shows similar trends as Figure 2.5. As can be seen in Figure 2.6a, for specimens S1-SI-D4-P00, S2-SI-D4-P30, and S3-SI-D4-P60 maximum strain was recorded at strain gauge 10 (Figure 2.3), which was located at 95 mm away from the center of the dent. The only different between these three specimens was internal pressure which was varied from $0.0p_y$ to $0.6p_y$. Hence, as the internal pressure increases the maximum strain value increases as

well. The maximum strain recorded was 1.25% for S1-SI-D4-P00, 1.92% for S2-SI-D4-P30 and 3.60% for S3-SI-D4-P60.

Figure 2.6b shows strain behaviour of specimens S4-SI-D2-P00, S1-SI-D4-P00, and S5-SI-D6-P00 after unloading. The operating (internal) pressure was kept unchanged while the dent depth was varied from 2% to 6% in these three specimens. From this figure it can be found that as the permanent depth increases the maximum strain increases as well. The highest values of strain were 1.6%, 1.25%, and 0.43% in specimens S5-SI-D6-P00, S1-SI-D4-P00, and S4-SI-D2-P00, respectively.

From Figure 2.6c it is evident that the smaller (rectangular) indenter showed more strain concentration than the longer (canoe) indenter though both specimens had same dent depth of 4%. This behaviour was also observed in the circumferential direction. The maximum strains recorded after removing the indenter were 1.92% for S2-SI-D4-P30 and 0.71% for S6-LI-D4-P30. Hence, the test data shows that the maximum strain in specimen with short dent (S2-SI-D4-P30) is much higher than the maximum strain in specimen with long dent (S6-LI-D4-P30). Therefore, the pipe specimen which was dented using short indenter experienced about 3 times higher strain (the difference between the maximum strain values is 1.21%). The dent depth in both specimens was same. Therefore, it is evident that the use of dent depth alone is not sufficient to assess the severity of a dent defect and the strain values and their distributions need to be considered for better assessment of dent defect.
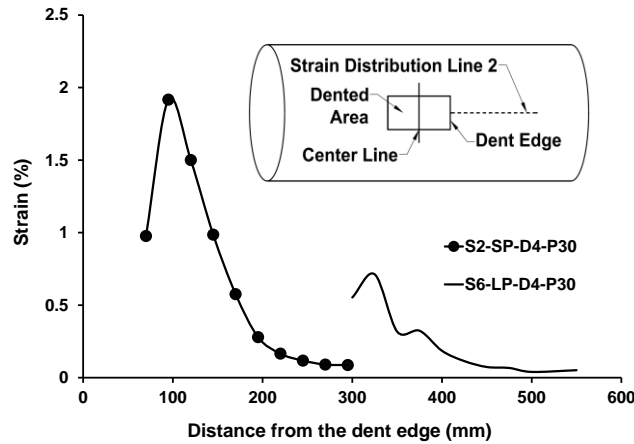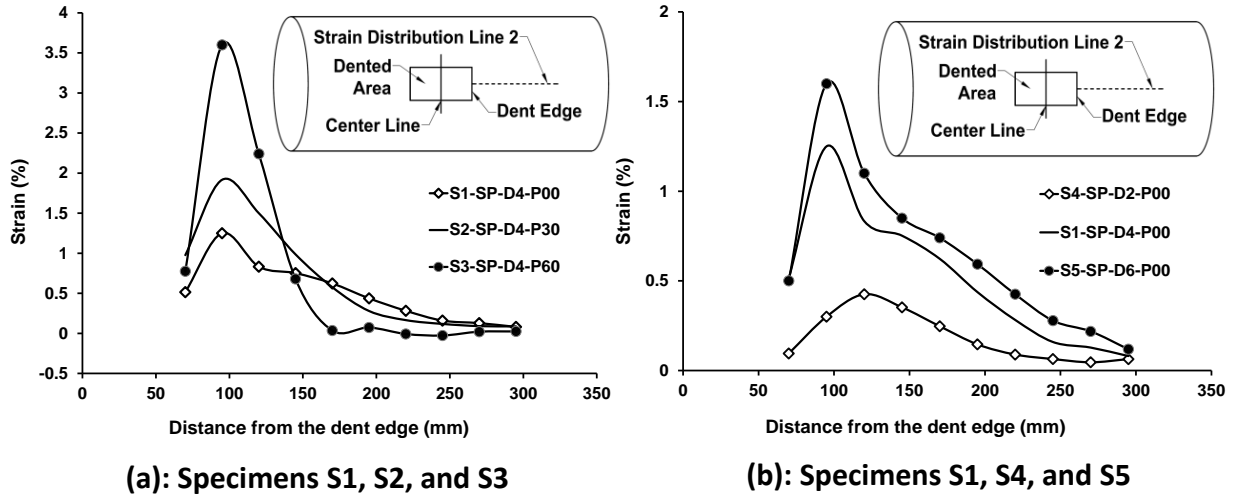
(a): Specimens S1, S2, and S3



(b): Specimens S1, S4, and S5



(c): Specimens S2 and S6

Figure 2.6: Strain distributions in longitudinal direction

## 2.4 FINITE ELEMENT ANALYSIS

The structural behaviour of the same pipe specimens under monotonically increasing denting load was studied numerically using nonlinear finite element method. The main purpose of developing the finite element models was to obtain the strains in the region underneath the indenter, which could not be obtained from the tests. The finite element models were validated using the test data obtained from this study.

**2.4.1 Finite element simulation**

In this study, numerical modeling technique considering both material and geometric nonlinearities was employed to simulate the behaviour of the test specimens. Commercially available general purpose finite element analysis code, ABAQUS/Standard version 6.11.2 distributed by SIMULIA [13] was used to model the pipe behaviour. The 20-node quadratic brick element with reduced integration (second order), C3D20R, was used in and around the load application area where stress concentration was expected to be high. For the rest of the pipe, 8-node linear brick elements with reduced integration C3D8R were used. The indenter and supports were modelled as discrete rigid body using the 4-node rigid quadrilateral elements, R3D4 to avoid any deformation in indenter and supports. In the tests, the indenter were very thick and rigid. A typical finite element mesh used in the present analysis is shown in Figure 2.7.
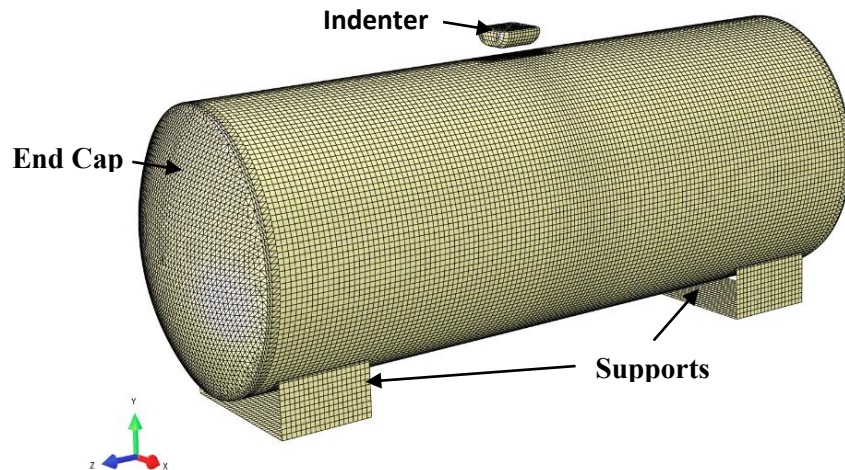


**Figure 2.7: Typical finite element model**

In the experimental program, the pipe specimen rested on the steel supports during the indentation process. Hence, there was a contact interaction between the pipe wall and the support. There was contact interaction between the pipe wall and the indenter as well. Therefore, a finite-sliding contact formulation was used to simulate the contact between the pipe and indenter and also between the pipe and the supports. The pipe material underneath and around the indenter experienced large plastic deformations. Therefore, an elastic-plastic actual material behaviour using von-Mises yield criterion and isotropic hardening with associated plastic flow rule was used in the numerical modeling.

The same loading and unloading steps which were used in the experimental program was applied to the FE models. Application of internal pressure was the first step in the loading scheme. After the application of the internal pressure, denting load was applied using displacement control algorithm to trace the nonlinear equilibrium paths. Finally, the denting load was removed gradually.

**2.4.2 Validation of FE models**

The finite element (FE) models were validated using the load-deformation behaviour and strain data obtained from the full-scale tests. The comparison of the load-deformation relationships for specimens S2-SI-D4-P30 and S6-LI-D4-P30 between the test data and finite element analyses are shown in Figures 2.8a and 2.8b, respectively. A good agreement between the test and numerical behaviours is observed. The circumferential and longitudinal strain for specimens S2-SI-D4-P30 and S3-SI-D4-P60 obtained from the test and FEA are shown in Figures 2.9, and 2.10 respectively. In these figures, the distance on the x-axis was measured from center of dented area. These figures also show a good agreement between the test and FEA strain distributions. Similar correlation between test

and FEA strain characteristics was also found for other test specimens. It is worth noting that the strain values underneath the indenter could only be obtained from finite element analysis. Figure 2.9a shows that the maximum circumferential strain value was compressive for specimen S2-SP-D4-P30 and it occurred inside the dent area. However, the maximum strain value in the longitudinal direction was tensile and the location of the maximum strain was outside the dent area (Figure 2.9b). Further, the maximum circumferential and longitudinal strains in the longer dent (for specimen S6-LI-D4-P30) were both tensile and both occurred outside the dent area.
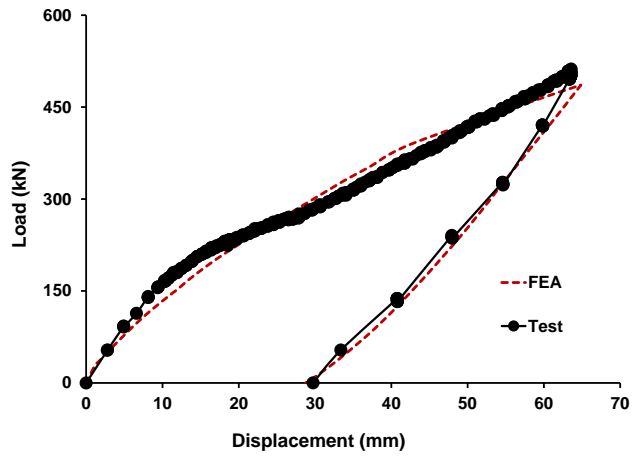
a) Specimen S2
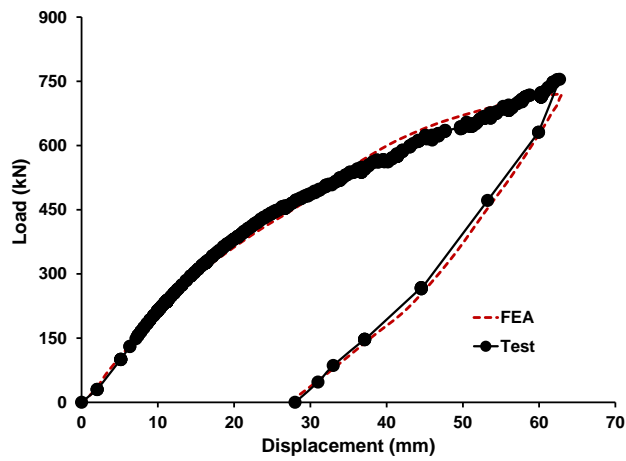


b) Specimen S6

**Figure 2.8: Comparison between experimental and numerical load-deformation behaviours**
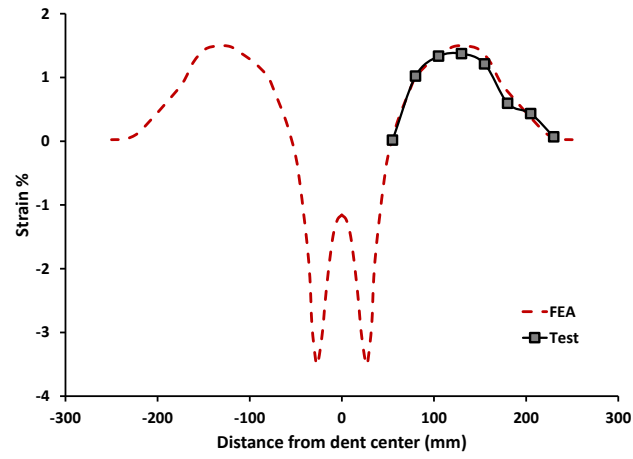
**a) Circumferential strains**
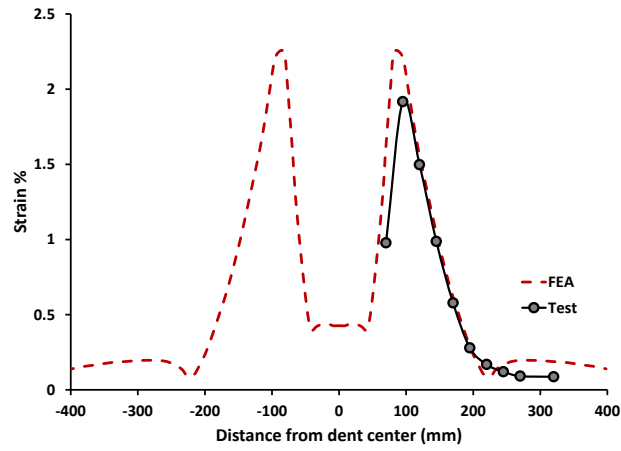


**b) Longitudinal strains**

**Figure 2.9: Comparison between experimental and numerical strain distributions for S2**
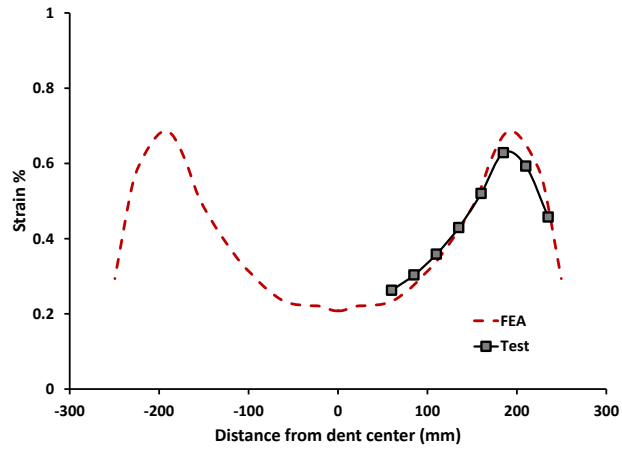
**a) Circumferential strains**
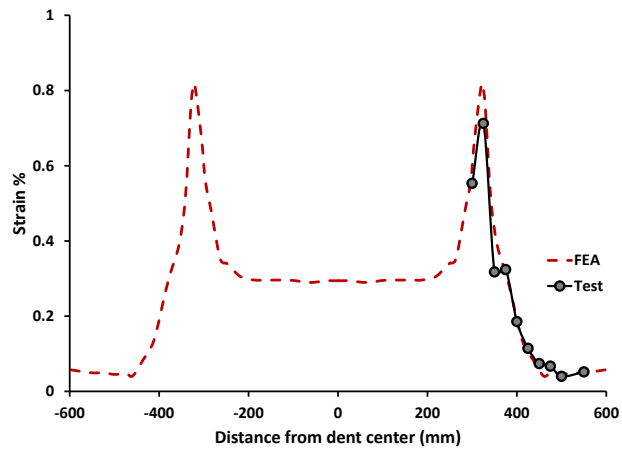


**b) Longitudinal strains**

**Figure 2.10: Comparison between experimental
and numerical strain distributions for S6**

**2.4.3 Parametric study**

Parametric study was undertaken to determine the effect of the D/t, operating (internal) pressure, dent depth, and shape of the indenter on the maximum strain of NPS30 X70 grade oil and gas pipe. Two shapes of indenter namely short and long were used in the parametric study. The short indenter simulates a sharp rock tip whereas the long shaped indenter simulates a relatively long rock tip.

Figure 2.11a shows the effect of two parameters: (i) level of internal (operating) pressure, p normalized by $p_y$ and (ii) dent depth, d normalized by outside diameter of the pipe, D on the maximum value of the compression strain in circumferential direction for NPS30 X70 steel pipe when load is applied using short indenter. It can be found from this figure that as the internal pressure increases the value of maximum strain increases. This is due to the fact that higher internal pressure results in larger re-rounding in the cross-section of the pipe and thus, causes more strain. It is worth noting that the strain values are reported in this figure are at unloaded condition in all specimens. The negative slopes in this figure is due to the fact that the strain values reported are negative or compressive since maximum strain was found to be compressive. Figure 2.11a also shows that as the dent depth-to-diameter ratio (d/D) increases the value of maximum strain increases as well. Figure 2.11b shows the effect of the same parameters on the maximum value of the tensile strain in longitudinal direction for NPS30 X70 steel pipe. Unlike circumferential direction, all the maximum strains are tensile in the longitudinal direction. This figure shows, as the level of internal pressure increases the maximum value of strain increases. Similar to Figure 2.11a, as the depth-to-diameter ratio (d/D) increases the value of maximum longitudinal strain increases as well as shown in Figure 2.11b.
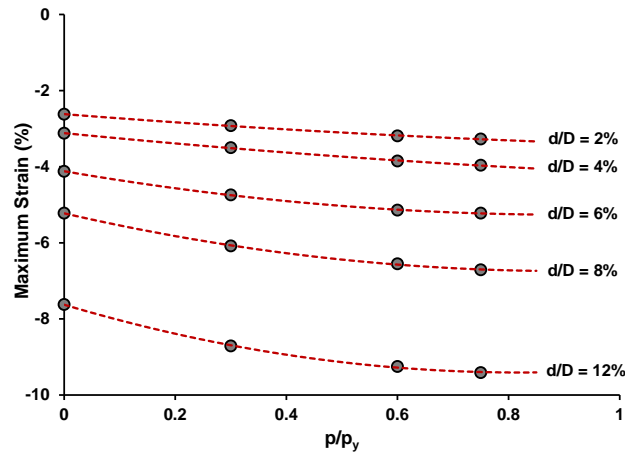
**a) Circumferential strains**
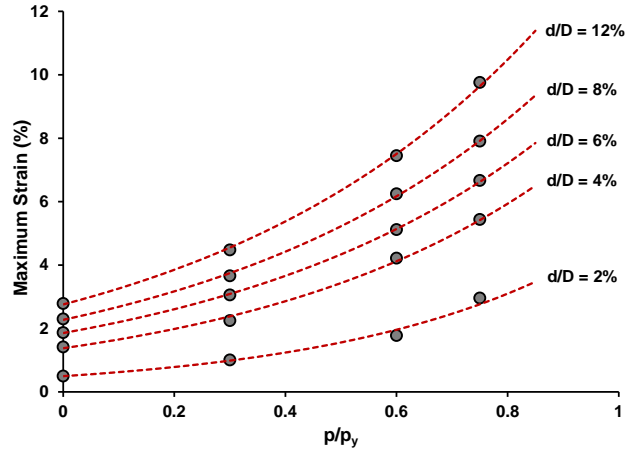


**b) Longitudinal strains**

**Figure 2.11: Effect of d/D and internal pressure on
maximum strain for short indenter**

Figure 2.12 shows the effect of the same parameters: (i) level of internal (operating) pressure and (ii) dent depth on the maximum value of the strain for the same steel pipe when load is applied using the longer indenter. Figures 2.12a and 2.12b show the effect of these two parameters on the maximum value of the strain in circumferential and longitudinal directions, respectively. It can be found that the effect of the two parameters on maximum strain are similar to those found from specimens loaded with short indenter.

However, for this specimen, the strains in the circumferential direction are tensile and the values of maximum strain for a specific internal pressure and same dent depth-to-diameter ratio (d/D) are much smaller when the specimen was loaded with long indenter. This is because short indenter caused more stress and strain concentrations around the dented area.
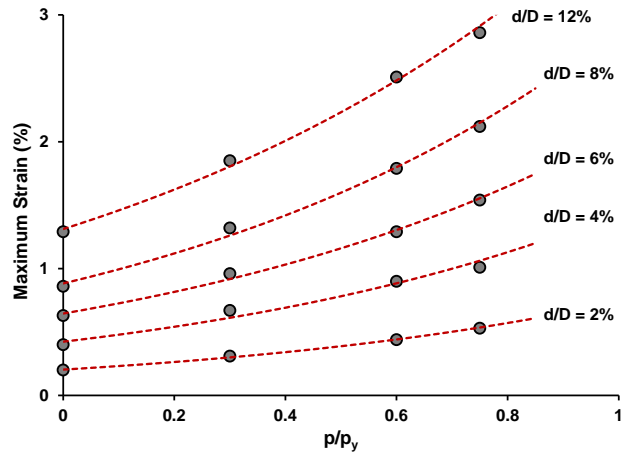


a) Circumferential strains
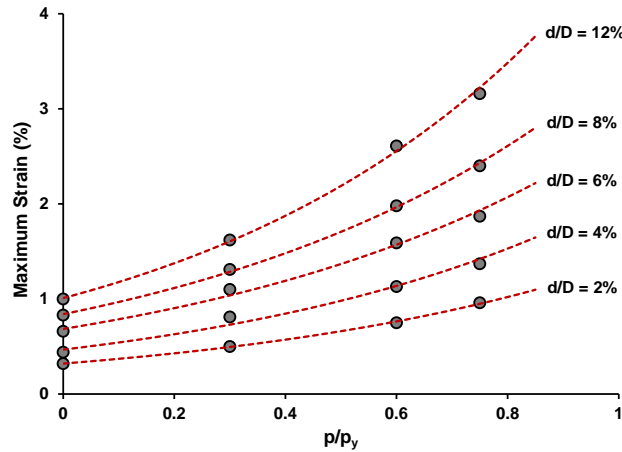


b) Longitudinal strains

**Figure 2.12: Effect of d/D and internal pressure on maximum strain for long indenter**

It is interesting to note that in the maximum allowable dent depth of 6% recommended by ASME B31.4 and CSA Z662 [7, 8] the pipeline which was loaded using short indenter exhibited much higher strain values than the pipe loaded with long indenter.

As an example, pipe with dent depth of 6% and internal pressure of $0.75p_y$. The maximum tensile longitudinal strain for longer dent shape was 1.87%, however, for the shorter dent, the maximum tensile strain in same direction was 6.67%. It is evident that for pipes with the dent depth of 6% or higher when load was applied using short indenter maximum value of strain is three time larger than maximum value of strain in the pipe with same dent depth but dented with the long indenter. Hence, this study found that the use of dent depth as the sole criterion for assessing the severity of a dent can be misleading and can result in unnecessary costly excavation and repair of many dents in the field which otherwise may not necessarily be harmful to the structural and operational integrity of the pipeline. On the other hand, it is also possible that a long dent may not be a threat to the structural integrity of the pipeline even if the dent depth is higher than 6%.

## 2.5 CONCLUSIONS

The following conclusions are made based on the tests and finite element analyses presented in this paper. Hence, the conclusions are limited to the findings associated with specific test specimens and finite element analyses presented in this paper.

1. All three parameters: level of internal or operating pressure, dent depth in pipe wall, and dent shape and length affect the maximum strain value and possibly its location as well.

2. Parametric study shows that as the internal pressure increases the maximum strain increases in both circumferential and longitudinal directions and this trend was found for both indenters.

3. The effect of indenter shape and length chosen in experimental program has significant effect on the value and location of maximum strain. Two different shapes

42

for the indenter used in the parametric study showed that a short indenter results in much higher strain values than the long indenter.

4. Maximum strain value increases as the d/D increases. However, the slope of trend is less when load is applied using long indenter.

5. Evaluation of severity of a dented pipeline solely based on dent depth is not appropriate. Rather, critical strain values must be included in the dent assessment criteria.

## 2.6 ACKNOWLEDGMENTS

## 2.7 REFERENCES

[1] Smith, R. B., and Gideon, D. N., 1979, "STATISTICAL ANALYSIS OF DOT-OPSO DATA," Proceedings, Annual Symposium - Society of Flight Test Engineers, pp. D. 1-D. 9.

[2] Wang, K., and Smith, E., 1982, The Effect of Mechanical Damage on Fracture Initiation in Line Pipe, Part I: Dents, Energy, Mines and Resources Canada, Canada Centre for Mineral and Energy Technology.

[3] Zarea, M. F., Toumbas, D. N., Philibert, C. E., and Deo, I., "Numerical models for static denting and dynamic puncture of gas transmission linepipe and their validation," Proc. Proceedings of the 1996 1st International Pipeline Conference, IPC. Part 2 (of 2), June 9, 1996 - June 13, 1996, ASME, pp. 777-784.

[4] Lancaster, E. R., 1996, "Burst pressures of pipes containing dents and gouges," Proceedings of the Institution of Mechanical Engineers, Part E: Journal of Process Mechanical Engineering, 210(1), pp. 19-27.

[5] Gresnigt, A. M., Karamanos, S. A., and Andreadakis, K. P., 2007, "Lateral loading of internally pressurized steel pipes," Transactions of the ASME.Journal of Pressure Vessel Technology, 129(4), pp. 630-638.

[6] Cosham, A., and Hopkins, P., 2004, "The effect of dents in pipelines-guidance in the pipeline defect assessment manual," International Journal of Pressure Vessels and Piping, 81(2), pp. 127-139.

[7] ASME, 2012, "B31.4: Pipeline Transportation Systems for Liquids and Slurries," ASME International, New York, NY, USA.

[8] CSA, 2007, "Z662-07: Oil and gas pipeline systems," Canadian Standard Association, Mississauga, ON, Canada.

[9] Gao, M., McNealy, R., Krishnamurthy, R., and Colquhoun, I., "Strain-Based Models for Dent Assessment: A Review," Proc. 2008 7th International Pipeline Conference, American Society of Mechanical Engineers, pp. 823-830.

[10] Baker, M., 2004, "Department of Transportation, Office of Pipeline Safety, TTO Number 10, Integrity management program–dent study," Delivery Order DTRS56-02-D-70036, final report.

[11] API, 2012, "Spec 5L: Specification for Line Pipe," American Petroleum Institute, Washington, DC, USA.

[12] ASTM, 2011, "E8/E8M-11: Standard Test Methods for Tension Testing of Metallic Materials," ASTM International West Conshohocken, Pennsylvania, USA.

[13] SIMULIA, 2011, Analysis User's Manuals, Dassault Systèmes Simulia Corp., Rising Sun Mills, Providence,  RI, USA.

# CHAPTER 3

# EFFECT OF CONCENTRATED LOAD ON OVALIZATION IN BURIED OIL AND GAS PIPELINE

## 3.1 INTRODUCTION

Despite many research and post-failure investigations on buried pipelines have been completed, external interference is still remains as the main cause of failure in oil and gas pipeline [1, 2]. External interference may cause surface defects such as dent, ovalization, puncture, gouge, and/or their combinations in pipelines. These defects, often called mechanical damages, may form as a result of contact with foreign objects such as a rock tip or impact from excavating equipment. It has been reported that the failure of oil and gas transmission pipelines resulting from mechanical damages ranges from 55% in the USA to around 70% in Europe [3-6]. A buried linepipe when resting on a rock tip or hard surface is subjected to concentrated load due to the overburden soil above the linepipe and hence, the section of the pipeline may experience plastic inward deformation known as dent and associated cross-sectional distortion known as ovalization or out-of-roundness [2] (Figure 3.1). Literature review found that several research projects were completed to study the behaviour of dent and its threat to the structural integrity of buried pipelines. Therefore, current design standards recommend the safe limit for a dent in terms of its permanent depth and strain values [7, 8]. A study was undertaken by Yeh and Kyriakides [9, 10] to determine the effect of ovalization on the collapse pressure of offshore pipeline. However, this study did not investigate how concentrated load affects the ovalization. Current pipeline design standards provide generic recommendations on ovalization limits resulting

45

from bending in pipeline and the limit value of ovalization recommended in these standards ranges from 2.5% to 3% [11-13]. Hence, the literature review did not find any previous research that was undertaken to study how a concentrated load resulting from a rock or others affect the cross-sectional distortion or ovalization of buried linepipe. However, Bai and Bai [14] based on their experience recommended a maximum allowable accumulated ovalization of 4% over the service life of the pipeline.
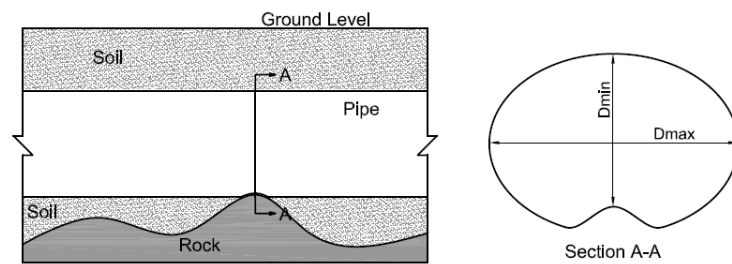


**Figure 3.1: Schematic of a section of buried pipe resting on a rock tip**

Figure 3.1 shows a schematic of a part of a buried linepipe resting on a tip of a rock. The overburden soil creates reaction force at the rock tip resulting in a concentrated load on the pipe wall. This concentrated load may create plastic deformation and associated ovalization. The ovalization of the pipe, $f_o$ is determined using the minimum and maximum pipe outer diameters, $D_{min}$ and $D_{max}$ as shown in Equation (1) and Figure 3.1 and this is measured at different positions around pipe circumference at a specific cross section [13, 14].

$$f_o = \frac{D_{max} - D_{min}}{D} \qquad (1)$$

The present study was designed to undertake the effect of concentrated load on the ovalization of NPS30 X70 [15] grade steel pipe used in oil and gas transmission. Both full-

scale tests and numerical analyses using finite element (FE) method were undertaken in this study. This paper discusses the test method, FE modeling used, and results obtained from this study.

## 3.2 EXPERIMENTAL PROCEDURE

### 3.2.1 Test specimen

This study was completed using both laboratory based full-scale tests and non-linear finite element analyses (FEA). NPS 30 X70 steel pipe [15] used in oil and gas onshore pipelines was used to prepare the test specimens. Six full-scale laboratory tests were completed to determine ovalization in the pipes cross section when subjected to concentrate load. Table 3.1 shows the matrix of the tests specimens used in this study. Specimens were named to reflect the primary attributes attached to each specimen. For example, specimen S2-SP-D4-P30, the first letter and number combination (S2) indicates that it is specimen number 2, the next two letters (SP) indicates that the specimen was loaded with short (square) loading plate, the next letter and number combination (D4) indicates that the inward permanent depth in the pipe wall due to loading in this specimen was 4% (~30 mm) of the diameter of the pipe, and the last combination of letter and number (P30) indicates that the internal pressure was held constant at $0.3p_y$ or 30% of $p_y$ which is about 3.8 MPa (550 psi). Hence, the specimen S6-LP-D4-P30 was the sixth and last specimen and this specimen was identical to specimen S2-SP-D4-P30 except the earlier one was loaded with long (canoe shaped) loading plate. The first specimen in Table 3.1, S1-SP-D4-P00 is considered as the reference specimen while considering the effect of internal pressure (no pressure, 3.8 MPa (550 psi), and 7.6 MPa (1100 psi), permanent dent

47

depth (2%, 4%, and 6% of diameter of pipe), and loading plate type (short and long) are evaluated.

The nominal pipe diameter (D) is 762 mm (30 in) and wall thickness (t) is 8.5 mm (0.33 in). Hence, all pipes had diameter-to-thickness ratio of approximately 90 (D/t ≈ 90). The length of the each pipe specimen was 2000 mm (78.74 in). Two ends of the specimen were welded to thick hemispherical steel end caps for the application of internal pressure during application of concentrated load. Water was used as the fluid in the test specimens. A number of tensile coupon specimens were cut from a virgin pipe section in its longitudinal direction and the standard material tensile test was carried out to determine the mechanical properties of the pipe material in accordance with ASTM E8 [16]. According to tensile tests, the actual yield strength ($\sigma_y$) of pipes material was found to be 543 MPa at 5% total strain; ultimate tensile strength ($\sigma_u$) was found to be 624 MPa; and modulus of elasticity (E) was determined at 204 GPa. Hence, the pressure required to yield the pipe material or yield pressure ($p_y$) was calculated at 12.7 MPa (1837 psi).

As can be found from Table 3.1, the parameters which were varied in the experimental work are: operating pressure (internal pressure during loading), permanent depth (plastic inward deformation) due to application of concentrated load, and the type of loading plate (square shaped or short and canoe shaped or long). The size and shape of loading plate was varied to simulate various shapes of the rock tip on which a section of buried linepipe may rest. The short loading plate simulates a tip of narrow rock whereas, the long loading plate simulates a relatively longer rock tip of a rock. Two different shapes and lengths of loading as shown in Figure 3.2 were used to apply concentrated load on the pipe wall. The length and width of the short loading plate were 100 mm and 50 mm,

respectively. The canoe shaped or long loading plate was 500 mm long and width at the

bottom part was 35 mm with gentle radius in all directions. The internal pressure was varied

from 0 to 7.6 MPa (0 to 1100 psi) which corresponds to 0% to 60% of the yield pressure

($p_y$) or 0 to $0.6p_y$ pressure to simulate various sections of a buried pipeline located at various

distances in the downstream.

**Table 3.1: Test matrix**

| Specimen name | Loading plate length (Type) | Plastic deformation (% of diameter) | Internal pressure during loading (% of $p_y$)* | Parameter |
|---|---|---|---|---|
| S1-SP-D4-P00 | 100 mm (short) | 30 mm (4%) | 0 MPa (0%) | Reference specimen |
| S2-SP-D4-P30 | 100 mm (short) | 30 mm (4%) | 3.8 MPa (30%) | Internal pressure |
| S3-SP-D4-P60 | 100 mm (short) | 30 mm (4%) | 7.6 MPa (60%) | |
| S4-SP-D2-P00 | 100 mm (short) | 15 mm (2%) | 0 MPa (0%) | Permanent deformation depth |
| S5-SP-D6-P00 | 100 mm (short) | 46 mm (6%) | 0 MPa (0%) | |
| S6-LP-D4-P30 | 500 mm (long) | 30 mm (4%) | 550 MPa (30%) | Loading plate type |

* Pressure held constant during application of concentrated load

In the experimental work, the load was applied to the pipe wall through the steel

loading plate using displacement control method. The total deformation applied in these

test specimens varied from 37 mm to 71 mm. These values were chosen such that the total

permanent or plastic deformations as shown in Table 3.1 could be obtained.  This

deformation caused a dent in the pipe wall under the loading plate (Figure 3.2). Hence, the

application of concentrated load created dents of two different lengths and slight two

different shapes.

| a) Short loading plate | b) Long loading plate |

**Figure 3.2: Two different loading plates used to apply concentrate load**

### 3.2.2 Test setup and instrumentation

The purpose of these tests was to study resulting ovalization in the pipe cross section due to application of stroke or displacement controlled concentrated load. Figure 3.3 schematically shows the test setup. The pipe specimen was placed on three T-shaped rigid steel supports. On the middle support, a steel was used to hold the specimen in place. Between the collar and pipe, a piece of rubber was placed in order to prevent sliding. Monotonically increasing displacement controlled load was applied on the top surface of the pipe wall through the steel loading plate using a universal loading actuator. The actuator and the loading plate was placed at the mid-length of the pipe (Figure 3.3). Figure 3.4 shows a photo of the test setup.
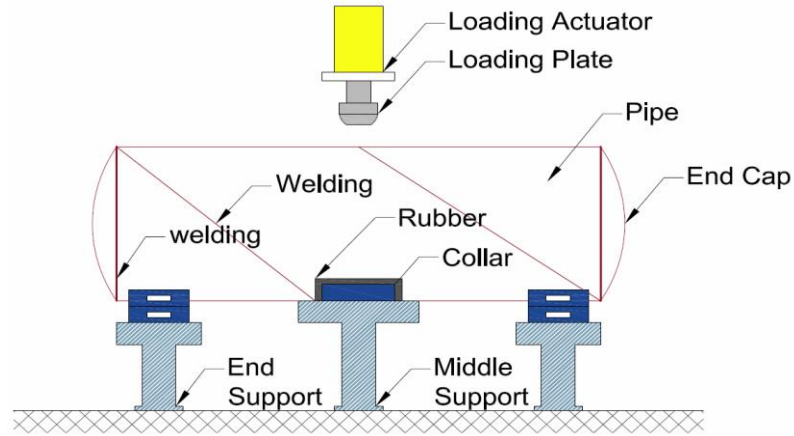
**Figure 3.3: Schematic of test setup**

The total and plastic deformations of the pipe due to application of concentrated load were controlled and measured using a linear variable differential transformers (LVDT). This LVDT was mounted with the actuator to measure the vertical displacements during loading and unloading. Another six LVDTs were mounted around the pipe circumference and perpendicular to the pipe surface to measure ovalization as shown in Figures 3.4, 3.5a, and 3.5b.



**Figure 3.4: Photo of test setup**

Hemispherical steel end caps were welded to the ends of each specimen to be able to apply internal pressure using water. A hydrostatic pump was used to apply the internal water pressure. Internal pressure was controlled and pressure data was acquired using a pressure transducer. Internal pressure during loading was varied in the specimens (Table 3.1). Though the primary objective of the study was to determine ovalization, pipe specimens were also instrumented with strain gauges to monitor and acquire the variations of strain data around the loading area and along the length of the pipe (Figure 3.6). Hence, ten strain gauges were installed in this line.



a) Schematic          b) Photo
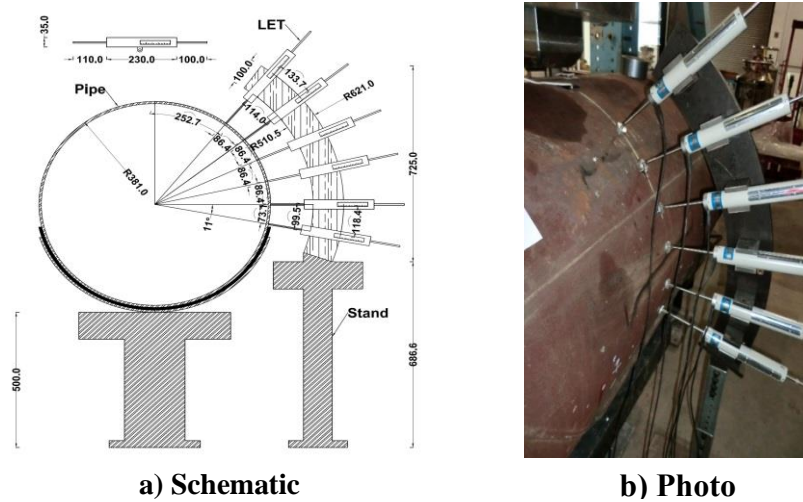
**Figure 3.5: Six LVDT's around the pipe**
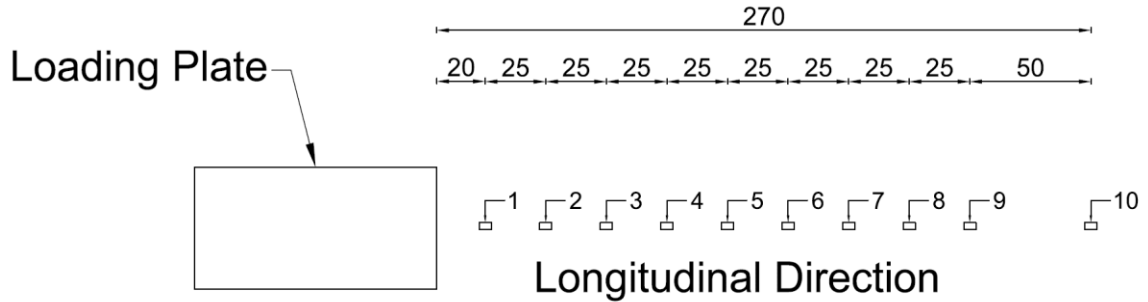
**Figure 3.6: Strain gauges layout**

## 3.3 TEST RESULTS

### 3.3.1 Load-deformation behaviour

For specimens S1, S2, S3, S4, and S5, the concentrate load was applied using the short (rectangular) loading plate while long (canoe) loading plate was used for the application of concentrated load on specimen S6 (Table 3.1). The load-deformation behaviours of these specimens are shown in Figures 3.7a to 3.7c.

Figure 3.7a shows the load-deformation for three specimens, S1-SP-D4-P00, S2-SP-D4-P30, and S3-SP-D4-P60. These three specimens were identical except the internal pressure during application of concentrated load was different and it ranged from no pressure to $0.6p_y$. This figure shows that as in the operating (internal) pressure of linepipe increases the maximum load increases as well. Also, as the operating pressure (internal) pressure increases the total displacement required to produce same permanent deformation depth (4%) increase as well. The maximum load required for these three specimens were 183 kN, 497 kN, and 812 kN, respectively. The total deformation required in these three specimen were 71 mm, 64 mm, and 49 mm respectively.

Figure 3.7b shows load-deformation behaviour of specimens S4-SP-D2-P00, S1-SP-D4-P00, and S5-SP-D6-P00. These three specimens had no internal pressure during application of the concentrated load and they were loaded with same short loading plate. The difference in these specimens was the permanent deformation depth due to application of the concentrated load which varied from 6% to 2%. From this figure it can be found that as the permanent depth reduces the maximum load and total deformation reduce as well.

Figure 3.7c shows load-deformation behaviour of specimens S2-SP-D4-P30 and S6-LP-D4-P30. The only difference between these two specimens was the length and shape of the loading plate. For specimen S2-SP-D4-P30, the length was short and shape was rectangular whereas, the shape and length of loading plate for S6-LP-D4-P30 were canoe and relatively long. This figure shows that longer loading plate required much higher load than the shorter loading plate and the maximum load values for these two specimens were 755 kN and 497 kN, respectively. However, total deformation required during application of concentrated load was about 64 mm for both specimens. Hence, this figure shows that shape of and length of rock tip may be an important factor if the load applied on the buried linepipe is in load control mode. However, the shape and length of rock tip is irrelevant if the concentrated load is applied in displacement control mode.
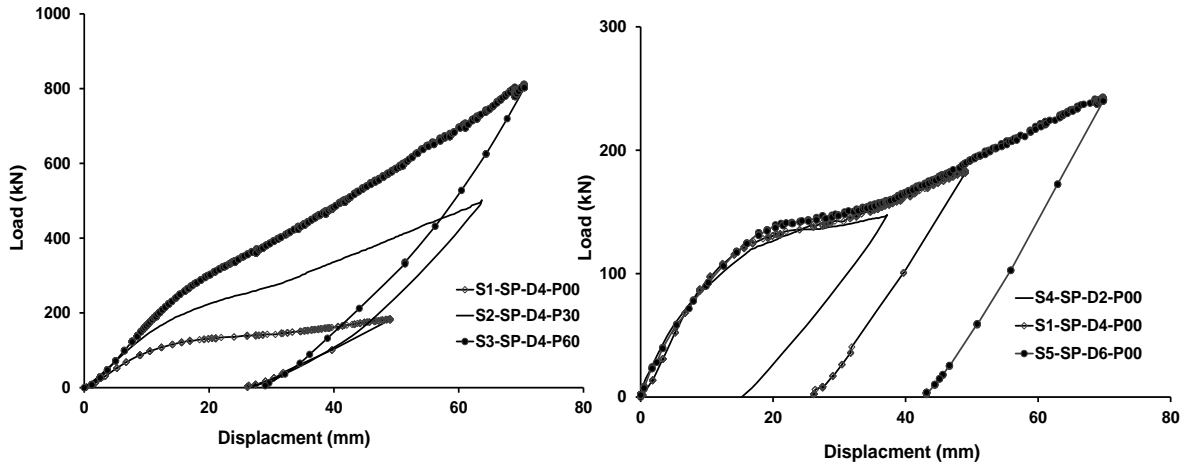
a) Specimens S1, S2, and S3          b) Specimens S1, S4, and S5
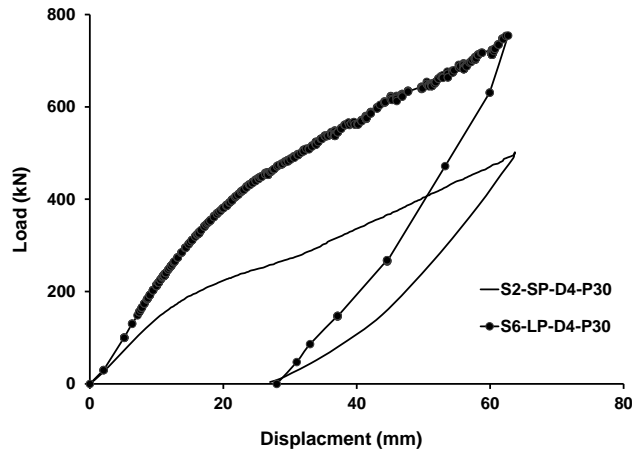


c) Specimens S2 and S6

**Figure 3.7: Load-deformation behaviours**

## 3.3.2 Strain distributions

Only strain gauges along the mid-width of the loading area and along the length of pipe specimens were installed to study if the strain distribution along that line varies during application of concentrated load. Figures 3.8a to 3.8c show the effect of various parameters (Table 3.1) on the strain distribution. It can be observed that the pattern of strain distribution, value of maximum strain, and location of maximum strain change when

operating (internal) pressure, permanent depth caused by loading, and shape of rock tip (shape of loading plate) change. This study did not focus on the detailed behaviour of strain distributions in and around the loading area. However, based on the outcome of this study it is recommended that a detailed study needs to be undertaken to understand the strain distributions along various axes and in and around the loading area in the future to be able to conclude the effect of these parameters on strain and stress concentrations in berried linepipe.

**a) Specimens S1, S2, and S3**

**b) Specimens S4, S1, and S5**

**c) Specimens S1 and S6**
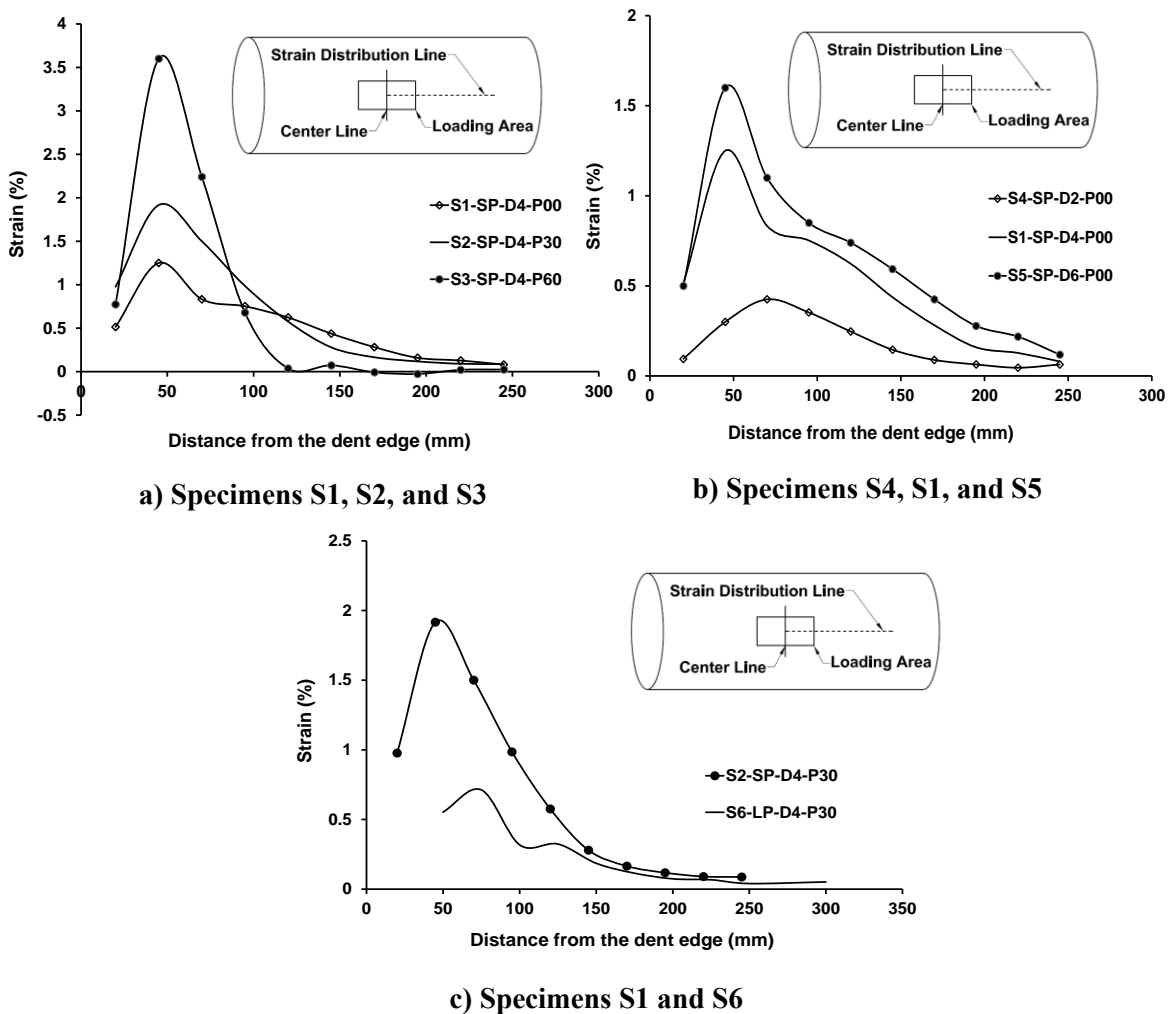
**Figure 3.8: Strain distributions for strain in axial direction**

### 3.3.3 Ovalization

As recommended by Bai and Bai [14], the allowable limit of accumulated ovalization in an oil and gas buried pipe subjected to a concentrate load is 4%. The value of ovalization in this study was calculated after unloading the specimens and hence, the ovalization values reported in this paper are at total plastic deformation level which the specimen experienced. The minimum diameter, $D_{min}$ was located exactly under loading area as it can be observed in Figures 3.1 and 3.9. However, the maximum diameter of the pipe was found away from the location of the loading point. It can be found from Figures 3.10a to 3.10c, location and value of $D_{max}$ varied depending on the internal pressure, total depth caused by loading, and shape of the loading plate.

Ovalization calculated using Equation (1) for all the specimens are shown in Table 3.2. From Figure 3.10a and Table 3.2, it is found that as the internal pressure increased from $0.0p_y$ to $0.6p_y$, the value of maximum ovalization increased from 3.9% to 6.9% and hence, the increase of ovalization is 3%. Similarly, as the value of total plastic deformation increased from 15 mm to 46 mm the value of maximum ovalization increased from 2.1% to 7.1% (Figure 3.10b). The change in maximum ovalization between specimens with 2% and 4% plastic deformations is only about 1.8% whereas, the increase in maximum ovalization from 4% to 6% plastic deformation is about 3.2% which is significant. It should be noted that no internal pressure was applied when deformation depth was varied. The effect of the length and shape of the loading plate used in the experimental work was found to be insignificant and the long loading plate resulted in a marginally higher ovalization and the difference is only about 0.5% (Figure 3.10c). The test results found the maximum

value of ovalization was 7.1% which is much higher than the 4% limit recommended by

Bai and Bai [14].
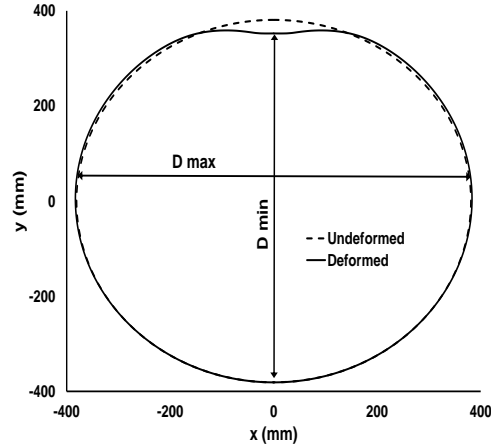


**Figure 3.9: Deformed and un-deformed cross sections of a pipe**

**Table 3.2: Maximum ovalization obtained from test specimens**

| Specimen name | Loading plate length (Type) | Plastic deformation (% of diameter) | Internal pressure during loading (% of $p_y$) | Ovalization (%) | Parameter |
|---|---|---|---|---|---|
| S1-SP-D4-P00 | 100 mm (short) | 30 mm (4%) | 0 MPa (0%) | 3.9 | Reference specimen |
| S2-SP-D4-P30 | | | 3.8 MPa (30%) | 5.7 | Internal pressure |
| S3-SP-D4-P60 | | | 7.6 MPa (60%) | 6.9 | |
| S4-SP-D2-P00 | 100 mm (short) | 15 mm (2%) | 0 MPa (0%) | 2.1 | Deformation depth |
| S5-SP-D6-P00 | | 46 mm (6%) | | 7.1 | |
| S6-LP-D4-P30 | 500 mm (long) | 30 mm (4%) | 3.8 MPa (30%) | 6.2 | Loading plate type |

a) Effect of internal pressure

b) Effect of plastic deformation

c) Effect of loading plate size
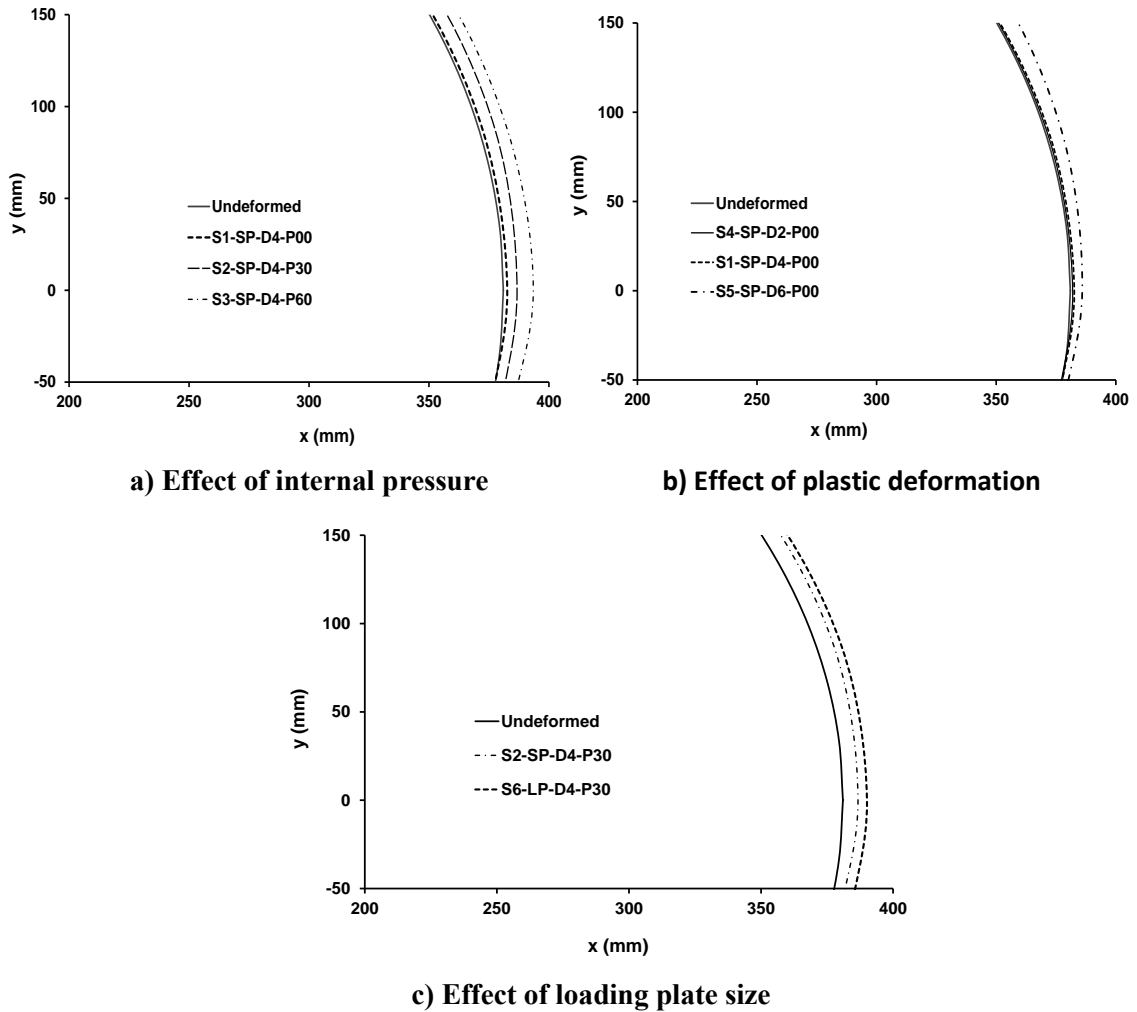
**Figure 3.10: Cross sectional distortion measured from various tests**
.

## 3.4 FINITE ELEMENT ANALYSIS AND PARAMERIC STUDY

Experimental testing is the most conventional and reliable way to study the behaviour of any structural component including pipe while subjected to concentrated load and/or other loads. However, it is impossible to obtain all the information required for a thorough understanding from the experimental data. Experimental testing is also expensive and time consuming. Hence, it is not viable to consider full-scale tests for a wide range of test parameters. An alternative method to study and predict the behaviour of such

specimens is to use numerical tools such as finite element analysis (FEA) method. In this study, numerical modeling technique considering both material and geometric nonlinearity was employed to simulate the behaviour of the test specimens. Commercially available general purpose finite element analysis code, ABAQUS/Standard distributed by SIMULIA [17] was used to model the pipe behaviour. It is often argued that load created by geotechnical causes can be either load control or displacement control. However, no general coconscious can be found on this. Hence, in the numerical study the concentrated load was applied using both load control and displacement control methods. The objective of developing the finite element model was to determine the ovalization of the NPS30 X70 grade pipe used in this study when subjected to both load controlled and displacement controlled concentrated load with various internal (operating) pressures, various permanent (dent) depths, and various diameter-to-thickness ratios.

One half-length of the full pipe was modeled to avail the opportunity of symmetry in the pipe geometry, loading, and boundary conditions, which saved computational effort. Full-length specimen of this pipe was also modeled and analyzed. However, the results were found to be identical from both full- and half-length models. Displacement boundary conditions were applied on the circumferential planes of the symmetry (z-plane). A 10-node quadratic (second order) tetrahedron solid element, C3D10, was used in and around the load application area where stress concentration was expected to be high. For the rest of the pipe, 8-node linear brick element with reduced integration was used. Each node of these elements has three translational degrees of freedom: u1, u2, and u3. The directions 1, 2, and 3 correspond to x, y, and z axes as shown in Figure 3.11. The u1 represents translation degree-of-freedom in x direction. This reduced number of integration points

increases computational efficiency and generally yields more accurate results than the corresponding fully integrated elements. Loading plate was modelled as discrete rigid body using the 4-node rigid quadrilateral elements, R3D4 to avoid any deformation in loading plate and supports. In the tests, the loading plates were at least 75 mm thick and hence, they were almost rigid if compared with the pipe wall. Figure 3.11 shows a typical meshed pipe.
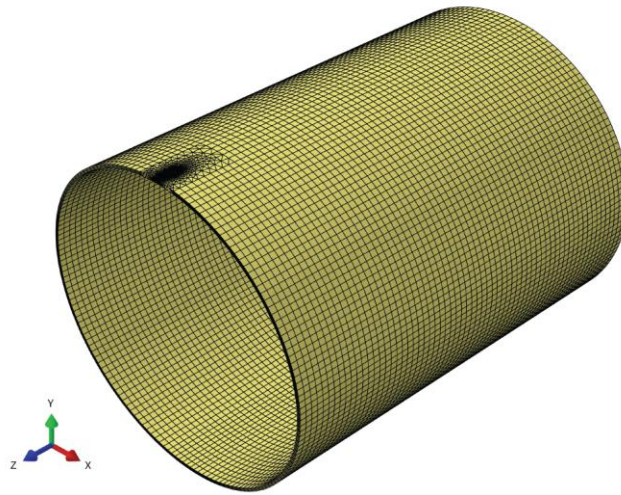


**Figure 3.11: FE model for half pipe with meshing scheme**

Mesh convergence studies were performed to obtain adequately refined finite element sizes. Minimum of four layers of element were used through the pipe wall thickness. The shape and geometric dimensions of the loading plate in finite element (FE) models were similar to those used in the tests as shown in Figure 3.11. The parameters chosen in the FEA based parametric study are: (1) D/t which was varied from 50 to 90 at an increment of 10, and (2) internal pressure which was varied during application of concentrated load. The internal pressures chosen were: 0, 3.8 MPa, 7.6 MPa, and 9.6 MPa

or $0p_y$, $0.3p_y$, $0.6p_y$, $0.8p_y$ (Table 3.3). In addition, the load in FE models was applied using both load controlled method and also displacement controlled method.

A surface-to-node contact with a hard contact algorithm was defined between the rectangular loading plate and the pipe wall surface during the loading process. Since the loading plate simulated as discreet rigid body, master surface allocated at the outer surface of that and the outside surface of the pipe was assigned as a slave surface in the contact algorithm. The internal (operating) pressure was applied to the inner surface of the pipe wall. This internal pressure was applied as a distributed load. In the full-scale tests, end caps were used at both ends of the pipe specimen to hold the water and to apply internal pressure. In the FEA model, these caps were modeled as elastic-plastic steel with modulus of elasticity of 204 GPa.

Supports conditions and dimensions were chosen in the FE models to simulate similar conditions to the test specimens. Extremely rigid steel supports were used in the tests and hence, they did not experience any measurable deformation. Therefore, these deformations, if any, were ignored in the FE models. Actual dimensions were used to model these supports. A surface-to-node contact algorithm was used to simulate contact and possible movement between supports and pipe wall.

Three tension coupon specimens from the pipe wall were prepared and tested to obtain the engineering or nominal stress-strain behaviour of the pipe material. Figure 3.12 shows the stress-strain curve. As can be found from this figure, point U is the ultimate or maximum stress point. The nominal values of fracture stress and fracture strain were determined after the completion of the material tests and the point F corresponding to the fracture nominal stress and fracture nominal strain. True elastic-plastic material model using von-Mises

yield criterion and isotropic hardening with associated plastic flow rule was used in the FE models.
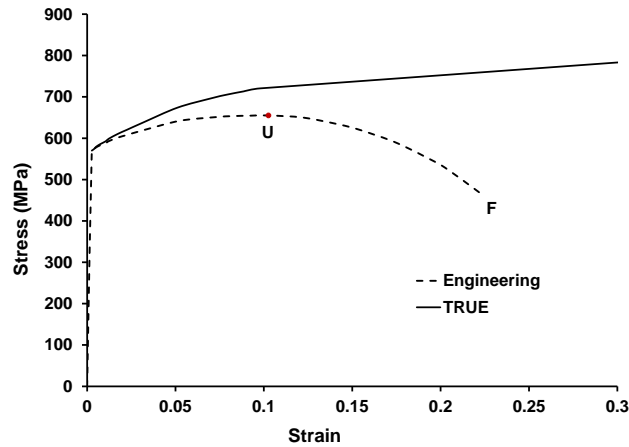


**Figure 3.12: Stress-strain relationship for pipe material**

### 3.4.1 FE model validation

The finite element (FE) models were validated using the load-deformation behaviour and ovalization data obtained from the full-scale tests. The comparison of the load-deformation relationships for specimens S2-SP-D4-P30 and S3-SP-D4-P60 between test and finite element analyses are shown in Figures 3.13a and 3.13b, respectively. A good agreement between the test and numerical behaviours is observed. The circumferential deformations indicating ovalization for specimens S2-SP-D4-P30 and S3-SP-D4-P60 obtained from the test and FEA are shown in Figures 3.14a and 3.14b, respectively. In these figures, the distance on the x-axis and y-axis were measured from center of the pipe cross-section which is also the center of load application area (Figure 3.9). These figures also show a good agreement between the test and FEA.

**a) Specimen S2-SP-D4-P30**  **b) Specimen S3-SP-D4-P60**
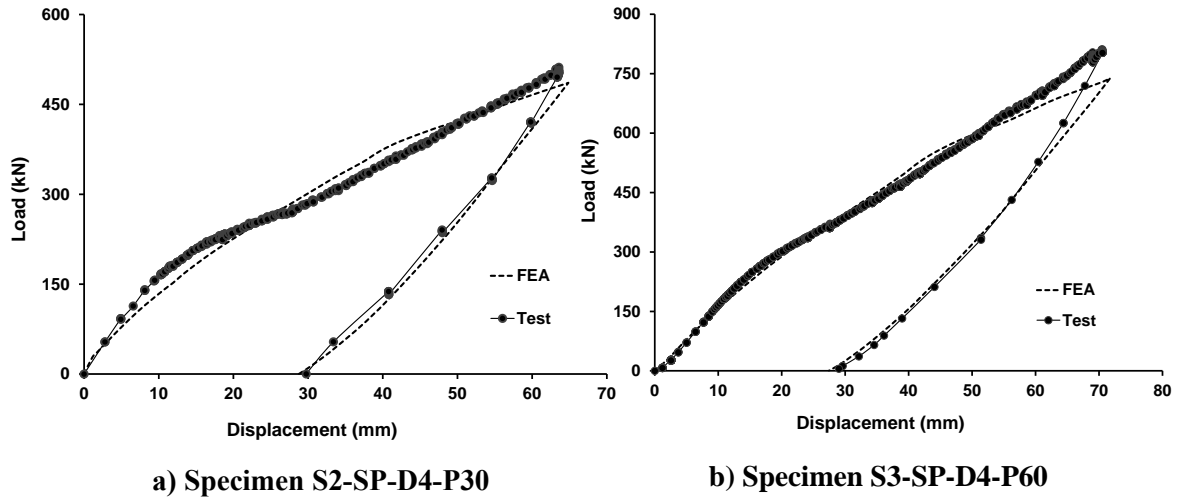
**Figure 3.13: Comparison of load-deformation behaviour for specimens S2 and S3**



**a) Specimen S2-SP-D4-P30**  **b) Specimen S3-SP-D4-P60**
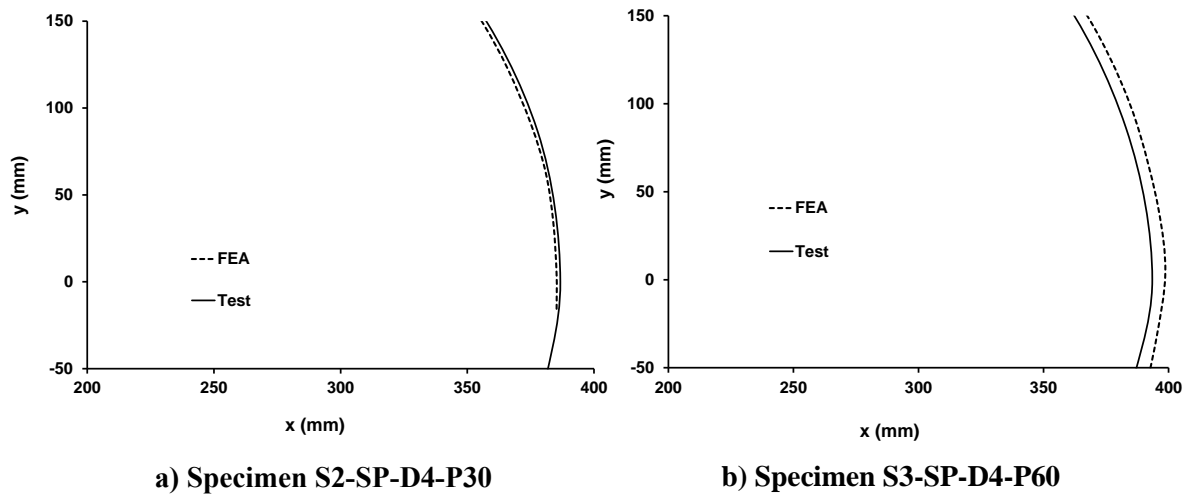
**Figure 3.14: Comparison of Cross sectional distortion for specimens S2 and S3**

The longitudinal strain distributions around the loading area for specimens S2-SP-D4-P30 and S3-SP-D4-P60 obtained from the test and FEA are shown in Figures 15a and 15b. The experimental strain data were acquired from the strain gauges located on a longitudinal line drawn through the centerline of the loading area (Figures 6). In Figure 15,

64

the distance on the x-axis was measured from the center of the loading area on the pipe. This figures also shows a good agreement in between the test and FEA. Similar correlations between test and FEA for longitudinal strain distributions were also found for other specimens.



(a) Specimen S2-SP-D4-P30          (b) Specimen S3-SP-D4-P60
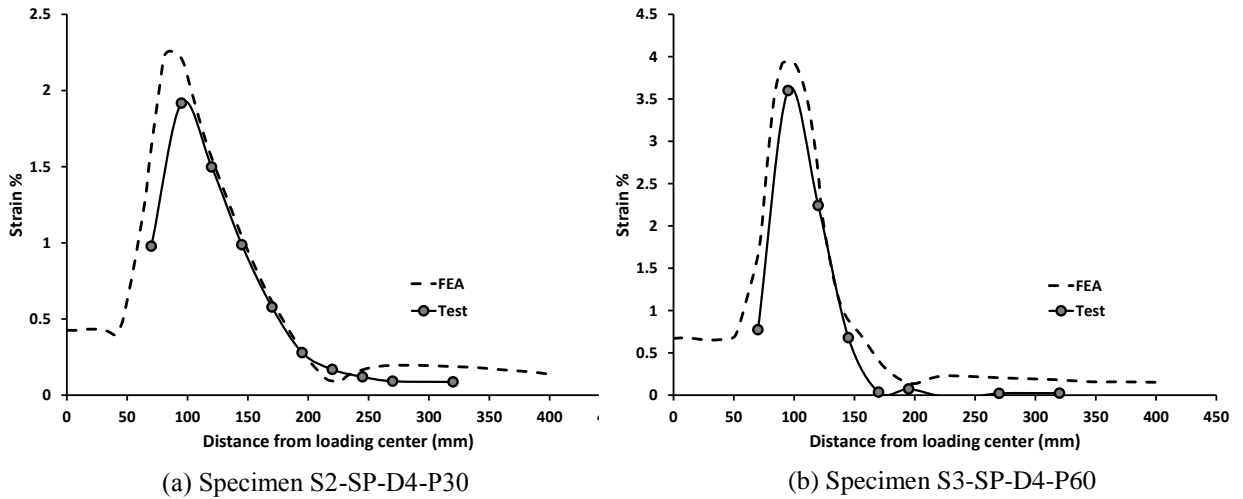
**Figure 3.15: Comparison of strain distribution for specimens S2 and S3**

### 3.4.2 Parametric study

Parametric study was undertaken to determine the effect of the D/t, operating (internal) pressure, and shape of the loading plate (rock) on the ovalization of NPS30 X70 grade oil and gas pipe (Table 3.3). In the experimental program, only displacement controlled concentrated load was applied. However, in the FEA based parametric study, the load was applied using both load and displacement control methods. As can be found from Table 3.3, total deformation or displacement applied in to parametric models for displacement control method is 65 mm and maximum load applied in the load control method was 800 kN. Total deformation of 65 mm was chosen since in the test specimens, total deformation ranged from 37 mm to 71 mm. The maximum load value of 800 kN was

chosen such that no FEA model collapses due to such load and thus, to avoid numerical instability in the FEA model. Two shapes of loading plates namely square and sphere were used in the parametric study (Figures 3.16a and 3.16b). The spherical shaped loading plate simulates a sharp rock tip whereas the rectangular shaped loading plate simulates a relatively wider rock tip.

**Table 3.3: Parameters and their ranges chosen**

| Parameters | Loading plate shape | | Load application method | | D/t | Internal pressure |
|---|---|---|---|---|---|---|
| Range | Rectangular | Sphere | Load control | Displacement control | 50 to 90 @ 10 | $0.0p_y$, $0.3p_y$, $0.6p_y$, $0.8p_y$ |
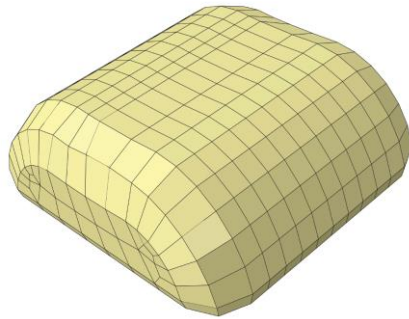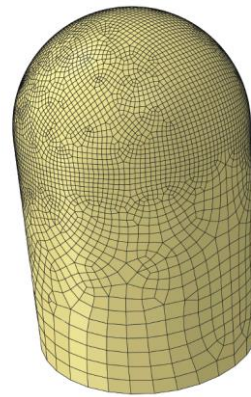


**a) Rectangular loading plate**      **b) Spherical loading plate**

**Figure 3.16: Loading plate shapes used in parametric study**

Figure 3.17 shows the effect of diameter-to-thickness ratio (D/t) on the maximum value of the ovalization for NPS30 X70 steel pipe when load is applied using square loading plate (Figure 16a). Figure 17a shows this effect when the load is applied using displacement or stroke control method. It can be found from this figure that as the diameter-to-thickness ratio (D/t) increases the value of maximum ovalization decreases. This is due to the fact that a higher D/t has thinner pipe wall and thus, experiences higher re-rounding

66

effect resulting in lesser ovalization. It is worth noting that the ovalization values are reported in this figure are at unloaded condition and the value of total deformation was kept unchanged at 65 mm in all specimens.

Figure 17b shows the effect of the same parameter on the maximum value of the ovalization for NPS30 X70 steel pipe [15] when load is applied using load control method. The maximum of 800 kN load was applied to all FE specimens. This figure shows that unlike displacement control method, as the diameter-to-thickness ratio (D/t) increases the value of maximum ovalization increases when load is applied using load control method. This is because of the fact that higher D/t means lower pipe wall thickness and hence, the pipe with higher D/t experiences higher total deformation at the maximum load of 800 kN resulting in higher ovalization.



**a) Displacement control method**          **b) Load control method**
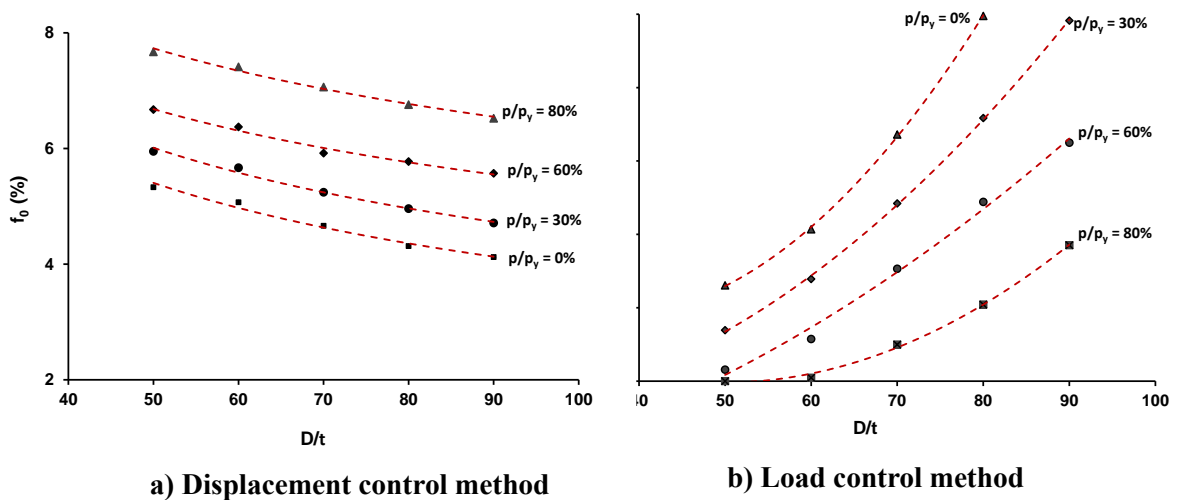
**Figure 3.17: Effect of D/t and internal pressure on maximum ovalization for square loading plate**

Figure 3.18 shows the effect of the diameter-to-thickness ratio (D/t) on the maximum value of the ovalization for the same steel pipe when load is applied using spherical loading plate (Figure 16b). Figures 18a and 18b show the effect of this parameter when load is applied

using displacement control and load control methods, respectively. It can be found that the effect of the D/t on ovalization are similar to those found from specimens loaded with rectangular plate. However, the values of maximum ovalization for a specific internal pressure and specific load is usually higher when the specimen is loaded with spherical loading plate in load control method. This is because spherical loading plate caused more stress and strain concentrations in and around the loading area.



a) Displacement control method

b) Load control method
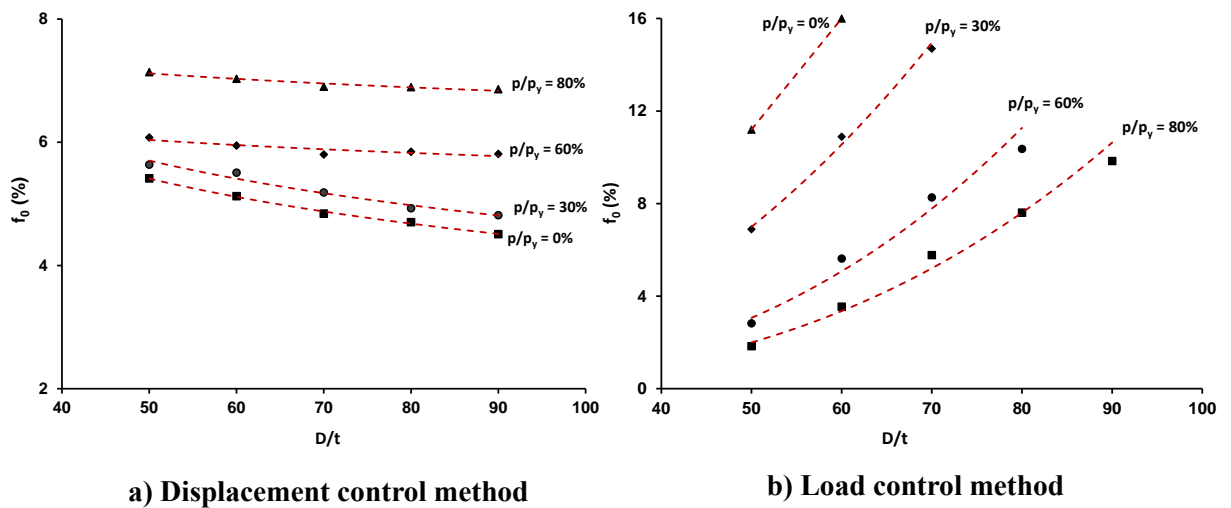
**Figure 3.18: Effect of D/t on maximum ovalization for spherical loading plate**

From Figure 3.17 and 3.18, it can also be concluded that as the internal pressure increases the value of maximum ovalization decreases. This can be more obvious if the relationship between internal pressure and ovalization is plotted as shown in Figure 19. This figure, however, shows the relationship between internal pressure and ovalization for pipe specimens loaded with spherical loading plate. Figures 19a and 19b show the effect of this parameter when pipe specimens loaded using displacement control and loading control method, respectively. Figures 19a and 19b show that the effect of internal pressure is significant on the pipe ovalization. As an example, for the pipes with D/t of 50 and for

68

no internal pressures the maximum out-of-roundness is 6.35% which is significant. It is worth noting that the internal (operating) pressure (p) is normalized by the yield pressure ($p_y$).



(a) Displacement control method

(b) Load control method
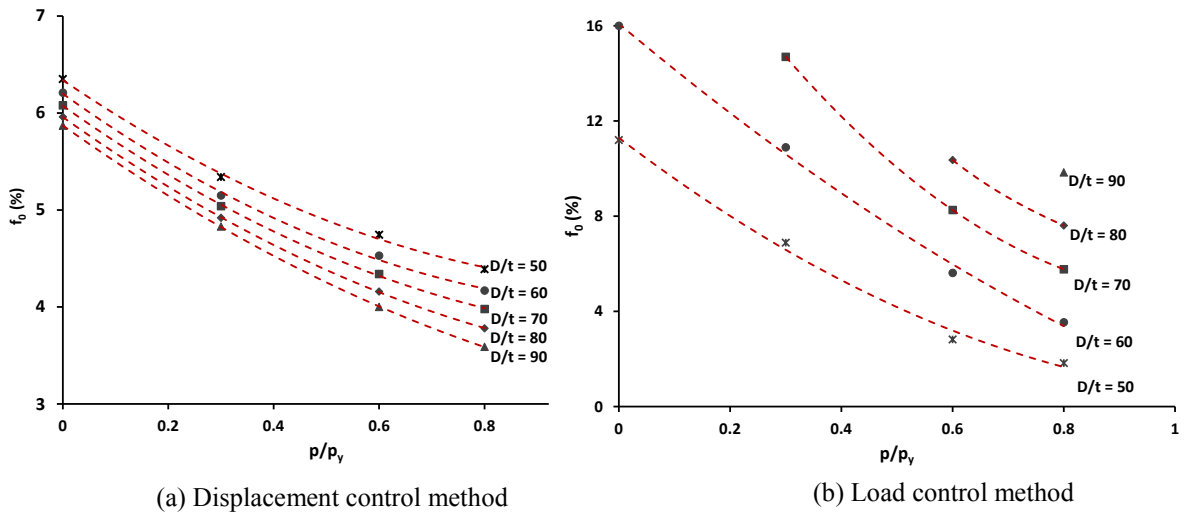
**Figure 18: Effect of internal pressure on maximum ovalization for spherical loading plate**

Figure 20 shows the relationship between D/t and dent depth and this figure shows that all of pipe specimens subjected to 30% and higher internal pressures were experienced dent depth of less than 6% and hence, according to ASME B31.4 [7] these pipe specimens are acceptable from dent assessment criterion.  However, from Figures 17a and 18a, it is found that the maximum ovalization value for all pipe specimens loaded in displacement control method exceeded 4% limit value recommended by Bai and Bai [14] when 65 mm displacement was applied and this is true irrespective of level of internal pressure applied, value of D/t chosen, and shape of the loading plate used. Hence, these pipe specimens are not be acceptable from ovalization criterion. Therefore, this study found that evaluation of dent defect solely based on the dent depth may not be an appropriate one. The study

recommends additional consideration of the severity of ovalization caused by a dent while assessing a dent defect.



(a) Rectangular loading plate          (b) Sphere loading plate
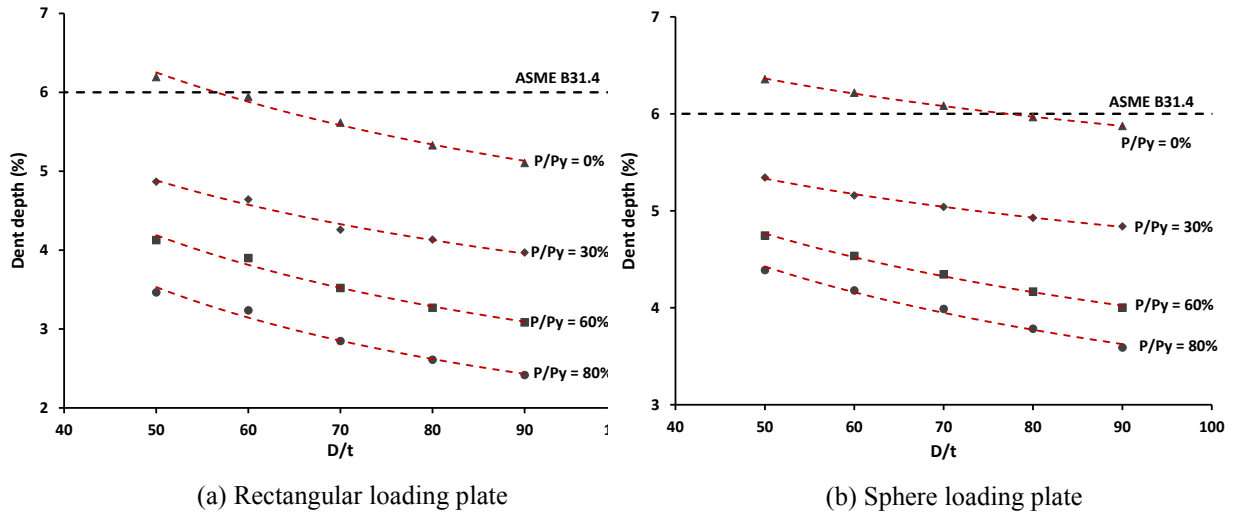
**Figure 19: Relationship between D/t and dent depth**

## 3.5 CONCLUSIONS

The following conclusions are made based on the full-scale tests and detailed FEA based parametric study undertaken under the scope of this study.

1. All three parameters: level of internal or operating pressure, permanent depth in pipe wall, and D/t of the pipe affect the maximum ovalization value.

2. Parametric study shows that as the internal pressure increases the maximum ovalization decreases and this trend was found for both displacement and load control methods and for both shapes of loading plates.

3. The effect of loading plate (rock tip shape) shape chosen in experimental program has insignificant effect on the ovalization. However, two different shapes for the

loading plates used in the parametric study showed that a spherical loading plate (rock tip) usually results in higher ovalization than the square rock tip.

4. Maximum ovalization value increases as the D/t increases when load is applied using load control method. However, the trend is opposite when load is applied using displacement control method.

5. Though total deformation of 65 mm may not be a safety concern from dent evaluation criterion, it is a concern when ovalization limit criterion is considered.

## 3.6 ACKNOWLEDGMENTS

## 3.7 REFERENCES

[1] Roovers P, Bood R, Galli M, Marewski U, Steiner M, Zaréa M., "EPRG methods for assessing the tolerance and resistance of pipelines to external damage," In: Denys R, editor, Proceedings of the Third International Pipeline Technology Conference, vol. II, Brugge, Belgium, Amsterdam: Elsevier; 2000. p. 405–425.

[2] Cosham, A., and Hopkins, P., 2004, "The effect of dents in pipelines-guidance in the pipeline defect assessment manual," International Journal of Pressure Vessels and Piping, 81(2), pp. 127-139.

[3] Smith, R. B., and Gideon, D. N., 1979, "STATISTICAL ANALYSIS OF DOT-OPSO DATA," Proceedings, Annual Symposium - Society of Flight Test Engineers, pp. D. 1-D. 9.

[4] Wang, K. C., and Smith, E. D., 1982, The effect of mechanical damage on fracture initiation in line pipe, part I dents, Energy, Mines and Resources Canada, Canada Centre for Mineral and Energy Technology, [Ottawa].

[5] Zarea, M. F., Toumbas, D. N., Philibert, C. E., and Deo, I., "Numerical models for static denting and dynamic puncture of gas transmission linepipe and their validation," Proc. Proceedings of the 1996 1st International Pipeline Conference, IPC. Part 2 (of 2), 1996, ASME, pp. 777-784.

[6] Lancaster, E. R., 1996, "Burst pressures of pipes containing dents and gouges," Proceedings of the Institution of Mechanical Engineers, Part E: Journal of Process Mechanical Engineering, 210(1), pp. 19-27.

[7] ASME, 2012, "B31.4: Pipeline Transportation Systems for Liquids and Slurries," ASME International, New York, NY, USA.

[8] ASME, 2012, "B31.8: Gas Transmission and Distribution Piping Systems," ASME International, New York, NY, USA.

[9] Yeh, M. K., and Kyriakides, S., 1986, "On the collapse of inelastic thick-walled tubes under external pressure," Journal of Energy Resources Technology, Transactions of the ASME, 108(1), pp. 35-47.

[10] Yeh, M. K., and Kyriakides, S., 1988, "COLLAPSE OF DEEPWATER PIPELINES," Journal of Energy Resources Technology, Transactions of the ASME, 110(1), pp. 1-11.

[11] CSA, 2007, "Z662-07: Oil and gas pipeline systems," Canadian Standard Association, Mississauga, ON, Canada.

[12] International-Standard, 2009, "Petroleum and natural gas industries - Pipeline transportation systems," ISO 13623, Switzerland.

[13] DNV, 2012, "OS-F101: Submarine Pipeline Systems," Det Norske Veritas.

[14] Bai, Y., and Bai, Q., 2005, Subsea Pipelines and Risers, Elsevier, Great Britain.

[15] API, 2012, "Spec 5L: Specification for Line Pipe," American Petroleum Institute, Washington, DC, USA.

[16] ASTM, 2011, "E8/E8M-11: Standard Test Methods for Tension Testing of Metallic Materials," ASTM International West Conshohocken, Pennsylvania, USA.

[17] SIMULIA, 2011, Analysis User's Manuals, Dassault Systèmes Simulia Corp., Rising Sun Mills, Providence, RI, USA.

# CHAPTER 4

# PRESSURE TESTS ON 30 IN DIAMETER X70 GRADE PIPES WITH DENT-CRACK DEFECT

## 4.1 INTRODUCTION

External interference causes various defects which significantly affect the transportation of oil and gas in pipelines. Corrosion, crack, puncture, dent, gouge, and combination of such damages from a variety of external interferences are some common examples of surface damage in pipelines. Gouges, dents, cracks, and punctures that form in the pipe wall as a result of contact and/or impact from foreign objects are often referred to as mechanical damage. Mechanical damage of oil and gas pipelines is referred as the major reason of failure of pipelines in service, and this damage may result in loss of product, explosions, fire, human and/or animal casualties, and pollution. It has been reported that the failure of oil and gas transmission pipelines resulting from mechanical damages ranges from 55% in the USA to around 70% in Europe [1-4].

Accidental impacts are common in onshore and offshore pipeline. However, they are formed in a different way. Construction and excavation cause mechanical defects in onshore pipeline while anchors or trawling gear cause mechanical damage in offshore pipelines. These damages are known as dents and gouges (with or without wall crack) in pipeline industry. A dent is an inward permanent plastic deformation of the pipe wall which causes a gross distortion of the pipe cross section [5]. A dent also causes stress and strain concentrations and a local reduction in the pipe diameter. A gouge is a metal loss defect that occurs in the pipeline due to the scraping action of the excavating equipment or due to

73

the rubbing action of the pipeline with a foreign object such as a rock. A gouge and dent can both form at the same time. Dents can also exist with a wall crack inside of it. These cracks occur mostly during the formation of dent or later due to corrosion or scratching the surface by external objects like gears. The other mentioned reason of having crack in pipeline surface is fatigue or cyclic loading [6-8].

Dent defects in energy pipelines have been a major concern for pipeline operators. Therefore, a significant number of investigations have been completed to understand the effect of dents of various shapes and sizes on the behaviour of energy pipes under monotonic and cyclic pressures. It has been found and generally accepted that dent defect alone is not a threat to the integrity of pipe structure under monotonic pressure load when the dent depth is up to 24% of the diameter of the pipe [9-11]. Extensive research has also been completed to understand how the burst strength of pipelines with part-wall defects (such as corrosion alone and crack alone) changes as the shape of corrosion and crack dimensions change. Detailed guidelines on predicting the burst strength of such pipes are available in various pipeline design and maintenance codes and standards for examples, ASME 2004, DNV 2004, and CSA 2007. Numerous studies have also been undertaken by various research groups and individuals to determine the burst pressure capacity of pipes that have developed a gouge in the dent (often known as dent-gouge defect). Various design guidelines and equations for calculating the burst strength of such pipes are available [6, 12].

The burst strength of pipes with defect with just one of the damage forms such as dent, crack, corrosion and combined dent-gouge has been subjected to extensive research. No studies have been undertaken to determine the burst strength of dented pipe that has

developed crack in the dent. Therefore, this study was undertaken to develop a detailed design guideline for determining the safe burst pressure limit for various oil and gas pipelines that have developed a crack in the dent (which will be called a dent-crack defect in the subsequent discussion).

## 4.2 EXPERIMENTAL WORK

### 4.2.1 Test specimen

This study was accomplished by performing laboratory based experimental tests. The purpose of performing full-scale tests was to determine experimentally the final burst strength of field defect pipes due to dent-crack damages and also to determine the critical strain values obtainable from the tests. As a result, X70 steel pipes which are mostly used in oil and gas pipelines, were selected as test specimens. six specimens were fabricated from pipe with nominal diameter of 762 mm and thickness of 8.2 mm and conforming to grade, X70 steel pipes. The outer diameter to thickness of pipe ratio (D/t) of the all specimens used in this experimental work was 93. The length of the each pipe specimen was 2050 mm. Two ends of the specimen were welded to thick caps for holding pressure during dent and burst test which will be explained later. A number of tensile specimens were cut from a virgin pipe section and the standard tensile test was carried out to determine the mechanical properties of the pipe material. The properties of the material which were obtained from the tensile test are: actual yield strength of 543 MPa; tensile strength of 624 MPa; and modulus of elasticity of 204 GPa.

The full size tests were completed in three different loading steps; fatigue or cyclic loading, dent loading and bursting. Each of these steps is explained in detail in the following sections. All the pipes have an EDM cut notch with 100 mm length and the depth

75

is 1 to 1.5 mm at the mid span. This area was subjected to local loads of fatigue and dent. The main parameters of this study were service pressure (when pipe subjected to the dent loads) and the indenter shape. In most of the cases where pipeline in the field is subjected to lateral loading it contains internal pressure. The pressure varied from 3.8 MPa to 7.6 MPa which represents 30% to 60% of the service pressure of oil and gas pipeline. Indenters of two different shapes were used to create dent of two different shapes. These were: (a) rectangular shape and (b) blunt shape as shown in Figure 4.1. Details of the test specimens are given in Table 4.1.

**Table 4.1: Properties of test specimens**

| Specimen | Crack length | Crack Depth | Dent length | Dent depth | Pressure* |
|---|---|---|---|---|---|
| X70-1 | 100 mm | ~ 2 mm | 100 mm | 30 (3.96%) | 3.8 MPa (30%) |
| X70-2 | 100 mm | ~ 2 mm | 100 mm | 28 (3.7%) | 6.3 MPa (50%) |
| X70-3 | 100 mm | ~ 2 mm | 100 mm | 28 (3.7%) | 7.6 MPa (60%) |
| X70-4 | 100 mm | ~ 2 mm | 500 (blunt) | 28 (3.7%) | 3.8 MPa (30%) |
| X70-5 | 100 mm | ~ 4 mm | 100 mm | 28 (3.7%) | 3.8 MPa (30%) |
| X70-6 | 100 mm | ~ 4 mm | 100 mm | 46 (6%) | 0 MPa (0%) |

~ it is almost impossible to measure the exact crack depth
* Service pressure during denting test

### 4.2.2 Test setup and instrumentation

*Fatigue test:*

Pipe specimens rested on three raised thick steel supports. The supports at the ends consisted of a pin and a roller. To keep specimens in location, a steel collar of the same radius as the pipes was used on the mid span support. Rubber pieces were placed between the pipe and the collar to minimize sliding between them as can be seen in Figure 4.2. Also, a small collar was used at the top of the specimens between the actuator and pipe in order

to prevent load concentration. Between the top collar and pipe a rubber was used as well. Notch was cut using EDM machine with depth of 1 mm and length of 100 mm. Notch is almost 20 cm below the actuator. The rubber is 11 cm from the notch (Figure 4.2). The universal loading actuator applied cyclic sine loading from 50 kN to 100 kN on the pipe. Number of cycles to reach approximately 1 mm crack depth was chosen based on CT tests that were completed in University of Windsor.



| a) Rectangular indenter | b) Blunt indenter |

**Figure 4.1: two different indenters**

*Denting test:*

The experimental program was carried out in the Structural Engineering Laboratory of the University of Windsor. Figure 4.3 schematically shows the test setup for denting test. The pipe specimens were placed on three thick steel supports. Hence, the boundary condition between the pipe and the support plane can be defined as a contact interaction. On the middle support, a steel collar with the same radius as the pipes was used to hold the specimen in place. Between the collar and pipe a piece of rubber was placed in order to prevent sliding. Denting load was applied on the top surface of the pipe wall using a

universal loading actuator. The notch was placed directly below the center of the indenter (Figure 4.3).



a) Test setup schematic

b) Test setup photo
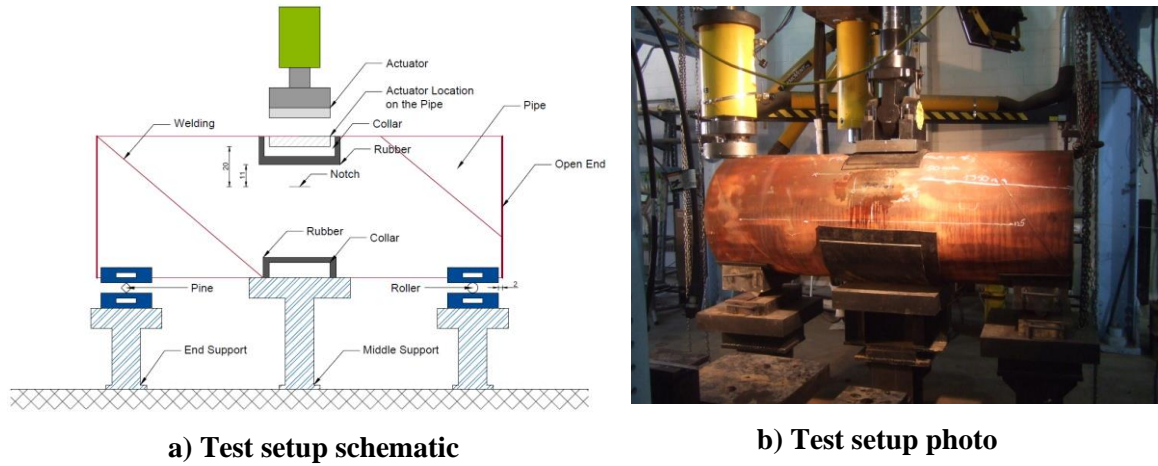
**Figure 4.2: Fatigue test setup**

The total and plastic deformation of the pipe due to application of denting load was measured using linear voltage displacement transducers (LVDTs). Two LVDTs were used. The LVDTs were located at the top of actuator at right angle to capture stroke of indenter. End caps were welded at the end of each specimen to pressurize the pipes using a hydrostatic pump. Internal pressure and indenter shape varied for different specimens. Specimens were instrumented with strain gauges to monitor and record the variations of strain around the dent. Four different lines of strain gages consisting of eight to ten strain gauges on each line were installed. Hence, a large area around the dent was covered to understand the critical strain location. The strain gauges layout is shown in Figure 4.3. No strain gauges were installed underneath the indenter because those strain gauges failed as soon as load was applied through the actuator.

a) Test setup schematic

b) Strain gauge layout
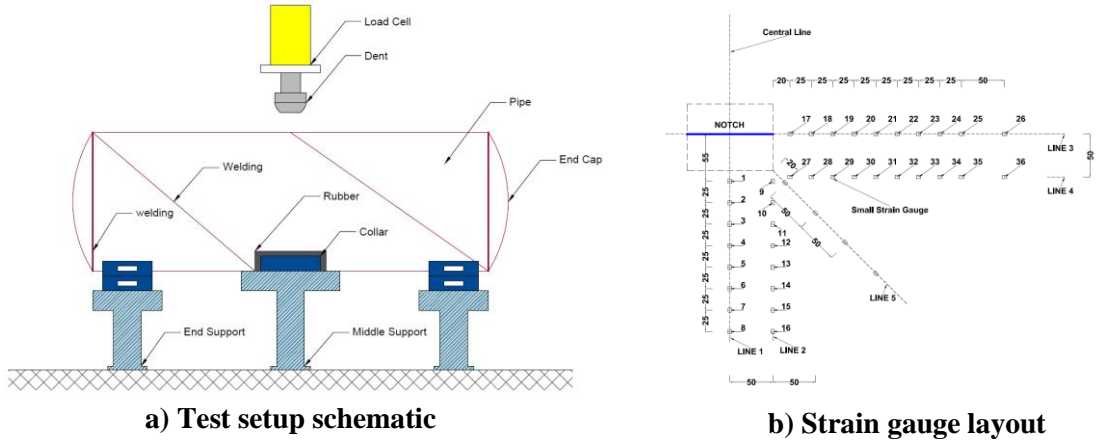
**Figure 4.3: Denting test setup**

*Bursting test:*

Specimens were pressurised with a pressure washer in order to quantify the ultimate bursting strength of pipe with dent-crack defect. A number of strain gauges are located inside and around the dented area. Concentration of load observed in these regions. The pressure was monitored using a digital pressure gauge that was located on an end cap.

### 4.2.3 Test procedure

For all four specimens, the same procedure was followed when performing fatigue, denting and bursting tests. First, the pipe was subjected to sine cyclic loading using a universal loading actuator. Next, pipe specimens were filled with water to a certain level of pressure that is a fraction of $p_y$ which is the water pressure required for yielding of pipe steel material in the circumferential direction. Following this, the universal loading actuator applied a dent load to the X70 steel pipe while the internal pressure was maintained at the same level. Denting load was applied in several loading and unloading steps. After completion of each load step, that is, after complete removal of denting load, the internal pressure in the pipe specimen was reduced to zero. The objective was to obtain strain data

when the pipe is completely unloaded. Finally, the pipe was pressurized using the pressure washer until bursting occurred. The objective was to find the bursting strength of the dent-crack pipe.

## 4.3 TEST RESULTS

### 4.3.1 Load deformation behaviour

For specimens X70-1, X70-2 and X70-3 the rectangular indenter was used while blunt indenter was used for specimen X70-4. For some specimens, denting load was applied in multiple loading and unloading steps. The load deformation behaviour of the specimens is shown in Figure 4.4. It can be seen from this figure, for a blunt shaped indenter (X70-2), a higher load is required for denting than that required for the rectangular shaped indenter (X70-1). Both specimens are equally pressurized to 3.8 MPa (.3$p_y$) and have 2 mm notch-crack depth. For instance, X70-1 showed total deformation of 10 mm at a load level of 226 kN. However, X70-4 which involved a blunt indenter required a load of 382 kN to achieve the same amount of deformation. The reason is specimen X70-4 was loaded with a longer dent. This longer dent results in the specimen to acting stiffer under dent load than the X70-1 with shorter rectangular dent. In the other words, the blunt shaped indenter had a larger area in contact with the indenter compared to the rectangular shaped indenter.
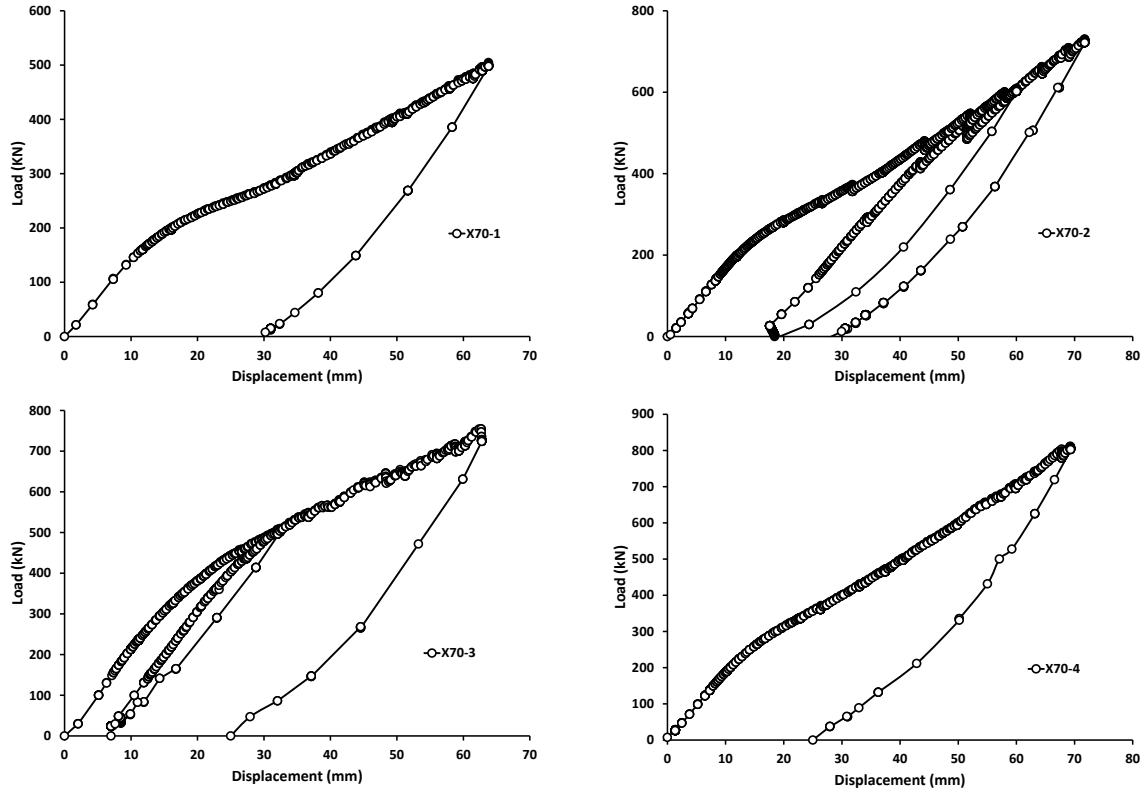
**Figure 4.4: Load-deformation behaviour**

For Specimen X70-1, X70-2 and X70-3 the indenter shape and the size remained constant while the internal pressure was $.3p_y$, $.5p_y$ and $.6p_y$ respectively. From the load-deformation behaviour, Yielding stress is almost same in all of these specimens Pipes undergo both elastic and plastic deformation during the process of denting. As the denting load was removed, elastic spring back always existed. The spring back influences the dent depth which is an important parameter influencing the strain concentration in a dent [5]. In Figure 4.4 it can be observed that specimens with the rectangular indenter and varying internal pressure, the amount of spring back due to removal of denting load is higher as the internal pressure increased. However, specimens at the same level of internal pressure and different indenter shape the spring back influence is negligible. For example 55.5% spring

back is observed for the X70-1 after the removal of indenter, while the amount of spring back are 60.6%, 60% and 54.1% for the X70-2, X70-3 and X70-4 respectively.

## 4.3.2 Strain distributions

Strain data obtained from the strain gauges installed in the circumferential direction is presented in Figure 4.5. Figure 4.5-a shows the comparison between the tensile circumferential strain between specimens X70-1, with rectangular indenter, and X70-4, blunt and longer indenter. Figure 4.5-b compares specimens, X70-1, X70-2 and X70-3, with the same rectangular indenter but different internal pressure. In case of the blunt shaped indenter (X70-4), maximum tensile circumferential strain was 0.63% obtained from strain gauge 6, which was located 185 mm away from the center of the notch along the perimeter of the pipe. Whereas, in the case of the rectangular shaped indenter (X70-1), maximum tensile strain was 1.37% at strain gauge 4, which was located 130 mm away from the indenter center along the perimeter of the pipe (Figure 4.3). Hence, the specimen with the smaller indenter (X70-1) was subjected to a higher strain. This strain occurred at a greater distance from the notch than the specimen with the blunt indenter (X70-4). From the strain gauge readings of Figure 4.5-b, it is observed that as the internal pressure increases the values of maximum circumferential strains increase as well. However, the highest strain was observed in strain gauge number 4 which was located 130 mm away from the notch. The highest circumferential strain for specimens X70-1, X70-2, and X70-3 after unloading was 1.37%, 1.91% and 2.17% respectively. None of these specimens show compressive strain values around the dented area.
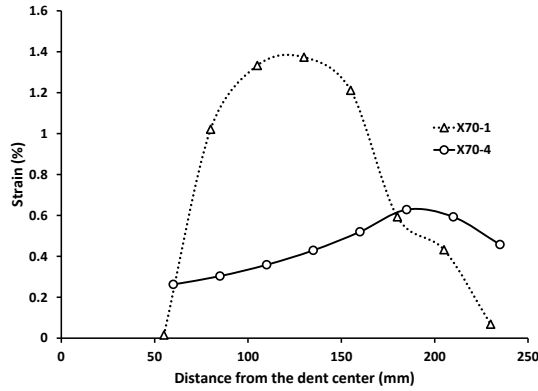
**a) Comparison between X70-1
and X70-4**
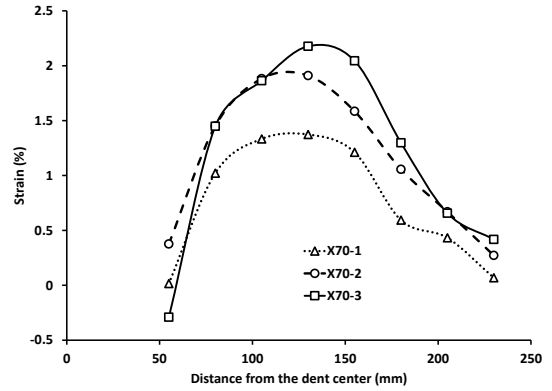
**b) Comparison between X70-1,
X70-2, and X70-3**

**Figure 4.5: Circumferential strain distributions**
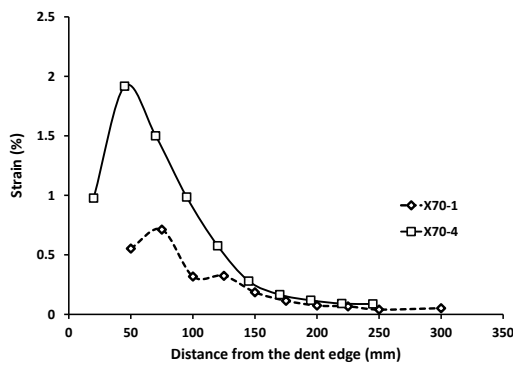


**a) Comparison between X70-1
and X70-4**
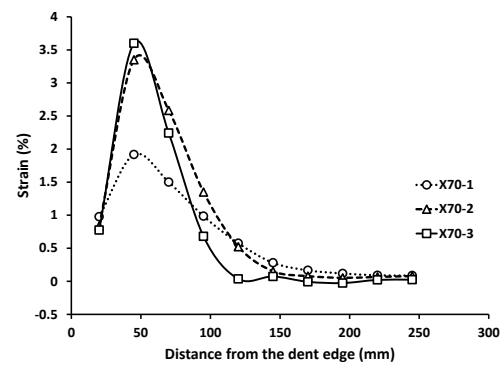
**b) Comparison between X70-1,
X70-2, and X70-3**

**Figure 4.6: Longitudinal strain distributions**

Figure 4.6 shows the distributions of strains in the longitudinal direction and it shows similar trends as in Figure 4.5. From Figure 4.6 it is evident that, same as in the circumferential direction, the smaller rectangular indenter showed more strain concentration than the longer blunt indenter. For all specimens (X70-1, X70-2 and X70-3) maximum strain was recorded at strain gauge 18, which was located at 45 mm away from the edge of the notch. The maximum strain recorded was 3.6% for X70-3, 3.35% for X70-

2 and 1.92% for X70-3. It should be noted that all the strain values recorded from the test specimens are tensile.

### 4.3.3 Burst strength

The value of $p_y$ for X70 grade pipe specimen is 12.67 MPa (1837 psi). The bursting pressure for the specimen with a small rectangular indenter (X70-1) was 13.96 MPa (2024 psi) while the bursting pressure for the specimen with a longer indenter (X70-4) was 14.9 MPa (2160 psi). Hence, X70-4 showed a higher bursting pressure by 6.3%. However, both specimens had higher bursting pressure than the yielding pressure of 12.67 MPa (1837 psi) as defined by codes. Specimens X70-1 and X70-4 had a bursting pressure of $1.10p_y$ and $1.18p_y$. In the case of specimens with different internal pressure during denting (X70-1, X70-2 and X70-3), bursting pressure did not vary by more than 0.4 MPa. The value of bursting pressure was 13.96 MPa (2024 psi), 14.34 MPa (2080 psi) and 14.3 MPa (2074 psi) for specimens X70-1, X70-2 and X70-3 respectively. Alternatively states, bursting pressure was equal to $1.10p_y$, $1.13p_y$ and $1.13p_y$ for X70-1, X70-2 and X70-3 respectively. Therefore, when the crack depth is less than 2 mm, the internal pressure and the indenter shape was not found to have a considerable effect the final bursting pressure of the crack-dented pipes.

Specimen X70-5 and X70-1 had the same specifications except for the crack depth. Crack depth of X70-5 was 4 mm but crack depth of X70-1 was 2 mm. The burst pressure for specimen X70-5 was 8.96 MPa (1300 psi). The burst pressure of X70-1 was 13.96 MPa (2024 psi). Hence, X70-5 sustained 36% less pressure than the same crack-dented pipe with 2 mm crack depth. In fact, the bursting pressure of X70-5 was $0.7p_y$ which is less than the allowable pressure of $0.8p_y$. Specimen X70-6 had the same bursting strength of 8.96

MPa (1300 psi) as specimen X70-5. All specifications were the same except for the dent depth (46 mm or 6%). Dent depth of X70-5 was 28 mm or 3.7%. The X70-6 bursting strength was equal to $0.7p_y$.

The only parameter that had a considerable effect on bursting strength of the crack-dented pipe is crack depth after 4 mm.

## 4.4 CONCLUSION

After completing a number of full-scale experiments on X70 grade pipe the following conclusions can be made.

1. The indenter shape affects the strain distribution and maximum magnitude of dent. The blunt indenter required a larger load application to reach the same dent depth.

2. Pressure during denting affected the strain magnitude away from the dent. The smaller the pressure during denting the larger the stress was found to be. It must be noted that this pattern was not observed very close to the dent.

3. Bursting pressure was not significantly affected by dent shape, internal pressure during denting or by cracks with depths less than 2 mm. The only parameter to significantly affect bursting pressure was crack depth if it was at least 4 mm.

## 4.5 REFERENCES

[1] Smith, R.B. and Gideon, D.N. (1979). "Statistical analysis of DOT-OPSO data". AGA 6th Symposium on Linepipe Research, Huston, Texas, pp. D.1-D.9.

[2] Wang, K.C. and Smith, E.D. (1982). "The effect of mechanical damage on fracture initiation in linepipes: Part I-dents". An internal report submitted to Physical Metallurgical Research Laboratories of CANMET, Ottawa, Canada, Report No. ERP/PMRL 82-11(TR).

[3] Zarea, M.F.; Toumbas, D.N.; Philibert, C.E.; and Deo, I. (1996). "Numerical models for static and dynamic puncture of gas transmission linepipe and their validation". International Pipeline Conference, June 9-14, Vol. 2, pp. 777-784.

[4] Lancaster, E.R. and Palmer, S.C. (1996a). "Burst pressure of pipes containing dents and gouges". Journal of Process Mechanical Engineering, Part E, pp. 19-27.

[5] Cosham, A., and Hopkins, P. 2004. The Effect of Dent in Pipelines-Guidance in the Pipeline Defect Assessment Manual. International Journal of Pressure Vessels and Piping, ELSEVIER, 81: 127-139.

[6] Lancaster, E.R. and Palmer, S.C. (1996). "Strain concentrations in pressurized dented pipes". Journal of Process Mechanical Engineering, Part E, pp. 29-38.

[7] Iflefel, I.B., Moffat, D.G., and Mistry, J. (2004). "The interaction of pressure and bending on dented pipe". International Journal of Pressure Vessel and Piping, Vol. 82, pp. 761-769.

[8] Karamanos, S.A. and Andreadakis, K.P (2006). "Denting of internally pressurized tubes under lateral loads". International Journal of Mechanical Science, vol. 48, pp. 1080-1094.

[9] Gresnigt, A.M.; Karamanos, S.A.; and Andreadakis, K.P. (2007). "Lateral loading of internally pressurized steel pipes". Journal of Pressure Vessel technology, Vol. 129, pp. 630-637.

[10] Dama, E.; Karamanos, S.A.; and Gresnigt, A.M. (2007). "Failure of locally buckled pipelines". Journal of Pressure Vessel technology, Vol. 129, pp. 272-279.

[11] Pinheiro, B.C. and Pasqualino, I.P. (2009). "Fatigue analysis of damaged steel pipelines under cyclic internal pressure". International Journal of Fatigue, Vol. 31, pp. 962-973.

[12] Maxey W.A. (1986). "Outside force defect behaviour". A technical report submitted to the Pipeline Research Committee of the American Gas Association, Report No. 162, AGA Catalogue No. L51518.

# CHAPTER 5

# EFFECT OF OPERATING PRESSURE AND DENT DEPTH ON BURST STRENGTH OF NPS30 LINEPIPE WITH DENT-CRACK DEFECT

## 5.1 INTRODUCTION

Steel pipelines are the primary mode of transporting natural gas, crude oil, and various petroleum products in North America. In Canada alone, more than 110,000 km of buried energy transmission pipelines are in operation [1]. Damages or defects resulting from third party interference, more commonly known as mechanical damages are serious threat to the structural integrity of buried pipelines. Corrosion, crack, puncture, dent, gouge, and combination of such damages are some common examples of mechanical damage in pipelines. Mechanical damage of oil and gas pipelines is believed to be the major cause of failure of pipelines in service, and this damage may result in loss of product, explosions, fire, human and/or animal casualties, and pollution. It has been reported that the failure of oil and gas transmission pipelines resulting from mechanical damages ranges from 55% in the USA to around 70% in Europe [2-5].

Incidents of accidental impacts are not uncommon in onshore and offshore pipelines. Construction and excavation equipment can accidently impact the field pipeline causing mechanical damages such as dent and/or gouge with or without cracks. A dent is an inward permanent deformation in the pipe wall which causes a gross distortion of the pipe cross section [6]. A dent also causes stress and strain concentrations, ovalization, and

a local reduction in the pipe diameter. A gouge is a metal loss defect that occurs in the pipe wall due to the scraping action of the excavating equipment or due to the rubbing action of the pipeline with a foreign object such as rock or hard ground surface. Crack can also develop in a dent or gouge as a result of impact action and/or because of exposure to the corrosive environment and/or due to fatigue loading arising from pressure fluctuation and geotechnical movements [7].

Dent defects in energy pipeline have been a concern for pipeline operators. As a result, several research works were completed to understand the behaviour of various dent defects such as plain-smooth dents [8, 9], plain-kinked dents, confined or unconfined conditions [6], and fatigue life of a dent [6]. Based on the outcome of these studies, it is generally accepted that a dent defect alone is not a threat to the structural integrity of pipe structure when the dent depth is up to 6% of the diameter of the pipe [10, 11] and any crack on the surface of pipe wall less than 12.5% of wall thickness of the pipe can be removed by grinding [10, 11].

Various studies were also completed using analytical and experimental techniques to understand the effect of metal loss of the pipe wall such as corrosion or crack on the burst strength of pipeline [12]. Detailed guidelines on predicting the burst strength of such pipes are available in various pipeline design and maintenance codes and standards [11, 13, 14]. Studies were also undertaken by various research groups and individuals to determine the burst pressure capacity (burst strength) of pipes with dent-gouge defect that is, pipe with combined defect of dent and gouge [15]. Various design guidelines and equations for calculating the burst strength of such pipes are available [16].

The burst strength of pipe with single defect such as dent or crack or corrosion has been the subject of many previous research works. Behaviour of pipes with dent-gouge defect was studied as well. However, review of literatures available in the public domain reveals that no studies were undertaken to determine the burst strength of dented pipe that has developed crack in the dent. Such combined defect is called dent-crack defect in this study. Therefore, this study was completed at the Centre of Engineering Research in Pipelines (CERP), University of Windsor to determine the burst strength of NPS30 X70 pipe with dent-crack defect with various dent depths and operating pressure. This paper discusses the results obtained from this study.

## 5.2 EXPERIMENTAL PROCEDURE

### 5.2.1 Test specimen

The purpose of this study was to determine the burst strength of field linepipes that have developed dent-crack damage. This project was completed using both laboratory based experimental work and numerical study using non-linear finite element method (FEM). NPS 30 X70 [17] steel pipe used in oil and gas transmission pipelines was chosen to make the test specimens. The pipe specimens were spiral welded. Five pipe specimens were fabricated from this pipe. The nominal diameter of the pipe is 762 mm (30 in) and the thickness of the pipe wall is 8.5 mm (0.33 in) and hence, the outer diameter-to-thickness ratio (D/t) of the pipe specimens used in the experimental work is about 90. The length of each pipe specimen was 2000 mm (78.74 in). Two ends of the specimen were welded to thick hemispherical steel end caps for holding water pressure during dent formation process and also during burst strength test. A number of tensile material specimens were cut from a virgin pipe wall and the standard material tensile tests were carried out to determine the

mechanical properties of the pipe material in accordance with ASTM E8 [18]. The properties of the material obtained from theses tensile tests are: actual yield strength of 543 MPa at 0.5% total strain; tensile strength of 624 MPa; and average modulus of elasticity of 204 GPa. The nominal (engineering) values of fracture stress and fracture strain were determined after the completion of the material tests. In addition to tensile test, Charpy V notch impact test were conducted on five subsize specimens (full wall thickness specimens) in room temperature (22°C) to ensure the pipe material has sufficient ductility. Average Charpy toughness found to be 152 J.

Each test specimens was required to go through three different sub-tests and hence, each pipe specimen was required to go through three different test setups, three different instrumentations, and three different loading steps. These three loading steps are: (i) fatigue load test, (ii) denting load test, and (iii) finally, the burst or pressure loading test. These loading steps and sub-tests are explained in the following sections.

All the pipes had an electro-discharging machine (EDM) cut crack-like V-notch of 100 mm long and 4 mm deep. Previous study completed at the Centre of Engineering Research in Pipeline (CERP) found that a crack with depth less than 2 mm does not affect the burst strength of this dented pipe [19]. The notches were located at the mid-length of the pipe specimens and it was oriented in the direction of the length of the pipe specimen. The width of the V-notch was about 0.3 mm. A total of five full-scale tests were completed under the scope of this study. Table 5.1 shows the matrix of the tests specimens used in this study. Specimens were named to reflect the primary attributes attached to each specimen. For example, specimen SP5-P30-D4, the first two letters and number combination (SP5) indicates that it is specimen number 5, the next letter and number

combination (P30) indicates that the internal pressure was held constant at $0.3p_y$ or 30% of $p_y$ which is about 3.8 MPa (550 psi) during denting process, the next letter and number combination (D4) indicates that the inward permanent depth or permanent dent depth in the pipe wall due to loading in this specimen was 4% (~30 mm) of the diameter of the pipe. Hence, the specimen SP3-P00-D4 was the second specimen and this specimen was identical to specimen SP5-P30-D4 except the earlier one maintained zero internal pressure during denting test. As can be seen from this table, the parameters that were varied in the experimental work are: (a) permanent dent depth and (b) internal pressure applied during denting process. The pressure was varied from 0 MPa (no internal pressure) to 3.8 MPa (550 psi) and hence, the internal pressure was varied from $0.0p_y$ to $0.3p_y$ where $p_y$ is the pressure required to cause yielding of the pipe material. The yield pressure for this pipe was calculated at 12.67 MPa (1837 psi). A rectangular indenter was used to create the dent as can be seen in Figure 5.1. The length (dimension in the direction of the length of the pipe) and width (dimension in the circumferential direction of the pipe) for the indenter were 100 mm and 50 mm, respectively. The indenter was made by machining a solid steel slab. The permanent dent depth for these specimens was varied from 0% to 6% of the outer diameter of the pipe (Table 5.1). The permanent dent depth is the plastic deformation resulted from denting process and calculated after removal of the indenter.

**Table 5.1: Test matrix**

| Specimen | Crack length | Crack Depth | Dent depth | Pressure* | Parameter |
|---|---|---|---|---|---|
| SP1-P00-D0 | 100 mm | 4 mm | 0.00 (0%) | 0 MPa (0%) | Dent Depth |
| SP2-P00-D2 | 100 mm | 4 mm | 15.2 (2%) | 0 MPa (0%) | |
| SP3-P00-D4 | 100 mm | 4 mm | 28.2 (4%) | 0 MPa (0%) | |
| SP4-P00-D6 | 100 mm | 4 mm | 45.7 (6%) | 0 MPa (0%) | |
| SP5-P30-D4 | 100 mm | 4 mm | 28.2 (4%) | 3.8 MPa (30%) | Internal Pressure |

*Pressure was held constant during denting test

**Figure 5.1: Rectangular indenter used to create dent**

## 5.2.2 Test setup and instrumentation

The purpose of these tests was to study how burst strength of this linepipe is affected by crack-dent defect. The same loading procedure and same loading sequence was followed for all five tests specimens. First fatigue load was applied, followed by denting load, and finally pipes were subjected to monotonically increasing water pressure until rupture occurred in the dent-crack defect. All these experimental works were completed in the structural engineering laboratory of the University of Windsor.

*Fatigue load test*

The purpose of the fatigue load was to create a crack at the tip of the V-notch through the thickness of the pipe wall (Figure 5.2a). Hence, a crack-like fine V-notch which was first created using EDM (electro-discharging machine) technique. The dimensions of the notch were: 100 mm long ($\pm1\%$) along the length of the pipe, 0.3 mm ($\pm3\%$) wide at the top of the outside surface of the pipe wall, and 4 mm ($\pm1\%$) deep (Figure 5.2a). Then, the notched pipe was subjected to fatigue load cycles with stress ratio of 0.5 and the fatigue

loading continued until a crack at the tip of the V-notch of about 0.3 mm deep was obtained. As a result, the notch tip was associated with a true crack at the tip of the V-notch (see Figure 5.2a). Ten small samples were cut, after completion of fatigue and burst tests, from various locations on V-notch-crack area and examined under the Scanning Electron Microscope (SEM) to determine true depth of the cracks in all the pipes. Figure 5.2b shows how the samples were numbered and where they were located. Figure 5.3 shows a SEM (Scanning Electron Microscope) pictures taken at different locations of the wall cross-section after fatigue crack was obtained.
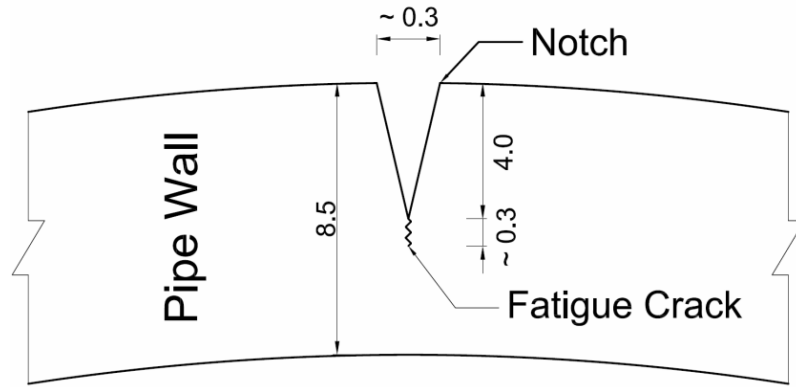


**a) Pipe wall section showing V- notch and crack**
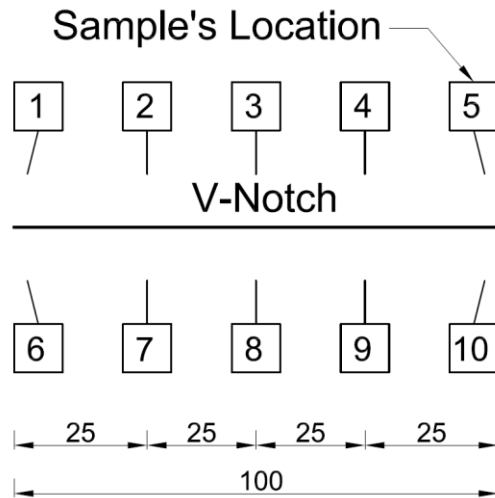


**b) Sample's location on the V-notch**

**Figure 5.2: EDM cut V- notch on pipe wall**
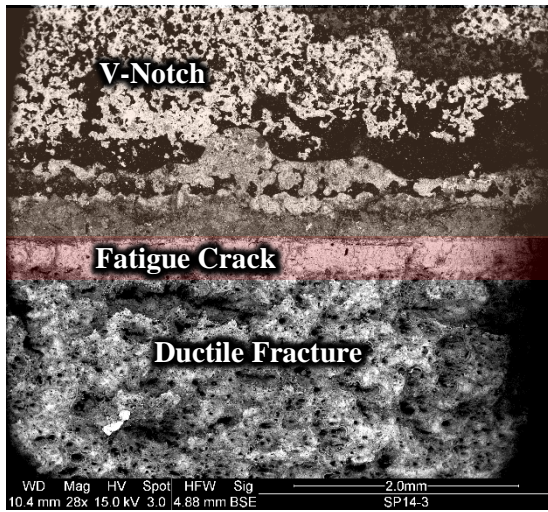
a) V-notch, Fatigue Crack, and Ductile
Fracture area under SEM in sample location 3
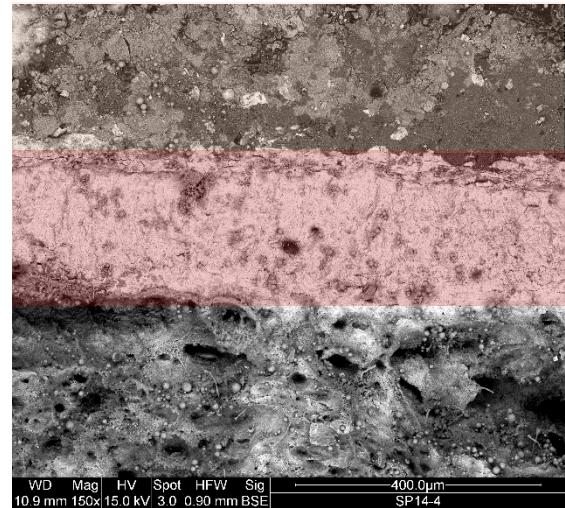
b) Sample location 4 under SEM

**Figure 5.3: Pictures taken by SEM at different locations of the V-notch after fatigue and burst test**

A schematic and a photo of the test setup used for fatigue load step are shown in Figure 5.4. The test specimen rested on three T-shaped stiff steel supports. On the middle support, a steel collar with the same radius as the pipes was installed to secure the pipe specimen onto the steel support. A steel roller and a steel pin were installed in between the pipe and the T-support at two ends of the pipe specimen. The fatigue load cycles were simulated using a ±500 kN fatigue loading actuator and the load ratio was 0.5. Fatigue load cycles continued for 50,000 cycles to introduce a crack with depth of about 0.3 mm through the thickness of the pipe wall and at the tip of the V-notch. Number of cycles required to reach 0.3 mm crack depth was predicted from the test data obtained from CT (compact tension) specimens completed in a previous research completed by the CERP at the University of Windsor [20] and from previous trial tests on full-scale pipes specimens.
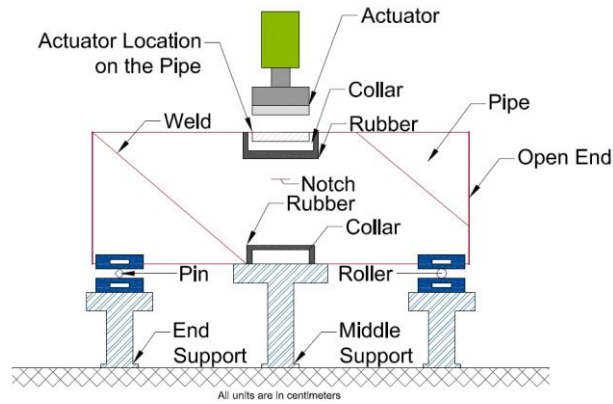
**a) Schematic**



**b) Photo**

**Figure 5.4: Schematic and photo of fatigue load test setup**

*Denting load test*

In the next loading step, a dent of rectangular shape and required depth (Table 5.1) was created on the pipe wall at the notch-crack defect location by applying a load through the steel indenter using displacement control method. Figure 5.5 shows the schematic and a photo of the test setup used in the dent test. The pipe specimen during this loading step was placed on three rigid T-shaped steel supports. The load was applied to the pipe wall at the mid-length through the steel indenter. A universal loading actuator was used to apply

this load through the steel indenter. The internal pressure (Table 5.1) was held constant during this indentation process and the internal pressure was applied using a hydrostatic pump and the pressure was controlled through a pressure transducer which was connected to the computerized data acquisition system. The pre-cracked V-notch part of the pipe wall was placed directly underneath the center of the indenter (Figure 5.5).
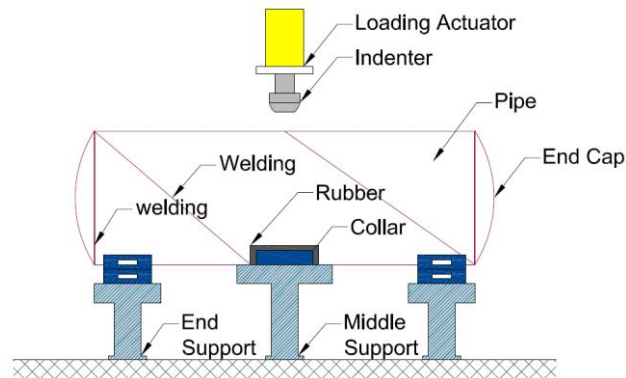


**a) Schematics**



**b) Photo**

**Figure 5.5: Schematic and photo of denting test setup**

The total and plastic deformations of the pipe due to application of denting load were measured using linear variable differential transducers (LVDTs). Two LVDTs were used. The LVDTs were located at the top of the actuator to measure the linear vertical

displacement of indenter. Steel hemispherical steel end caps were welded to the both ends of the pipe specimen to be able to apply internal water pressure. The internal pressure was applied using a hydrostatic pump. Each pipe specimen was instrumented with several strain gauges installed along the crack length to acquire the strain data during this denting loading process. These strains were later used to validate finite element (FE) model.

*Burst pressure test*

The pipe specimen with dent-crack defect was then subjected to monotonically increasing water pressure until a leak or a rupture occurred in the dent-crack defect. The pipe specimen in this loading step was placed on semi-circular bed trolley (Figure 5.6). Pressure was monitored using an electronic pressure transducer and also through a mechanical pressure gauge. Both were mounted on one of the end caps. The pipe specimen was then pressurized with a high capacity hydrostatic pressure pump to determine the burst strength of the pipe with dent-crack defect.



**Figure 5.6: Burst test setup**

## 5.3 TEST RESULTS

### 5.3.1 Load-deformation behaviour

For specimens SP2-P00-D2, SP3-P00-D4, SP4-P00-D6, and SP5-P30-D4, desired permanent dent depth was reached on the pipe using the rectangular indenter. The load-deformation behaviours of these specimens are shown in Figures 5.7a and 5.7b. The load in these figures represents the quasi-static load applied through the indenter during the indentation process and the deformation is the vertical movement of the indenter. Specimen SP1-P00-D0 did not have any dent and hence, no load-deformation plot is available for this specimen.

Figure 5.7a shows the load-deformation for three specimens, SP2-P00-D2, SP3-P00-D4, and SP4-P00-D6. These three specimens had no internal pressure during application of the denting load and they were dented with same indenter. The difference in these specimens was the permanent dent depth which varied from 2% to 6%. From this figure it can be found that as the permanent depth reduces the maximum load and total deformation reduce as well.

Figure 5.7b shows load-deformation behaviour of specimens SP3-P00-D4 and SP5-P30-D4. These two specimens were identical except the internal pressure during application of denting load was different and it ranged from no pressure to $0.3p_y$. This figure shows that as the operating (internal) pressure of linepipe increases the maximum load and total displacement required to produce same permanent deformation depth (4%) increase as well. The maximum load required for these two specimens were 497 kN and 183 kN, respectively. The total deformation required for these two specimen were 64 mm and 49 mm, respectively. Further, SP3-P00-D4 showed a total deformation of 11 mm at a

load level of 100 kN. However, SP5-P30-D4 required a load of 157 kN to achieve the same amount of deformation of 11 mm.  Hence, specimen SP5-P30-D4 behaved stiffer than specimen SP3-P00-D4. The reason for this is the specimen SP5-P30-D4 was subjected to internal pressure of 3.8 MPa (550 psi) whereas, specimen SP3-P00-D4 did not have any internal pressure during denting process.

In specimens SP2-P00-D2, SP3-P00-D4, and SP4-P00-D6 no internal pressure was applied during denting process. However, the dent depth for these three specimens was varied to 2%, 4%, and 6%, respectively (see Figure 5.7a).  This figure shows that the yield load capacity for these three specimens is almost same (~110 kN). However, the maximum load increased by 40%, that is, it increased from 147 kN to 241 kN as the dent depth increased from 2% to 6%.



| a) Specimens SP2, SP3, and SP4 | b) Specimens SP3 and SP5 |
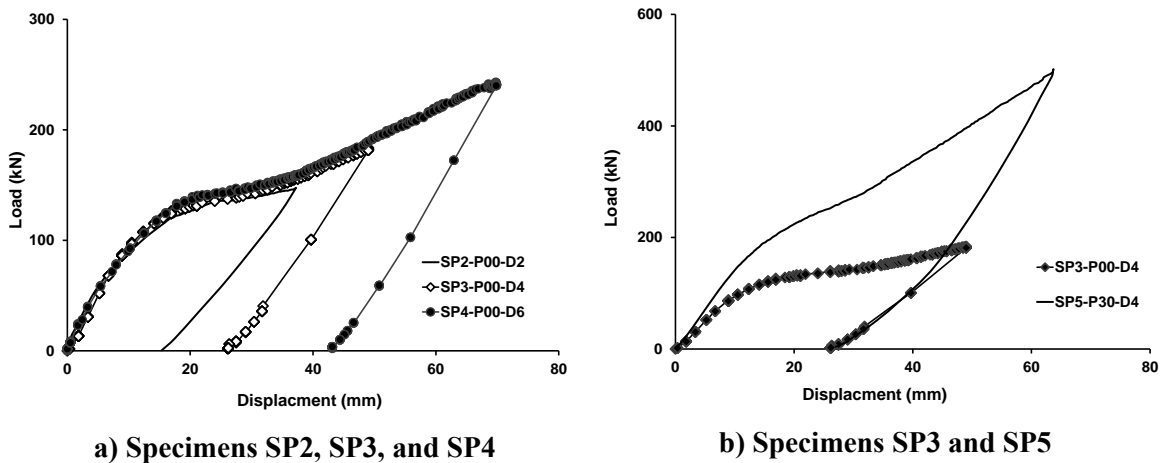
**Figure 5.7: Load-deformation behaviours**

### 5.3.2 Burst strength

The value of yield pressure ($p_y$) for NPS30 X70 grade pipe specimen used in this study is 12.67 MPa (1837 psi). For specimens SP1-P00-D0, SP2-P00-D2, SP3-P00-D4, and SP4-P00-D6 which had four different dent depths ranging from no dent to 6%, the burst strength varied by more than 3.1 MPa (450 psi) which is considerable. The value of burst pressure for these four specimens was found to be 12.01 MPa (1749 psi), 10.5 MPa (1520 psi), 9.6 MPa (1385 psi), and 8.9 MPa (1293 psi), respectively (Figure 5.8). In other words, it can be said that the burst strength of these four specimens was found to be $0.95p_y$, $0.83p_y$, $0.75p_y$, and $0.7p_y$, respectively. Hence, the pressure strength of SP1-P00-D0 that had no dent (0% dent depth) was 26% higher than the same pipe with 6% dent depth, that is, the specimen SP4-P00-D6. It is worth mentioning that the dent in these four specimens was formed with no internal pressure. As can be found from Figure 5.8, the burst pressure of specimens SP1-P00-D0 and SP2-P00-D2 are more than the maximum allowable operating pressure (MAOP) which is assumed to be $0.8p_y$. However, the burst pressures of specimens SP3-P00-D4 and SP4-P00-D6 which had dent depths of 4% and 6% are less than MAOP. Hence, The study found that the burst strength of this pipe with dent-crack defect is significantly affected by the dent depth and Figure 5.8 shows that linepipe with dent-crack defect with dent depth above 2.5% is not able to sustain MAOP.

All specimens in Table 5.1 had crack depth of 4 mm. All these specimens exhibited burst strength lower than the yield pressure or $p_y$. The MAOP in field linepipes is usually restricted to $0.8p_y$. However, the linepipes are expected to subject to $1.05p_y$ to $1.10p_y$ during hydro test. Therefore, the test results of this study found that this linepipe with dent-crack defect for any dent depth and with crack depth being 4 mm or higher will pose a threat to

the structural integrity of the pipeline while subjected to hydro test (Figure 5.8). In other words, the study found that this pipe with crack defect alone where crack depth is 4 mm or higher is unable to sustain the yield pressure or $p_y$.

Specimens SP3-P00-D4 and SP5-P30-D4 had same dent depth of 4%; however, the internal pressure during denting varied between no internal pressure in specimen SP3-P00-D4 and internal pressure of 3.8 MPa (550 psi) or $0.3p_y$ in specimen SP5-P30-D4. The burst pressure for specimen SP5-P30-D4 was 9.4 MPa (1367 psi) which is $0.74p_y$ (Figure 5.8). The burst pressure of SP3-P00-D4 was 9.6 MPa (1385 psi) which is 0.75py. Hence, experimental data of this study showed that the burst strength of pipes with dent-crack defect is not affected by the level of internal or operating pressure during the formation of the dent. Nonetheless, the burst pressure of both specimens (SP3-P00-D4 and SP5-P30-D4) is less than the maximum allowable operating pressure (MAOP) of $0.8p_y$ (Figure 5.8).
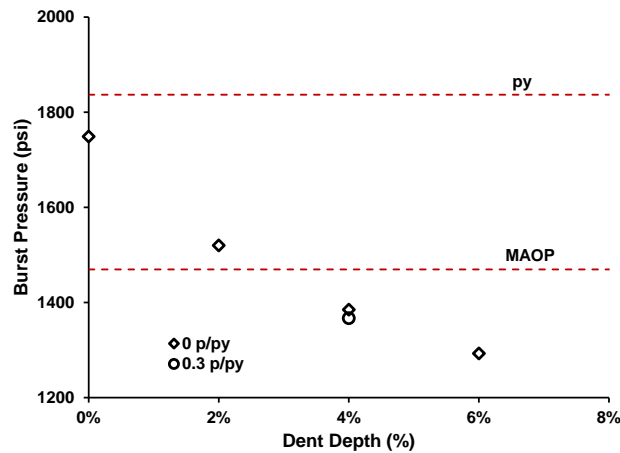


**Figure 5.8: Burst pressure of test specimens**

Test data of this study found that between the two parameters: dent depth and internal pressure during denting (operating pressure), the former has greater effect on the

burst strength of this pipe when a dent-crack defect forms. However, this observation may be valid only with the depth of the crack remains unchanged to 4 mm.

### 5.3.3 Failure mode

Figure 5.9 shows the failure area of the pipe specimens SP1-P00-D0, SP3-P00-D4, SP4-P00-D6, and SP5-P30-D4. Figures 5.9a, 5.9b, and 5.9c show the opening at the crack-notch location due to burst pressure test for specimens SP1-P00-D0, SP3-P00-D4, SP4-P00-D6. All these three specimens were similar except the dent depth varying from no dent to 6%. These figures show that as in the permanent dent depth increases the amount of opening of the crack after failure decreases. This indicates that specimen SP4-P00-D6 exhibited most ductile fracture at the crack-notch defect leading to leaking. On the other hand, specimen SP1-P00-D0 had no dent and thus, had no plastic deformation which resulted in violent rupture at the crack-notch location. In the other word, SP4-P00-D6 had a ductile failure (or leaking) while SP1-P00-D0 experienced a rupture failure. Further, it can be found from Figures 5.9b and 5.9d, the pipe specimen SP5-P30-D4 which maintained internal pressure of $0.3p_y$ during indentation process exhibited much higher ductile failure (leaking) in comparison with the pipe specimen SP3-P00-D4 which had no internal pressure during denting process. Specimen SP3-P00-D4 exhibited a rupture failure in the dent-crack location. It is worth noting that both pipe specimens experienced same dent depth of 4%. Hence, this study shows that internal pressure or operating pressure of the linepipe has significant effect on the failure mode of pipe with dent-crack defect.

**a) Fracture area in SP1-P00-D0**


**b) Fracture area in SP3-P00-D4**


**c) Fracture area in SP4-P00-D6**


**d) Fracture area in SP5-P30-D4**

**Figure 5.9: Fracture area after burst test on pipe**

## 5.4 FINITE ELEMENT MODELING AND ANALYSIS

Experimental testing is the most conventional and reliable way to study the behaviour of pipe. However, it is impossible to obtain all the information required for a thorough understanding from the experimental data alone. Experimental method is also expensive and time consuming. Hence, it is not viable to consider full-scale tests for a wide range of test parameters. An alternative method to study and predict the behaviour of such

specimens is to use numerical tools such as finite element analysis (FEA) method. In the current study, numerical modeling technique considering both material and geometric nonlinearity was used to simulate the behaviour of the test specimens. Commercially available general purpose finite element analysis code, ABAQUS/Standard version 6.11.2 distributed by SIMULIA [21] was used to model the pipe behaviour. It is often argued that load created by geotechnical causes can be either load control or displacement control. However, no general consensus on this can be found. The objective of developing the finite element model was to determine the burst strength of the NPS30 X70 grade pipe used in this study when a crack-dent defect has developed on the pipe surface with various internal (operating) pressures and various permanent (dent) depths.

Only half of the pipe length was modeled since the pipe was symmetric about its mid-length or mid-span which saved computational time. This half-length FEA model was compared with the full-length FEA model and a good agreement between the full-length and half-length FEA models was obtained. Displacement boundary conditions were applied on the circumferential planes of the symmetry (z-plane symmetry) in the half-length model. The model was created to closely reflect the test specimen and loading steps (see Figures 5.5, 5.6, and 5.10).

First order solid element, C3D8R (8-node linear brick), with reduced integration was used to model pipe wall. Minimum of four elements were used through the wall thickness. First order element was used to minimize solution time. However, the 10-node quadratic (second order) tetrahedron solid element, C3D10, was used in and around the notch area where geometry was complex and stress concentration was expected to be high.

The indenter and the T-shaped supports were modeled as discrete rigid body using 4-node rigid quadrilateral element, R3D4, because these supports and the indenter were relatively much more rigid than the pipe specimen and the deformations in these supports and the indenter were negligible. Figures 5.10a to 5.10d show typical meshing schemes used or the pipe specimen, meshing scheme around notch and dented area of the pipe specimen, meshing of rigid supports, and meshing of the indenter. Mesh convergence studies were performed to obtain optimum sizes of various elements used in the FEA model.

A surface-to-node contact using a hard contact algorithm was assigned between the rectangular indenter and the pipe wall during the dent loading process. The internal pressure was applied to the inner surface of the pipe wall. In the tests, thick hemispherical steel end caps were used at both ends of the pipe specimen to hold the water and to apply internal pressure. Hence, in the FEA model, these end caps were modeled as an elastic-plastic steel with modulus of elasticity of 204 GPa. Actual dimensions as used in the test setup were used. A surface-to-node contact algorithm was also used to simulate possible sliding movement between the T-supports and the pipe specimen. An elastic-plastic material behaviour as obtained from the material tension tests and as shown in Figure 5.11 using von-Mises yield criterion and isotropic hardening with associated plastic flow rule was used in the FE models. In the FE model, it was assumed that a failure occurs when the maximum equivalent plastic (MEP) strain at any integration point reaches the maximum equivalent plastic strain at rupture obtained from material tensile tests. In this study, the value of this strain is considered as 100% [22].

**c) End Support**

**a) Pipe**

**d) Indenter**

**b) Crack**
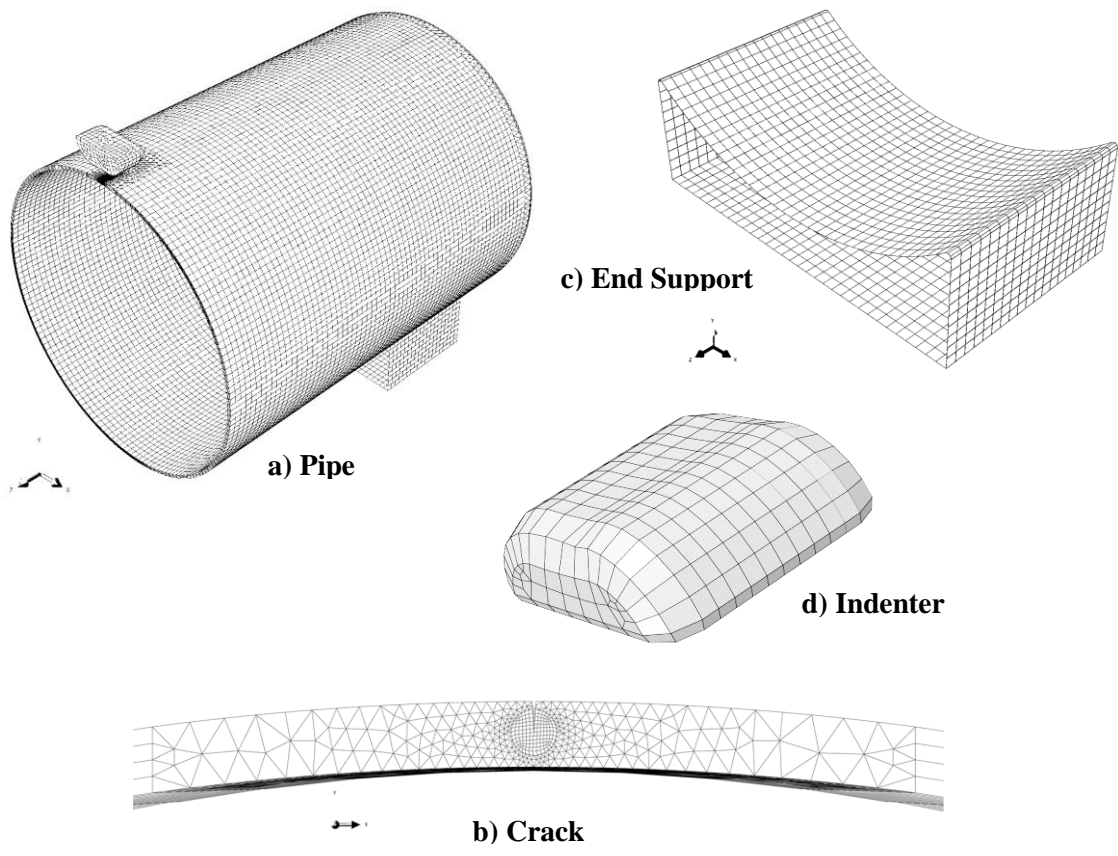
**Figure 5.10: Meshed pipe and notch area**
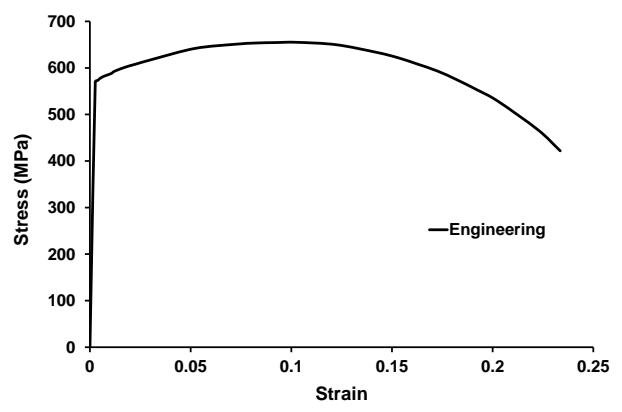


**Figure 5.11: Stress-strain relationship for pipe material**

**5.4.1 FEA model validation**

The finite element (FE) models were validated using the load-deformation behaviour and strain data obtained from the tests. The comparison of the load-deformation relationships for specimens SP3-P00-D4 and SP5-P30-D4 between test and finite element analyses are shown in Figures 5.12a and 5.12b, respectively. In these figures actual test data and actual FE data are plotted. A good agreement between the test and numerical behaviours is observed. The longitudinal strain distribution in the dented area for specimens SP3-P00-D4 and SP5-P30-D4 obtained from the tests and FEA are shown in Figures 5.13a and 5.13b, respectively. The experimental strain data were acquired from the strain gauges located on the longitudinal line drawn through the centerline of the dent and hence, this line coincides with the orientation of the crack. In Figures 5.13a and 5.13b, the distance on the x-axis were measured from the edge of the dent of the pipe. These figures also show a good agreement between the test and FEA. Similar correlation between test and FEA for longitudinal strain distributions was also found for other specimens.
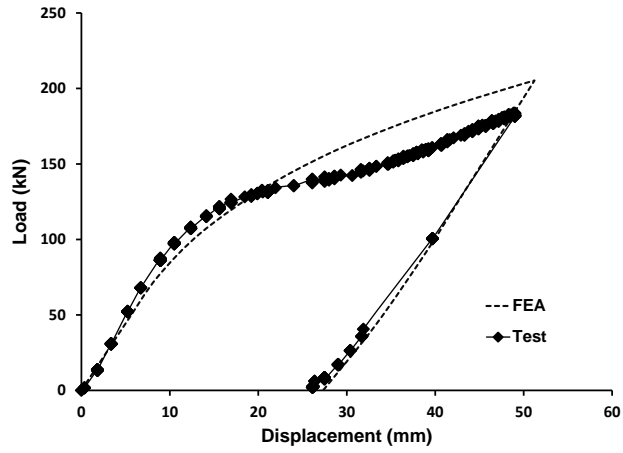
**a) Comparison of SP3-P00-D4 and
FEA model**
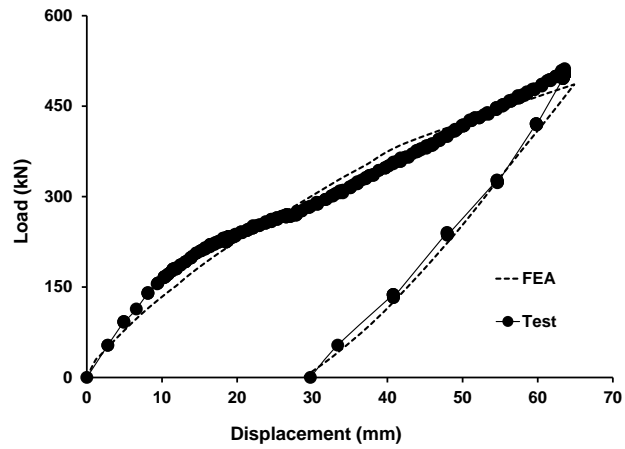


**b) Comparison of SP5-P30-D4
and FEA model**

**Figure 5.12: The load-deformation of tests and FEA models**
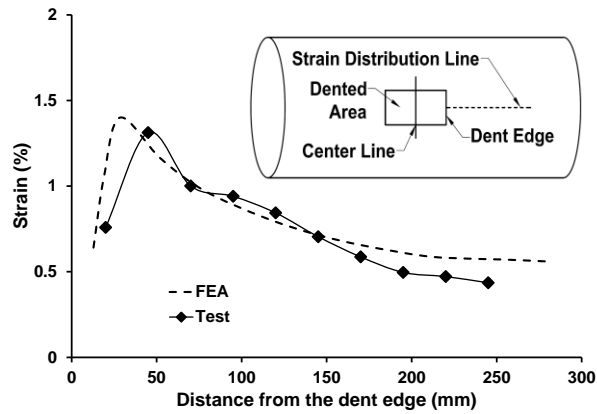
**a) Comparison of SP3-P00-D4
and FEA model**
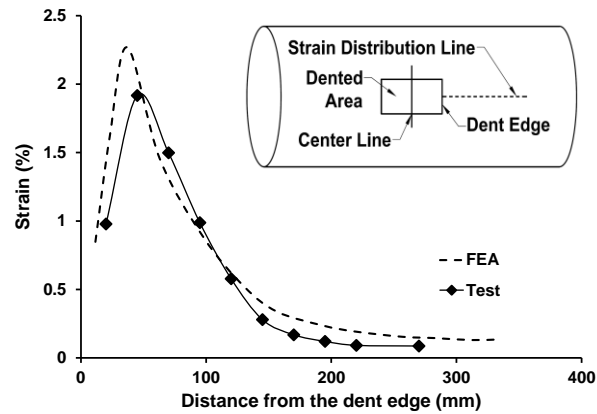


**b) Comparison of SP5-P30-D4
and FEA model**

**Figure 5.13: The longitudinal strain of the tests and FEA models**

## 5.4.2 Parametric study

Parametric study was undertaken to determine the effect of the dent depth and operating (internal) pressure on the burst strength of NPS30 X70 grade oil and gas pipe with dent-crack defect with dent depth and operating pressure of wider ranges than those chosen in the tests. The parameters chosen in the FEA based parametric study are: (1) dent depth which was varied from 0% to 12% of the outer diameter at an increment of 2% and

(2) internal pressure applied during denting process (operating pressure of linepipe) was varied from no internal pressure ($0.0p_y$ to $0.75p_y$). The internal pressures chosen for the FEA based parametric study are: 0 MPa, 3.8 MPa MPa, 7.6 MPa, and 9.5 MPa which correspond to $0.0p_y$, $0.3p_y$, 0.6, and $0.75p_y$, respectively. Figure 5.14 shows the effect of two parameters: (i) level of internal (operating) pressure ($p/p_y$) and (ii) permanent dent depth on the burst strength of NPS30 X70 steel pipe with a crack-dent defect when load is applied using rectangular indenter (Figure 5.10d). As it can be found from Figure 5.14, the internal (operating) pressure (p) and the burst pressure are normalized by the yield pressure ($p_y$). The permanent dent depth is normalized by the outer diameter of the pipe and then converted to percentage. From Figure 5.14, it is evident that the burst strength decreases as the permanent dent depth increase. It is due to the fact that as the dent depth increases, area around crack experienced more strain concentration and more plastic deformation resulting in lesser amount of burst pressure capacity. Figure 5.14 also shows that as the internal (operating) pressure increases the burst pressure decreases, though the effect of internal pressure is not significant. As an example, for the pipes with dent depth of 12% and for various internal pressures the maximum difference between the burst strength is only $0.05p_y$ or 0.63 MPa. Thus, the lowest burst strength was obtained when the internal pressure and the dent depth were at the maximum values. The minimum value of the burst strength for this pipe was obtained at $0.62p_y$ which is much lower than the MAOP. In the other word, burst pressure of pipe with 12% of permanent dent depth and 4 mm crack depth is 38% less than the specimen with no dent but with same crack depth of 4 mm. Such lower burst pressure capacity will result in problem of the structural integrity of this linepipe.
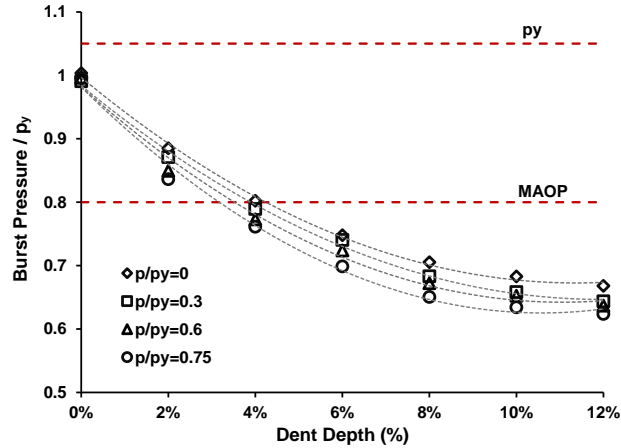
**Figure 5.14: Effect of dent depth and internal pressure on burst pressure
of pipe specimens**


## 5.5 CONCLUSIONS

The conclusions made in this paper are based on full-scale tests and finite element analyses completed. Hence, these conclusions are limited to the pipe specimen, test method, and parametric study used in this research work.

1. The burst pressure or burst strength of this pipe with dent-crack defect is influenced by both internal or pipeline operating pressure and the dent depth. However, the dent depth has much greater effect whereas; the operating pressure does not have much effect assuming that crack depth remains unchanged.

2. This linepipe with dent-crack defect with dent depth above 2.5% is not able to sustain MAOP.

3. This linepipe with dent-crack defect with crack depth of 4 mm or larger but with or without any dent can pose a threat to the structural integrity of the pipeline while subjected to hydro test.

111

4. The failure mode at dent-crack defect is influenced by the level of operating pressure.

5. Parametric study shows that burst strength in this pipe can reduce by as much as 38% when a dent-crack defect develops in the pipe wall and this could be a matter of serious concern for structural integrity of this linepipe.

## 5.6 ACKNOWLEDGEMENTS

## 5.7 REFERENCES

[1] CEPA, "Canadian Energy Pipeline Association", www.cepa.com, Viewed: Jan 28th, 2014

[2] Smith, R. B., and Gideon, D. N., 1979, "Statistical Analysis of Dot-Opso Data," *Proceedings, Annual Symposium - Society of Flight Test Engineers*, pp. D. 1-D. 9.

[3] Wang, K., and Smith, E., 1982, The Effect of Mechanical Damage on Fracture Initiation in Line Pipe, Part I: Dents, Energy, Mines and Resources Canada, Canada Centre for Mineral and Energy Technology.

[4] Zarea, M. F., Toumbas, D. N., Philibert, C. E., and Deo, I., "Numerical models for static denting and dynamic puncture of gas transmission linepipe and their validation," *Proceedings of the 1996 1st International Pipeline Conference*, IPC. Part 2 (of 2), June 9, 1996 - June 13, 1996, ASME, pp. 777-784.

[5] Lancaster, E. R., 1996, "Burst pressures of pipes containing dents and gouges," *Proceedings of the Institution of Mechanical Engineers*, Part E: Journal of Process Mechanical Engineering, 210(1), pp. 19-27.

[6] Cosham, A., and Hopkins, P., 2004, "The effect of dents in pipelines-guidance in the pipeline defect assessment manual," International Journal of Pressure Vessels and Piping, **81**(2), pp. 127-139.

[7] Karamanos, S. A., and Andreadakis, K. P., 2006, "Denting of internally pressurized tubes under lateral loads," International Journal of Mechanical Sciences, **48**(10), pp. 1080-1094.

[8] Hopkins, P., Jones, D., and Clyne, A., "The Significance of Dents and Defects in Transmission Pipelines," *Proceedings of the International Conference on Pipework Engineering and Operations*, London, UK.

[9] Bjornoy, O. H., Rengard, O., Fredheim, S., and Bruce, P., "Residual Strength of Dented Pipelines, DNV Test Results," *Proc. Proceedings of the 10th International Offshore and Polar Engineering Conference*, May 28, 2000 - June 2, 2000, ISOPE, pp. 182-188.

[10] ASME, 2012, "B31.4: Pipeline Transportation Systems for Liquids and Slurries," ASME International, New York, NY, USA.

[11] CSA, 2007, "Z662-07: Oil and Gas Pipeline Systems," Canadian Standard Association, Mississauga, ON, Canada.

[12] Staat, M., and Duc Khoi, V., 2013, "Limit Analysis of Flaws in Pressurized Pipes and Cylindrical Vessels. Part II: Circumferential Defects," Engineering Fracture Mechanics, **97**, pp. 314-333.

[13] ASME, 2004, "B31G-1991 (R2004): Manual for Determining Remaining Strength of Corroded Pipelines: Supplement to B31 Code-Pressure Piping," ASME International, New York, NY, USA.

[14] DNV, 2012, "OS-F101: Submarine Pipeline Systems," Det Norske Veritas.

[15] Bachut, J., and Iflefel, I. B., 2011, "Analysis of Pipes Containing Plain and Gouged Dents," Strain, **47**(SUPPL. 1), pp. e34-e51.

[16] Maxey, W. A., 1986, "Topical Report on Outside Force Defect Behaviour: To Line Pipe Research Supervisory Committee of the Pipeline Research Committee of the American Gas Association, " NG-18 Report No. 162, AGA Catalogue No. L51518, Batelle.

[17] API, 2012, "Spec 5L: Specification for Line Pipe," American Petroleum Institute, Washington, DC, USA.

[18] ASTM, 2011, "E8/E8M-11: Standard Test Methods for Tension Testing of Metallic Materials," ASTM International West Conshohocken, Pennsylvania, USA.

[19] Ghaednia, H., Silva, J., Kenno, S., Das, S., Wang, R., and Kania, R., 2013, "Pressure Tests on 30-In Diameter X65 Grade Pipes with Dent-Crack Defects," The Journal of Pipeline Engineering, **12**(1), p. 7.

[20] Silva, J., Ghaednia, H., and Das, S., "Fatigue Life Assessment for Nps30 Steel Pipe," *Proc. 2012 9th International Pipeline Conference*, IPC 2012, September 24, 2012 - September 28, 2012, American Society of Mechanical Engineers, pp. 619-624.

[21] SIMULIA, 2011, Analysis User's Manuals, Dassault Systèmes Simulia Corp., Rising Sun Mills, Providence,  RI, USA.

[22] Das, S., Cheng, J. J. R., and Murray, D. W., 2007, "Prediction of Fracture In Wrinkled Energy Pipelines Subjected to Cyclic Deformations," International Journal of Offshore and Polar Engineering, **17**(3), pp. 205-212.

# CHAPTER 6

# DEPENDENCE OF BURST STRENGTH ON CRACK LENGTH AND CRACK DEPTH OF A PIPE WITH DENT-CRACK DEFECT

## 6.1 INTRODUCTION

In-service inspections of existing metal pipelines have indicated that the most common cause for pipeline failure is the mechanical damage [1]. Corrosion, crack, puncture, dent, gouge, and combination of such damages are some common examples of surface defects found in the field pipeline. These damages may occur due to many different reasons; construction and excavation activities can cause impact loads resulting in mechanical damages in onshore pipeline while anchors or trawling gear actions can cause mechanical damages in offshore pipelines. It has been reported that the failure of oil and gas transmission pipelines resulting from mechanical damages ranges from 55% in the USA to around 70% in Europe [2-5].

A concentrated lateral load resulting from rock tip or hard surface can also create a dent in the field buried pipeline. A dent is an inward plastic deformation in the pipe wall which causes a gross distortion of the pipe cross section and reduction in pipe diameter locally [1]. The ability of the pipeline to sustain the concentrated loading and transform it into plastic deformation is of particular interest for safeguarding their structural integrity against such loading [1, 6]. Formation of a dent results in localized stress and strain concentrations in the pipe wall which can lead to a leak or a rupture causing loss of

containment, damage to environment, and threat to the safety of habitants living nearby, and also interruption in oil and gas supply, and a loss in the pipeline industry's revenue. A dent also causes local reduction in the pipe diameter and ovalization in the pipe cross-section. Hence, the dent defect has been a major concern for the pipeline operators for many years. Several investigations in the past was completed to understand the effect of dent defect on the structural behaviour of energy pipes under monotonic and cyclic pressures. Based on these research works, it is generally accepted that dent defect alone is not a threat to the integrity of pipe structure under monotonic pressure load when the dent depth is up to 6% of the diameter of the pipe [7, 8].

A dent can be followed by a crack or crack can also develop in a dent as a result of impact action and/or because of exposure to the corrosive environment and/or due to fatigue loading arising from pressure fluctuations and geotechnical movements [9]. Various studies were completed using analytical and experimental techniques to understand the effect of metal loss of the pipe wall such as corrosion or crack on the burst strength of pipeline [10]. Detailed guidelines on predicting the burst strength of such pipes are available in various pipeline design and maintenance codes and standards [7, 8, 11, 12]. Any crack on the surface of pipe wall less than 12.5% of wall thickness of the pipe can be removed by grinding [7, 8]; however, there is no studies to support that.

The burst strength of pipe with single defect such as dent or crack or corrosion has been the subject of many previous research works. Behaviour of pipes with dent-gouge defect was studied as well. However, review of literatures available in the public domain reveals that no studies were undertaken to determine the burst strength of dented pipe that

116

has developed crack in the dent. Such combined defect is called dent-crack defect in this study.

Therefore, this study was completed at the Centre for Engineering Research in Pipelines (CERP), University of Windsor to determine the burst strength of NPS30 X70 pipe with dent-crack defect with various crack depths and crack lengths. This work was completed using a combined method of laboratory based experimental study and finite element method (FEM) based numerical study. This paper discusses the results obtained from this research.

## 6.2 EXPERIMENTAL PROCEDURE

### 6.2.1 Test specimen

The purpose of this study was to determine the burst strength of oil and gas transmitting linepipes that have developed dent-crack defect. This project was completed using both laboratory based experimental work and numerical study using non-linear finite element method (FEM). NPS 30 X70 grade [13] steel pipe used in oil and gas transmission pipelines was chosen to make the test specimens. Six pipe specimens were fabricated from this pipe. The nominal diameter of the pipe is 762 mm (30 in) and the thickness of the pipe wall is 8.5 mm (0.33 in) and hence, the outer diameter-to-thickness ratio (D/t) of the pipe specimens used in the experimental work is about 90. The length of each pipe specimen was 2500 mm (78.74 in) in total. A number of tensile material specimens were cut from a virgin pipe wall and the standard material tensile tests were carried out to determine the mechanical properties of the pipe material in accordance with ASTM E8 [14]. The properties of the material obtained from theses tensile tests are: actual yield strength of 543 MPa at 5% total strain; tensile strength of 624 MPa; and modulus of elasticity of about 204

GPa. The nominal (engineering) values of fracture stress and fracture strain were determined after the completion of the material tests. In addition to tensile test, Charpy V notch impact test were conducted on five subsize specimens (full wall thickness specimens) to ensure the pipe material has sufficient ductility. Average value of Charpy toughness was found to be 152 J.

Two ends of the specimen were welded to thick hemispherical steel end caps for holding water pressure during dent formation process and also during burst strength test. Water was used as the fluid in the test specimens. The internal pressure was held constant at 0.3py or 30% of $p_y$ which is about 3.8 MPa (550 psi) during the denting process. The yield pressure for this pipe was calculated at 12.67 MPa (1837 psi). A rectangular indenter was used to create the dent as can be seen in Figure 6.1. The length (dimension in the direction of the length of the pipe) and the width (dimension in the circumferential direction of the pipe) for the indenter were 100 mm and 50 mm, respectively. The indenter was made by machining a solid steel slab. The permanent dent depth (plastic deformation due to denting) for these specimens was kept unchanged at 4% of the outer diameter of the pipe or 28 mm which is less than allowable dent depth of 6% defined by ASME B31.4 [7]. The permanent dent depth is the plastic deformation resulted from denting process and calculated after removal of the indenter.

Each test specimens was required to go through three different load tests and hence, each pipe specimen was required to go through three different test setups, three different instrumentations, and three different loading steps. These three loading steps are: (i) fatigue load test, (ii) denting load test, and (iii) finally, the burst or monotonically increasing pressure loading test. These loading steps are explained in the following sections.

Table 6.1 shows the matrix of the test specimens used in this study. All the pipes had an EDM (electro-discharging machine) cut crack-like V-notch. The notches were located at the mid-length of the pipe specimens and it was oriented in the direction of the length of the pipe specimen. The width of the V-notch was about 0.3 mm and the notch length was varied to 20 mm, 100mm, and 200 mm (Table 6.1). A total of six full-scale tests were completed under the scope of this study. Specimens were named to reflect the primary attributes attached to each specimen. For example, specimen SP2-D4-L20, the first two letters and a number combination (SP2) indicates that it is specimen number 2, the next letter and a number (D4) indicates that the specimen had a 4 mm deep crack depth, and the last combination of letter and number (L20) indicates that the crack length on the pipe was 20 mm. Hence, the specimen SP3-D4-L200 was the third specimen and this specimen was identical to specimen SP2-D4-L20 except in the former specimen, the crack length was 200 mm. The first specimen in Table 6.1, SP1-D4-L100 is considered as the reference specimen while considering the effect of crack length (20 mm, 100 mm, and 200 mm), and crack depth (2 mm, 3 mm, 4 mm, and 5 mm), are evaluated.

**Table 6.1: Test matrix**

| Specimen name (SP) | Crack Depth (D) | Crack Length (L) | Parameter |
|---|---|---|---|
| SP1-D4-L100 | 4 mm | 100 mm | Reference specimen |
| SP2-D4-L20 | 4 mm | 20 mm | Crack length |
| SP3-D4-L200 | 4 mm | 200 mm | |
| SP4-D2-L100 | 2 mm | 100 mm | Crack depth |
| SP5-D3-L100 | 3 mm | 100 mm | |
| SP6-D5-L100 | 5 mm | 100 mm | |

**\* Pressure held constant at 3.8 MPa (0.3$p_y$) during application of denting load**
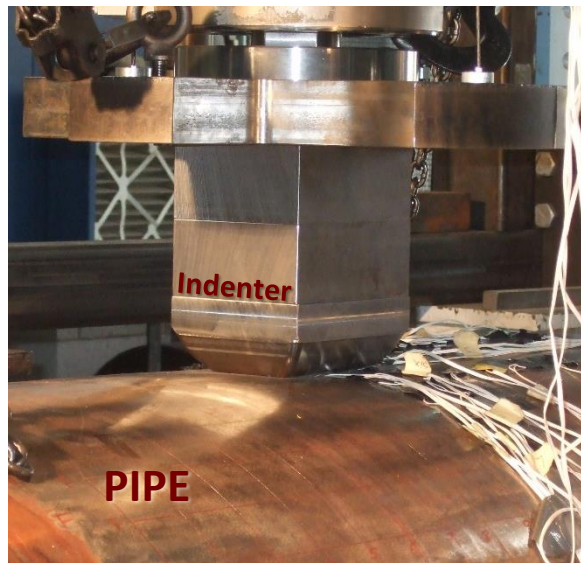**\* Dent depth was kept unchanged at 28 mm (4%)**



**Figure 6.1: Rectangular indenter used to create dent**

## 6.2.2 Test setup and instrumentation

The purpose of these tests was to study how burst strength of pipes with dent-crack defect is affected by crack length and crack depth. All the full-scale specimens were subjected to the same loading procedure. First, the fatigue load was applied to precrack the specimens, followed by denting load to have dent-crack defect, and finally pipes were subjected to monotonically increasing water pressure until rupture occurred in the dent-crack defect to measure burst strength of pipe specimens. All the experimental work was completed by CERP in the structural engineering laboratory of the University of Windsor.

### *Fatigue load test*

Fatigue load was applied to create a crack at the tip of the V-notch through the thickness of the pipe wall (Figure 6.2a). Hence, an EDM (electro-discharging machine) cut crack-like fine V-notch was created. The dimensions of the notch were: 100 mm long (±1%) along the longitudinal direction, 0.3 mm (±3%) wide at the top of the outside surface of the pipe wall, and 2 mm to 4 mm (±1%) deep (Figure 6.2a). Previous study completed at the CERP found that pipe with dent-crack defect and a crack depth less than 2 mm does not affect the burst strength of this dented pipe [15] and hence the minimum notch depth chosen in the current study is 2mm. Then, the pipe specimen with a notch on its surface was subjected to fatigue load cycles with load ratio of 0.5 and the fatigue loading continued until a precrack at the tip of the V-notch of about 0.3 mm deep was obtained. As a result, a true crack developed at the notch tip (see Figure 6.2a). After completion of burst test, ten small samples were cut from various locations on notch-crack area of each specimen and examined under the Scanning Electron Microscope (SEM) to determine true depth of the crack in all the pipe specimens. Figure 6.2b shows how the samples were numbered and

where they were located. Figure 6.3 shows SEM pictures taken at two different locations

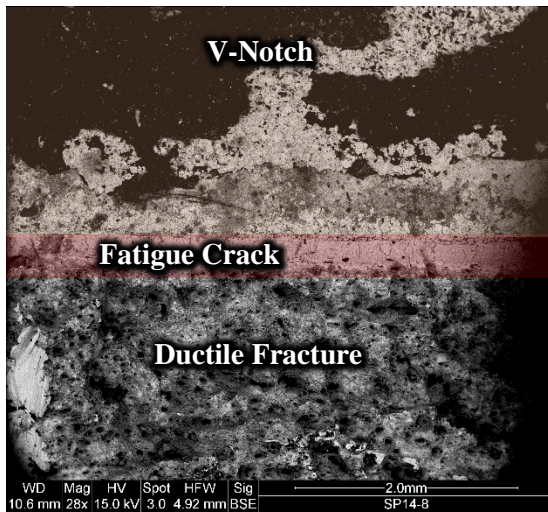of the wall cross-section after fatigue crack was obtained.
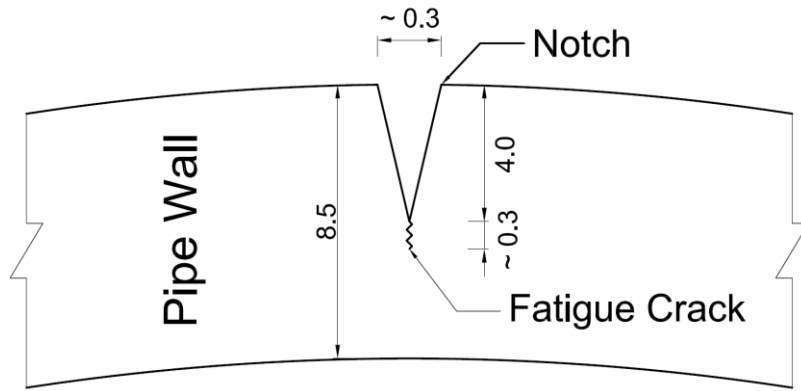


**a) Pipe wall section showing V- notch and crack**
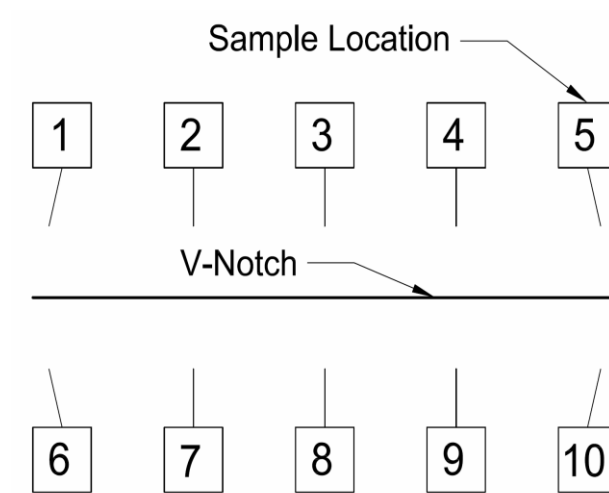


**b) Sample location on the V-notch**

**Figure 6.2: EDM cut V- notch on pipe wall**

**a) V-notch, fatigue crack, and ductile fracture areas for location 8**
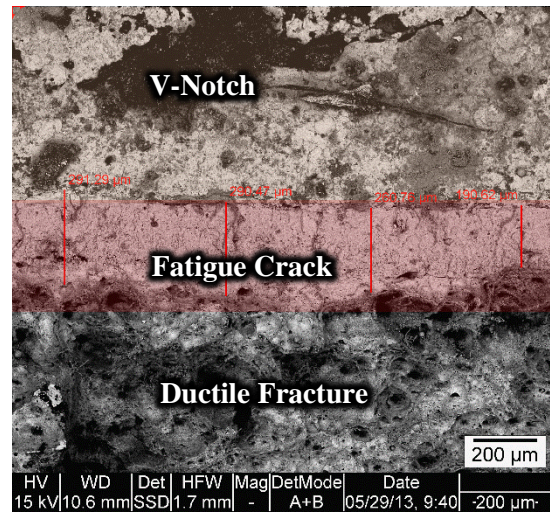


**b) V-notch, fatigue crack, and ductile fracture areas for location 4**

**Figure 6.3: Pictures taken by SEM at different locations of the V-notch**

A schematic and a photo of the test setup used in the fatigue load step are shown in Figure 6.4. The test specimen rested on three T-shaped stiff steel supports. The fatigue load cycles were applied using a ±500 kN fatigue loading actuator with the load ratio of 0.5. Fatigue load cycles continued for 50,000 cycles to introduce a precrack with depth of about 0.3 mm through the thickness of the pipe wall and at the tip of the V-notch. Number of cycles required to reach 0.3 mm crack depth was predicted from the test data obtained from CT (compact tension) specimens completed in a previous research completed by the CERP at the University of Windsor [15] and this was verified in previous trial tests on full-scale pipes specimens.
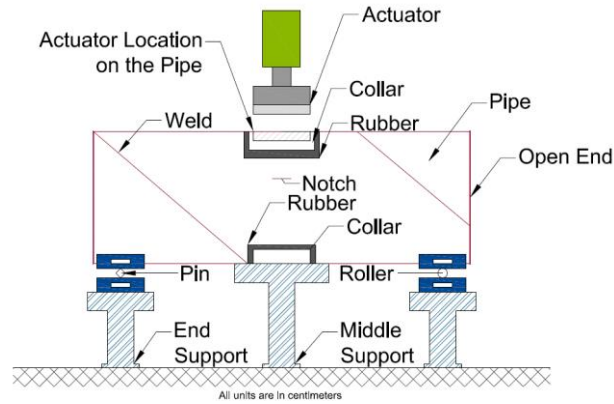
**a) Schematic**



**b) Photo**

**Figure 6.4: Schematic and photo of fatigue load**

*Denting test*

In the dent load step, a dent of rectangular shape was created on the pipe wall such a way that the V-notch defect was located at the mid-length of the dent. Figure 6.5a schematically shows the test setup. The pipe specimen was placed on three very thick and rigid T-shaped steel supports. Denting load was applied on the top surface of the pipe wall using a universal loading actuator (Figures 6.5a and 6.5b). The internal pressure (Table 6.1) was held constant at 3.8 MPa (550 psi) during this indentation process and the internal pressure was applied using a hydrostatic pump. The pressure was monitored through a

manual pressure gage and also through a digital pressure transducer which was connected

to the computerized data acquisition system for acquiring the pressure data.
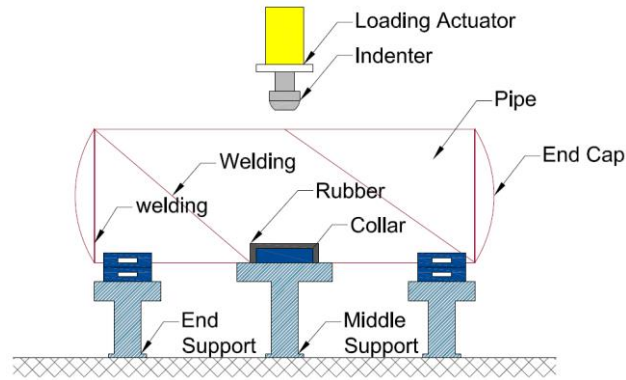


**a) Schematic**



**b) Photo**

**Figure 6.5: Schematic and photo of denting test**

The total (elastic plus plastic) and plastic deformation (dent depth) of the pipe due

to application of denting load was measured using linear variable differential transformers

(LVDTs). Two LVDTs were used. The LVDTs were located on the actuator to acquire

downward displacement of the indenter. Hemispherical steel end caps were welded at the

end of each specimen to hold the water and pressurize the pipes using a hydrostatic pump.

Specimens were instrumented with strain gauges to monitor and record strain distributions

around the dent. The layout of the strain gauges is shown in Figure 6.6. In this figure,

dimension are shown in mm. These strains were later used to validate finite element (FE) model.
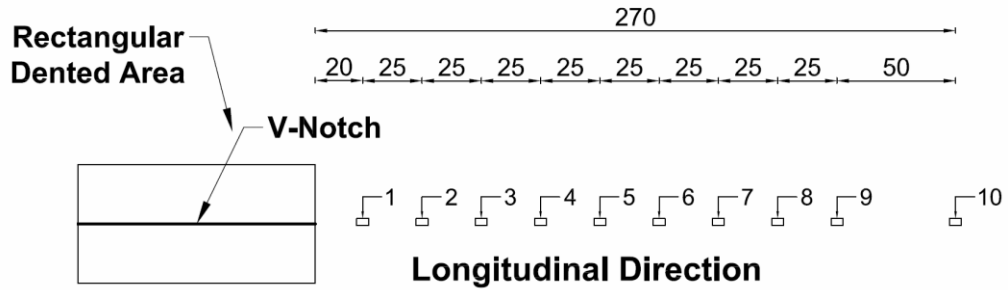


**Figure 6.6: Strain gauge layout**

The load-deformation behaviours of these specimens are shown in Figures 6.7a and 6.7b. The load in these figures represents the quasi-static load applied through the indenter during the indentation process and the deformation is the vertical movement of the indenter. It can be found from these figures that all specimens showed very similar load-deformation behaviour. Also, after unloading, all specimens experienced almost same amount of plastic deformation or dent depth of 28 mm which is 4% of the pipe diameter and hence, it is referred to as 4% dent depth.
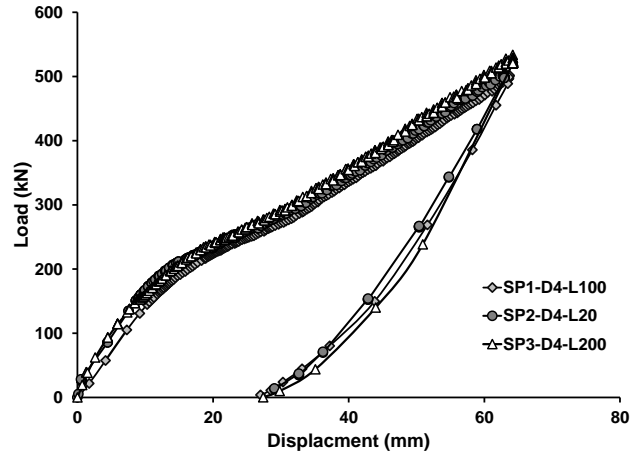
**(a): Specimens SP1, SP2, and SP3**
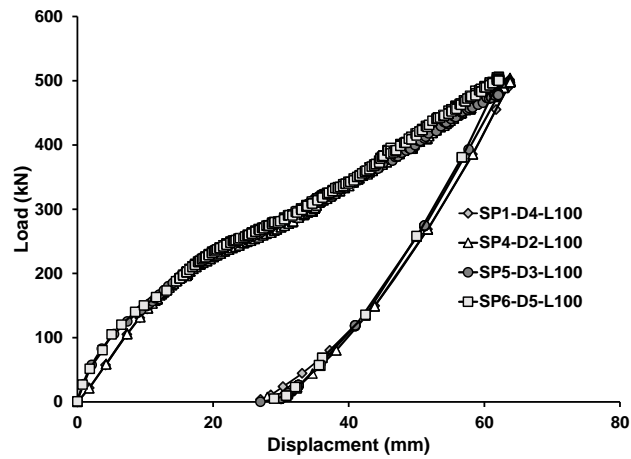


**(b): Specimens SP1, SP4, SP5 and SP6**

**Figure 6.7: Load-deformation behaviours**

## *Burst pressure test*

The pipe specimen with dent-crack defect was then subjected to monotonically increasing water pressure until a leak or a rupture failure occurred in the dent-crack defect. The pipe specimen in this step was placed on semi-circular bed trolley (Figure 6.8). Pressure was monitored using a digital pressure transducer and also through a mechanical pressure gauge. Both were mounted on one of the two end caps. The pipe specimen was

127

then pressurized with a high capacity hydrostatic pressure pump to determine the burst strength of the pipe with dent-crack defect.



**Figure 6.8: Burst test setup**

## 6.3 TEST RESULTS

### 6.3.1 Burst strength

The value of yield pressure ($p_y$) for NPS30 X70 grade pipe specimen used in this study is 12.67 MPa (1837 psi). For specimens SP1-D4-L100, SP2-D4-L20, and SP3-D4-L200 which had three different crack lengths ranging from 20 mm to 200 mm, the burst strength varied by 5.7 MPa (831 psi) or 73.0% which is significant. The value of burst pressure for these three specimens was found to be 9.43 MPa (1367 psi), 13.55 MPa (1966 psi), and 7.82 MPa (1135 psi), respectively (Figure 6.9). In other words, it can be said that the burst strength of these three specimens was found to be 0.74$p_y$, 1.07$p_y$, and 0.62$p_y$, respectively (Figure 6.9). Hence, the pressure strength of SP2-D4-L20 that had 20 mm long crack was 73.0% higher than the same pipe with 200 mm long crack, that is, the specimen

SP3-D4-L200. It is worth mentioning that the dent depth was kept unchanged at 4% and operating pressure during indentation process was also kept unchanged at 3.8 MPa (550 psi) in all these three specimens. As it can be found from Figure 6.9, the burst pressure of specimens SP2-D4-L20 was 13.55 MPa (1966 psi) which is higher than the maximum allowable operating pressure (MAOP) which is assumed to be $0.8p_y$ or 12.67 MPa (1837 psi). However, the burst pressures of specimens SP1-D4-L100 and SP3-D4-L200 which had crack lengths of 100 mm and 200 mm, respectively are less than MAOP. Hence, the study found that the burst strength of this pipe with dent-crack defect is significantly affected by the crack length and Figure 6.9 shows that this linepipe with dent-crack defect with crack length above 80 mm is not able to sustain MAOP and hence, the operating pressure needs to be reduced. In other words, the linepipe with such a dent-crack defect and a crack length of less than 80 mm is still safe to operate at MAOP. It is worth noting, ASME B31.4 code does not provide any guideline on the limiting crack length.
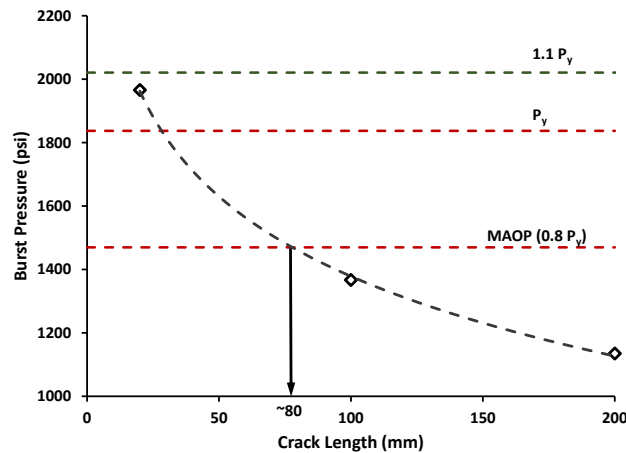


**Figure 6.9: Burst pressure of test specimens**

Specimens SP1-D4-L100, SP4-D2-L100, SP5-D3-L100, and SP6-D5-L100 had same dent depth of 4% and crack length of 100 mm; however, the crack depth varied from 2 mm to 5 mm. Figure 6.10 shows that the burst pressures for these specimens were found

to be 9.43 MPa (1367 psi), 13.95 MPa (2024 psi), 9.89 MPa (1435 psi), and 7.90 MPa (1146 psi), respectively. In other words, the burst strength of these specimens were found to be $0.74p_y$, $1.1p_y$, $0.78p_y$, and $0.62p_y$, respectively. Hence, the difference between pressure strength of SP4-D2-L100 and SP6-D5-L100 that had crack depth of 2 mm and 5 mm, respectively, was about 77% or 6.05 MPa (878 psi). This difference is notably a significant one. As it can be found from Figure 6.10, the burst pressure of specimens SP4-D2-L100 is 13.95 MPa (2024 psi) which is much higher than MAOP. However, the burst pressures of specimens SP1-D4-L100, SP5-D3-L100, and SP6-D5-L100 are less than MAOP. Hence, it was found that the burst strength of this pipe with dent-crack defect is highly affected by the crack depth. It can also be found from Figure 6.10 that linepipe with dent-crack defect and crack depth of more than 3.5 mm (0.4t) is not able to sustain MAOP and the operating pressure needs to be lowered if it is kept in service. In other words, a crack with depth of 2 mm or less is not a threat to safety and structural integrity of these pipes with dent-crack defect when subject to under monotonically increasing pressure load.
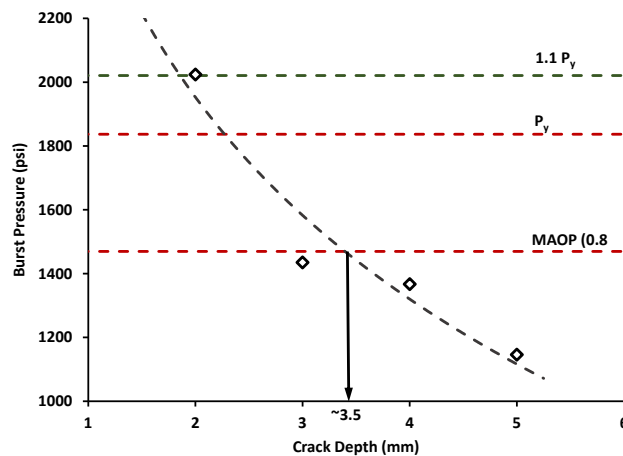


**Figure 6.10: Burst pressure of test**

The MAOP in field linepipes is usually restricted to $0.8p_y$. However, the linepipes are expected to subject to a pressure of 1.05py to $1.10p_y$ during the hydro test. Therefore,

the test results of this study found that this linepipe with dent-crack defect for any crack depth of more than 2 mm and with crack length 20 mm or higher will pose a threat to the structural integrity of the pipeline while subjected to hydro test (Figure 6.9 and 6.10). In other words, the study found that this linepipe with dent depth of 4% where crack depth is 3 mm or higher is unable to sustain the yield pressure or $p_y$.

Test data of this study found that both parameters: crack depth and crack length, have great effect on the burst strength of this pipe when a dent-crack defect forms. However, this observation may be valid only with the depth of the dent remains unchanged to 4%.

**6.3.2 Failure mode**

Figures 6.11a, 6.11b, 6.11c, and 6.11d show the opening at the dent-crack defect due to burst pressure tests on specimens SP1-D4-L100, SP4-D2-L100, SP5-D3-L100 and SP6-D5-L100. All these four specimens were similar except the crack depth which varied from 2 mm to 5 mm. These figures show that as in the crack depth increases the amount of opening of the crack after failure decreases. This indicates that specimen SP6-D5-L100 which had largest crack depth of 5 mm exhibited most ductile fracture at the dent-crack area leading to a leaking failure. On the other hand, specimen SP4-D2-L100 had the least crack depth of 2 mm resulted in a violent rupture failure at the dent-crack location. In the other word, SP6-D5-L100 had a ductile failure (or leaking) while SP4-D2-L100 experienced a rupture failure.
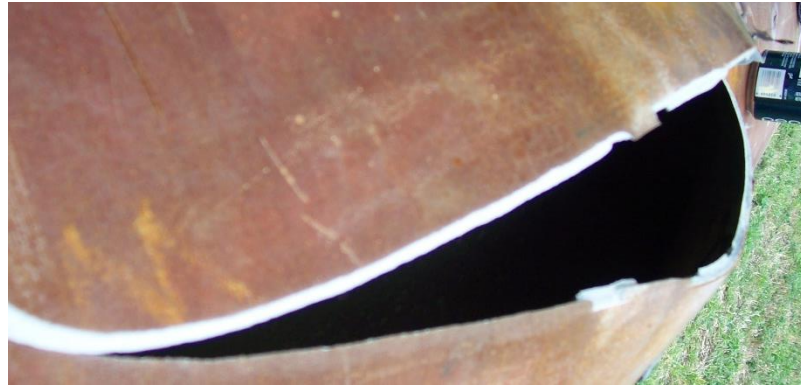
**a) Fracture area in SP4-D2-L100**


**b) Fracture area in SP5-D3-L100**


**c) Fracture area in SP1-D4-L100**


**d) Fracture area in SP6-D5-L100**

**Figure 6.11: Fracture area after burst test on pipe specimens**

Further, it can be found from Figures 6.12a, 6.12b, and 6.12c that the pipe specimen SP1-D4-L100 which had crack length of 100 mm exhibited more ductile failure (leaking) in comparison with the pipe specimens SP2-D4-L20 and SP3-D4-L200 which had 20 mm and 200 mm crack lengths, respectively. These two Specimens exhibited a rupture failure in the dent-crack defect location. In specimen SP3-D4-L200 the crack was larger than dent length and hence, a part of the crack did not experience plastic deformation from the

denting process. As a result, the mode of failure was rupture for this specimen. Hence, it can be conducted that if the entire crack is located inside the dented area, leaking failure is expected to happen. It is worth noting that all pipe specimens experienced same dent depth of 4% and had same internal pressure of 3.8 MPa ($0.3p_y$) during indentation process. Hence, both crack depth and crack length have significant effect on the failure mode of pipe with dent-crack defect. Furthermore, this study suggests that there may be a range of optimum crack length that leads to leakage than rupture. Further study is needed to understand the effect of crack length on failure mode.



a) Fracture area in SP2-D4-L20



b) Fracture area in SP1-D4-L100



c) Fracture area in SP3-D4-L200

**Figure 6.12: Fracture area after burst test on pipe specimens**

## 6.4 FINITE ELEMENT MODELING AND ANALYSIS

In this study, numerical modeling technique considering both material and geometric nonlinearities was used to simulate the behaviour of the test specimens. Commercially available general purpose finite element analysis code, ABAQUS/Standard version 6.13 distributed by SIMULIA [16] was used to model the pipe behaviour. The objective of developing the finite element (FE) model was to determine the burst strength of NPS30 X70 grade pipe used in this study when a crack-dent defect has developed on the pipe surface with wide ranges of internal (operating) pressure, crack depth, and crack length.

Due to the symmetry of the structure (specimen) about its mid-length or mid-span, a half-length FE model, with the axial length of about $3D_0$, was adopted. This half-length FEA model was compared with the full-length FEA model and a good agreement between the full-length and half-length FEA models was obtained. Appropriate boundary conditions for symmetry were applied along all edges of the half-length model. The model was created to closely reflect the test specimen and loading steps (see Figures 6.5 and 6.13).

Figure 6.13a shows a typical mesh used in numerical modelling. Vicinity of dented area was modeled with solid element, C3D8R (8-node linear brick), with reduced integration through the thickness. Minimum of four elements were used through the wall thickness. However, the 10-node quadratic (second order) tetrahedron solid element, C3D10, was used in and around the dent where geometry was complex and stress concentration was expected to be high (Figure 6.13b). Notch tip was modeled using Solid element, C3D20R (Figure 6.13c). The indenter and the T-shaped steel supports were modeled as discrete rigid body using 4-node rigid quadrilateral element, R3D4, because

134

these supports and the indenter were relatively much more rigid than the pipe specimen and the deformations in these supports and the indenter were negligible. Mesh convergence studies were performed to obtain optimum sizes of various elements used in the FEA model.



**b) Crack simulation**

**a) Half-length pipe model**

**c) Meshing Around Crack Tip**
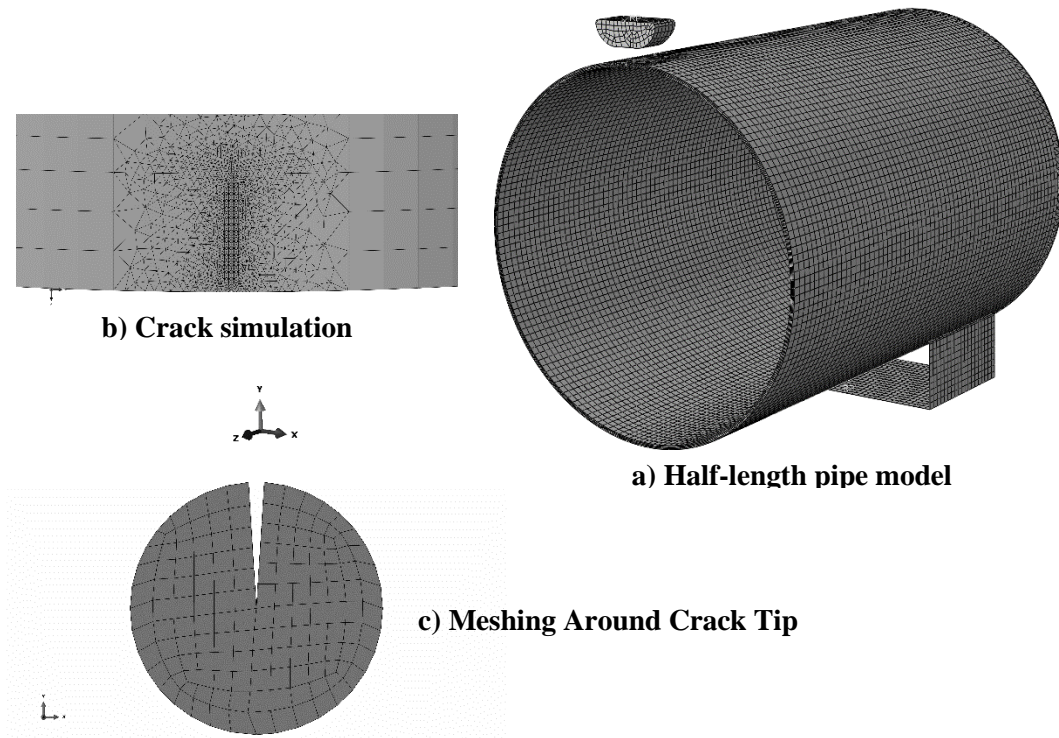
**Figure 6.13: Meshed pipe and notch area**

There were two contact areas in the FE model and these are contact between rectangular indenter and the pipe wall and between the pipe wall and the supports. A surface-to-node contact using a hard contact algorithm was assigned in these two regions while simulating the indentation process. The internal pressure was applied to the inner surface of the pipe wall. In the tests, very thick (12 mm) hemispherical steel end caps were used at both ends of the pipe specimen to hold the water and to apply internal pressure. Hence, in the FEA model, these end caps were modeled as an elastic-plastic steel with modulus of elasticity of 204 GPa. An elastic-plastic material model using von-Mises yield

criterion and isotropic hardening with associated plastic flow rule was used in the FE models.

The critical J integral ($J_{1c}$) can be used to predict the crack initiation in a pipe with dent-crack defect. Also, it can be assumed that a failure occurs when the maximum equivalent plastic (MEP) strain at any integration point reaches the maximum equivalent plastic strain at rupture obtained from material tensile tests. As result, the rupture strain can be conservatively considered as unit [17]. In the FE model, it was assumed that a failure occurs when the J-integral (J) at any integration point around crack tip reaches the maximum value of 1.15 $J_{1c}$ which is equivalent to plastic strain of unit value. The $J_{1c}$ for the pipe material obtained from fracture toughness tests in accordance with the ASTM E1820 [18]. The critical J integral ($J_{1c}$) was found to be 136 N/mm.

### 6.4.1 FEA model validation

The finite element (FE) models were validated using the load-deformation behaviour and strain data obtained from the full-scale tests discussed earlier. The comparison of the load-deformation relationships for specimen SP1-D4-L100 obtained from the test and the finite element analyses are shown in Figure 6.14. A good agreement between the test and numerical behaviours is observed. It is worth mentioning that all specimens had almost same load-deformation behaviour (see Figure 6.7). The longitudinal strain distributions in the dented area for specimens SP1-D4-L100 obtained from the test and FEA are shown in Figures 6.15. The experimental strain data were acquired from the strain gauges located on a longitudinal line drawn through the centerline of the dent and hence, this line coincides with the direction of the length of the crack as well (Figures 6.6 and 6.15). In Figures 6.15, the distance on the x-axis were measured from the edge of the

dent of the pipe. This figure also shows a good agreement in between the test and FEA. Similar correlations between test and FEA for longitudinal strain distributions were also found for other specimens.
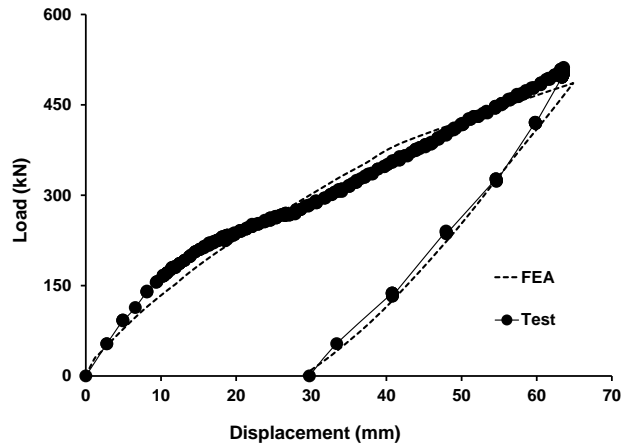


**Figure 6.14: The load-deformation behaviour comparison of SP1-D4-L100 and FEA model**
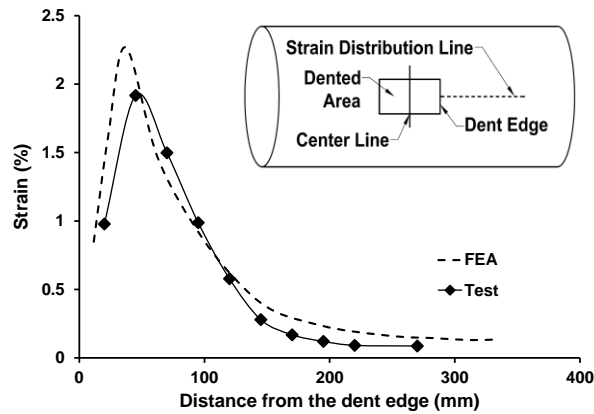


**Figure 6.15: Comparison of longitudinal strain of SP1-D4-L100**

The burst strength of the pipe specimens in FE model was predicted using $J_{1c}$ which was obtained from fracture toughness tests [18]. Crack initiation and burst strength of the specimen SP1-D4-L100 are shown in Figure 6.16. The $J_{1c}$ for crack initiation is assumed to be 136 N/mm and the $1.15J_{1c}$ for the burst pressure prediction is assumed to be 156.4

N/mm. Figure 6.16 also shows the burst strength of specimen SP1-D4-L100 obtained from the test and FEA. This figure indicates that the burst pressure obtained from FEA is slightly conservative.



**Figure 6.16: J-integral-pressure curve of SP1-D4-L100**

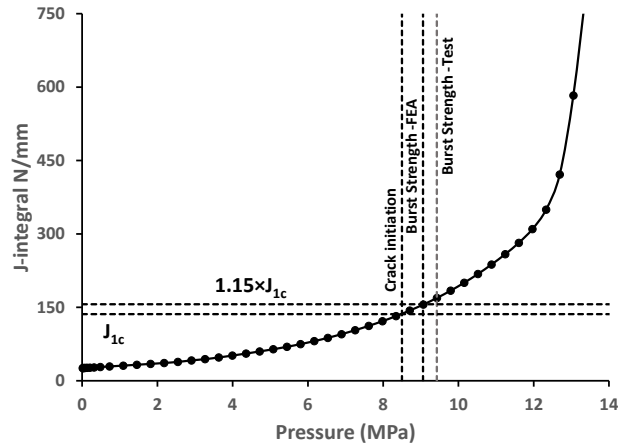## 6.4.2 Parametric study

Parametric study was undertaken to determine the effect of the crack depth, crack length, and operating (internal) pressure on the burst strength of NPS30 X70 grade oil and gas pipe with dent-crack defect with crack depth and length of wider ranges than those chosen in the tests. The parameters chosen in the FEA based parametric study are: (1) crack depth which was varied from 0.25 to 0.70 of pipe wall thickness, (2) crack length of 20 mm to 250 mm,  and (2) internal pressure applied during denting process (operating pressure of linepipe) was varied from no internal pressure ($0.0p_y$) to $0.75p_y$. The internal pressures chosen for the FEA based parametric study are: 0 MPa, 3.8 MPa, 7.6 MPa, and 9.5 MPa which correspond to $0.0p_y$, $0.3p_y$, 0.6, and $0.75p_y$, respectively.

Figure 6.17 shows the effect of two parameters: (i) level of internal (operating) pressure ($p/p_y$) and (ii) crack depth on the burst strength of NPS30 X70 steel pipe with a crack-dent defect when load is applied using rectangular indenter (Figure 6.13). As it can

be found from Figure 6.17, the internal (operating) pressure (p) and the burst pressure are normalized by the yield pressure ($p_y$). The crack depth is normalized by the thickness of the pipe wall. From Figure 6.17, it is evident that as the crack depth increase the burst strength decreases. It is due to the fact that as the crack depth increases, area around crack experienced more strain concentration and more plastic deformation and also loss of more area in the wall thickness resulting in lesser residual pressure capacity. Figure 6.17 also shows that as the internal (operating) pressure during indentation process increases the burst pressure decreases, though the effect of internal pressure is not that significant. As an example, for the pipes with crack depth of 6mm (0.70t) and for various internal pressures the maximum difference between the burst strength is only $0.07p_y$ or 0.89 MPa which is not that significant. Thus, the lowest burst strength was obtained when the internal pressure and the crack depth were at the maximum values. The minimum value of the burst strength for this pipe was obtained at $0.48p_y$ which is much lower than the MAOP. In other word, burst pressure of this pipe with 6 mm (0.70t) of crack depth and 4% of dent depth is 55% less than the specimen with 2 mm (0.25t) crack depth but with same dent depth of 4%. Such a lower burst pressure capacity threatens the structural integrity of this linepipe.
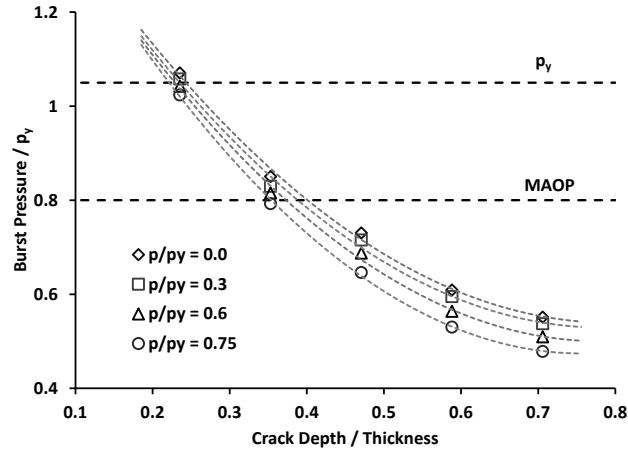
**Figure 6.17: Effect of crack depth and internal pressure on burst strength**

Figure 6.18 shows the effect of: (i) level of internal (operating) pressure (p/py) and (ii) crack length on the burst strength for this pipe. It can be found from this figure that the effect of these two parameters on burst strength are similar to those found from specimens with different crack depths. Figure 6.18 shows that as the crack length increases the burst strength decreases. It is due to the fact that as the crack length increases, more area on the pipe experienced strain concentration and more plastic deformation resulting in lesser amount of burst pressure capacity. Also, this figure shows that the effect of internal pressure is not as significant as the effect of crack length. However, as the internal (operating) pressure increases the burst pressure decreases. As an example, for the pipes with crack length of 250 mm and for various operating pressures the maximum difference between the burst strength is only $0.06p_y$ or 0.76 MPa. The lowest burst strength was obtained when the internal pressure and the crack length were at the maximum values and the lowest value for this pipe was obtained at $0.54p_y$ which is much lower than the MAOP. As a result, burst pressure of this pipe with 250 mm of crack length and 4 mm of crack

depth and 4% of dent depth is 49% less than the specimen with 20 mm crack length but with same crack and dent depths.
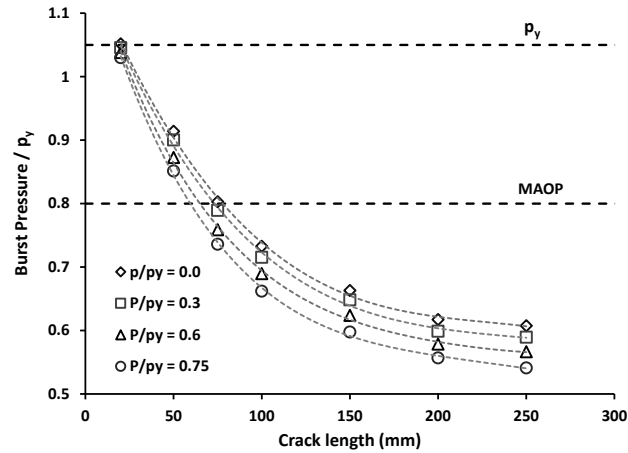


**Figure 6.18: Effect of crack length and internal pressure on burst strength**

## 6.5 CONCLUSIONS

The following conclusions are made in this paper based on the full-scale tests and the parametric study using finite element method completed in this study. Hence, these conclusions are limited to the pipe specimen, test method, defect type, and parametric study of this research work.

1. The burst pressure or burst strength of this pipe with dent-crack defect is influenced by internal or pipeline operating pressure, the crack depth, and the crack length. However, the crack depth and the crack length have much greater effect whereas; the operating pressure does not have much effect assuming that dent depth remains unchanged.

2. This linepipe with dent-crack defect with crack depth above 0.40 of wall thickness is not able to sustain MAOP. However, 40% is a lot more than what 12.5% crack depth which is limiting crack depth as least value recommended in ASME B31.4.

In other word, ASME code is over conservative in specifying limitation on the crack depth.

3. The failure mode for this pipe with a dent-crack defect is influenced by both the crack length and the crack depth.

4. FEA model developed in this study predicts the burst strength well-though the prediction is slightly conservative.

5. Parametric study shows that the dent-crack defect with crack length above 80 mm is not able to sustain MAOP. ASME B31.4 code does not provide any guideline on the limiting crack length.

6. This linepipe with dent-crack defect with crack depth of 0.40t or larger and crack length of 80 mm or above and dent depth of 4% can pose a threat to the structural integrity of the pipeline while subjected to hydro test.

7. Parametric study shows that burst strength in this pipe can reduce by as much as 55% when a dent-crack defect develops in the pipe wall and this could be a matter of serious concern for structural integrity of this linepipe.

## 6.6 ACKNOWLEDGEMENTS

## 6.7 REFERENCES

[1] Cosham, A., and Hopkins, P., 2004, "The effect of dents in pipelines-guidance in the pipeline defect assessment manual," International Journal of Pressure Vessels and Piping, 81(2), pp. 127-139.

[2] Smith, R. B., and Gideon, D. N., 1979, "STATISTICAL ANALYSIS OF DOT-OPSO DATA," Proceedings, Annual Symposium - Society of Flight Test Engineers, pp. D. 1-D. 9.

[3] Wang, K. C., and Smith, E. D., 1982, The effect of mechanical damage on fracture initiation in line pipe, part I dents, Energy, Mines and Resources Canada, Canada Centre for Mineral and Energy Technology, [Ottawa].

[4] Zarea, M. F., Toumbas, D. N., Philibert, C. E., and Deo, I., "Numerical models for static denting and dynamic puncture of gas transmission linepipe and their validation," Proc. Proceedings of the 1996 1st International Pipeline Conference, IPC. Part 2 (of 2), June 9, 1996 - June 13, 1996, ASME, pp. 777-784.

[5] Lancaster, E. R., 1996, "Burst pressures of pipes containing dents and gouges," Proceedings of the Institution of Mechanical Engineers, Part E: Journal of Process Mechanical Engineering, 210(1), pp. 19-27.

[6] Gresnigt, A. M., Karamanos, S. A., and Andreadakis, K. P., 2007, "Lateral loading of internally pressurized steel pipes," Transactions of the ASME.Journal of Pressure Vessel Technology, 129(4), pp. 630-638.

[7] ASME, 2012, "B31.4: Pipeline Transportation Systems for Liquids and Slurries," ASME International, New York, NY, USA.

[8] CSA, 2007, "Z662-07: Oil and gas pipeline systems," Canadian Standard Association, Mississauga, ON, Canada.

[9] Karamanos, S. A., and Andreadakis, K. P., 2006, "Denting of internally pressurized tubes under lateral loads," International Journal of Mechanical Sciences, 48(10), pp. 1080-1094.

[10] Staat, M., and Duc Khoi, V., 2013, "Limit analysis of flaws in pressurized pipes and cylindrical vessels. Part II: Circumferential defects," Engineering Fracture Mechanics, 97, pp. 314-333.

[11] ASME, 2004, "B31G-1991 (R2004): Manual for determining remaining strength of corroded pipelines: supplement to B31 code-pressure piping," ASME International, New York, NY, USA.

[12] DNV, 2012, "OS-F101: Submarine Pipeline Systems," Det Norske Veritas.

[13] API, 2012, "Spec 5L: Specification for Line Pipe," American Petroleum Institute, Washington, DC, USA.

[14] ASTM, 2011, "E8/E8M-11: Standard Test Methods for Tension Testing of Metallic Materials," ASTM International West Conshohocken, Pennsylvania, USA.
[15] Silva, J., Ghaednia, H., and Das, S., "Fatigue life assessment for nps30 steel pipe," Proc. 2012 9th International Pipeline Conference, IPC 2012, September 24, 2012 - September 28, 2012, American Society of Mechanical Engineers, pp. 619-624.

[16] SIMULIA, 2011, Analysis User's Manuals, Dassault Systèmes Simulia Corp., Rising Sun Mills, Providence, RI, USA.

[17] Das, S., Cheng, J. J. R., and Murray, D. W., 2007, "Prediction of fracture in wrinkled energy pipelines subjected to cyclic deformations," International Journal of Offshore and Polar Engineering, 17(3), pp. 205-212.

[18] ASTM, 2013, "E1820-13: Standard Test Method for Measurement of Fracture Toughness," ASTM International, West Conshohocken, Pennsylvania, USA.

# CHAPTER 7

# BURST STRENGTH OF NPS30 PIPES WITH VARIOUS CRACK LOCATIONS AND DENT DEPTHS

## 7.1 INTRODUCTION

Excavation operation often causes surface defects such as dent, gauge, crack, and/or their combinations in the field pipeline. These defects, often called mechanical damages, and it is widely accepted that mechanical damage is the most common cause for pipeline failure [1]. It has been reported that the failure of oil and gas transmission pipelines resulting from mechanical damages ranges from 55% in the USA to around 70% in Europe [2-5].

A dent is a permanent inward plastic deformation on the pipe surface which causes distortion in the cross-section of the pipe without causing any reduction in the wall thickness. Such a deformation causes stress and strain concentrations in the dented area of the pipeline [1]. Formation of a dent results in localized strain concentrations in the pipe wall which can lead to a leak or a rupture causing loss of containment, damage to environment, and threat to the safety of habitants living nearby, and also interruption in oil and gas supply, and a loss in the pipeline industry's revenue. Hence, the pipeline operators for many years have been concerned about the potential threat that may be posed by the dent defect. Several researches have been carried out to study the indentation issue and to understand of the relationship between the parameters such as dent depth and internal pressure. As a results of these studies, it is now widely accepted by the pipeline experts

that a dent depth of less than 6% is not a threat to the integrity of pipe structure under monotonically increasing pressure load [6, 7].

Excavation in and around a field buried pipeline can cause a combination of dent, crack, and metal loss (gauges) in a small area on a pipe surface. Many investigations have been carried out to understand the effect of metal loss on pipeline such as gauges or cracks to predict the burst strength of pipeline analytically and experimentally [8]. Detailed guidelines on predicting the burst strength of such pipes are available in various pipeline design and maintenance codes and standards [7, 9, 10]. Accordance to some of these standards, any pipe with a crack with the depth of more than 12.5% of wall thickness needs to be replaced [6, 7]; however, there is no studies to support that.

Several studies completed to determine the behaviour of pipe with single defect such as a dent or a crack or a gouge and the burst strength when such a single defect forms [11-14]. Also, pipes with dent-gouge defect was the subject of many previous studies [12, 15]. However, review of literatures available in the public domain reveals that no studies were undertaken to determine the burst strength of dented pipe that has developed crack in the dent. Such a combined defect is called dent-crack defect in this study. Therefore, this study was completed at the Centre for Engineering Research in Pipelines (CERP), University of Windsor to determine the burst strength of NPS30 X70 and X55 pipe with dent-crack defect with various dent depths, crack location, and two different material properties. This work was completed using a combined method of laboratory based experimental study and finite element method (FEM) based numerical study. This paper discusses the results obtained from this research.

## 7.2 EXPERIMENTAL PROCEDURE

### 7.2.1 Test specimen

The purpose of this study was to determine the burst strength of linepipes that have developed dent-crack defect. This project was completed using both laboratory based experimental study and numerical study using non-linear finite element method (FEM). NPS 30 grades X55 and X70 [16] steel pipes used in oil and gas transmission pipelines was chosen to prepare the test specimens. Four pipe specimens were fabricated from these pipes. The nominal diameter of the pipe is 762 mm (30 in) and the thickness of the pipe wall is 8.5 mm (0.35 in) and hence, the outer diameter-to-thickness ratio (D/t) of the pipe specimens used in the experimental work is about 90. The length of the each pipe specimen was 2500 mm (78.74 in). A number of material tensile specimens were cut from these pipe specimens and the standard material tensile tests were carried out to determine the mechanical properties of the pipe material in accordance with ASTM E8 [17]. The material properties obtained from theses tensile tests are shown in Table 7.1. The nominal (engineering) values of fracture stress and fracture strain were determined after the completion of the material tension tests. In addition to tensile test, Charpy V notch impact test were conducted on five subsize specimens (full wall thickness specimens) to ensure the pipe material has sufficient ductility (Table 7.1). Average value of Charpy toughness were found to be 152 J for X70 and 135 for X55 pipe material.

**Table 7.1: Material properties**

| Material type | Yield strength (MPa) | Tensile strength (MPa) | Modulus of elasticity (GPa) | Poisson's ratio | Charpy toughness (J) |
|---|---|---|---|---|---|
| X55 | 346 | 508 | 205 | 0.3 | 135 |
| X70 | 543 | 624 | 204 | 0.3 | 152 |

Two ends of the specimen were welded to thick (12mm) hemispherical steel end caps for holding water pressure during dent formation process and also during burst strength test. Water was used as the fluid in the test specimens. The internal pressure was held constant at $0.3p_y$ or 30% of $p_y$ which is about 3.8 MPa (550 psi) during denting process. The yield pressure for these pipe were calculated at 8.82 MPa (1279 psi) and 12.67 MPa (1837 psi) for X55 and X70 pipe materials, respectively. A rectangular indenter as can be seen in Figure 7.1 was used to create the dent. The length (dimension in the direction of the length of the pipe) and width (dimension in the circumferential direction of the pipe) for the indenter were 100 mm and 50 mm, respectively. The indenter was made by machining a solid steel slab. The permanent dent depth (plastic deformation due to denting) for these specimens was varied from 2% to 4% of the outer diameter of the pipe. The permanent dent depth is the plastic deformation resulted from denting process and calculated after removal of the indenter.



**Figure 7.1: Rectangular indenter used to create dent**

All the pipes had an EDM (electro-discharging machine) cut crack-like V-notch. Previous study completed at the Centre of Engineering Research in Pipeline (CERP) found that a crack with depth being less than 2 mm does not affect the burst strength of this dented pipe [18]. The notches were located at the mid-length of the pipe specimens and it was oriented in the direction of the length of the pipe specimen. The width of the V-notch was about 0.3 mm. A total of four full-scale tests were completed under the scope of this study. Table 7.2 shows the matrix of the test specimens used in this study. Specimens were named to reflect the primary attributes attached to each specimen. For example, specimen SP1-X70-D4-A, the combination of first two letters and a number (SP1) indicate that it is specimen number 1, the next combination of letter and number (X70) indicates that the specimen is made of X70 steel grade pipe, the next letter and a number (D4) indicates that the specimen had a dent depth of 4%, and the last letter (A) indicates that the dent located along the notch length or axial direction of the pipe (Figure 7.2). Hence, the specimen SP2-X70-D4-C was the second specimen and this specimen was identical to specimen SP1-X70-D4-A except in the earlier one crack located in the corner (indicated by letter, C) of the dent (Figure 7.3). The first and third specimens in Table 7.2, SP1-X70-D4-A and SP3-X55-D4-A, are considered as the reference specimens while considering the effect of Material (X55 and X70), crack location (Along the dent or crack located in the corner of the dent), and dent depth (2% and 4%), are evaluated.

**Table 7.2: Test matrix**

| Specimen name | Material type | Thickness | Dent depth | Crack location | Parameter |
|---|---|---|---|---|---|
| SP1-X70-D4-A | X70 | 8.5 mm | 28 mm (4%) | Notch along the length of dent | Reference specimen #1 |
| SP2-X70-D4-C | X70 | 8.5 mm | 28 mm (4%) | Notch at the corner of dent | crack Location |
| SP3-X55-D4-A | X55 | 8.5 mm | 28 mm (4%) | Notch along the length of dent | Reference specimen #2 and Material |
| SP4-X55-D2-A | X55 | 9.5 mm | 15 mm (2%) | Notch along the length of dent | Dent Depth |

**\* Pressure held constant at 3.8 MPa (550 psi) during application of denting load**
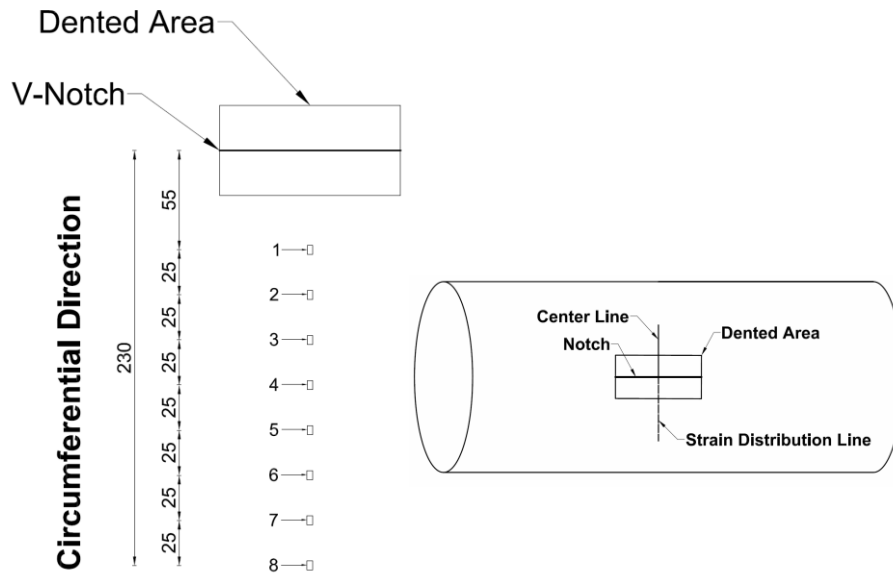


**Figure 7.2: Strain gauge layout for specimens SP1-X70-D4-A, SP3-X55-D4-A and SP4-X55-D2-A**
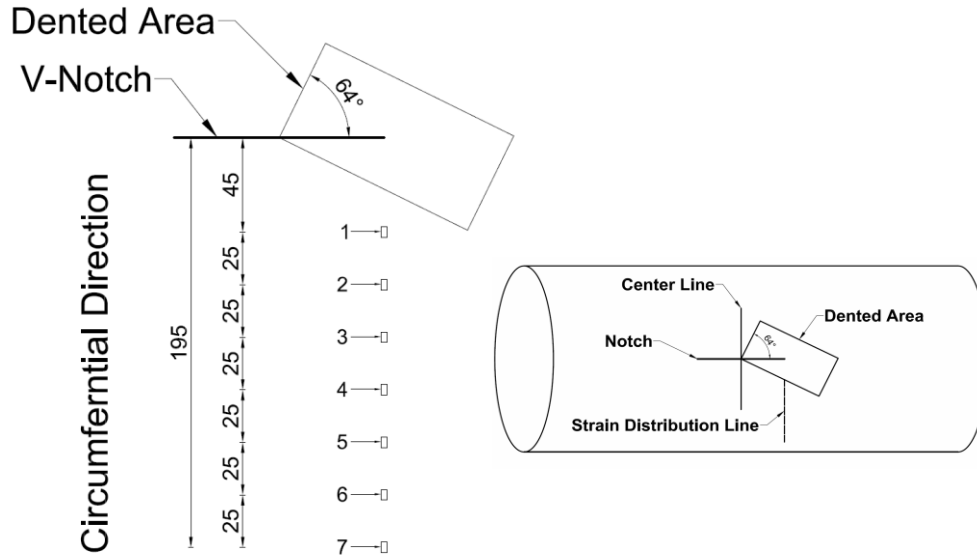
**Figure 7.3: Strain gauge layout for Specimen SP2-X70-D4-C**

Each test specimens was required to go through three different tests and hence, each pipe specimen was required to go through three different test setups, three different instrumentations, and three different loading steps. These three loading steps are: (i) fatigue load test, (ii) denting load test, and (iii) finally, the burst or pressure loading test. These loading steps are explained in the following sections.

### 7.2.2 Test Setup and Instrumentation

The purpose of these tests was to study how burst strength of pipes with dent-crack defect is affected by material, crack location, and dent depth. All the full-scale specimens went through the same loading procedure. First, fatigue load was applied to precrack the specimens at the tip of V-notch, followed by denting load to have dent-crack defect, and finally pipes were subjected to monotonically increasing water pressure until a rupture or a leak occurred in the dent-crack defect to determine burst strength of pipe specimens. All

these experimental works were completed in the structural engineering laboratory of the University of Windsor by CERP.

*Fatigue load test*

All specimens were subjected to fatigue load to create sharp tip or true crack at the tip of the V-Notch through the thickness of pipe wall. Figure 7.4a shows the V-notch associated with fatigue crack. An EDM (electro-discharging machine) was used to cut crack-like fine V-notch on pipe surface. The dimensions of the notch were: 100 mm long ($\pm 1\%$) along the longitudinal direction, 0.3 mm ($\pm 3\%$) wide at the top of the outside surface of the pipe wall, and 4 mm ($\pm 1\%$) deep (Figure 7.4a). Then, all the four specimens with a notch on their surface were subjected to fatigue load cycles. Fatigue load ratio of 0.5 was chosen and the fatigue loading continued until a precrack at the tip of the V-notch of about 0.3 mm deep was obtained. Ten small samples were cut from various locations on V-notch-crack area and examined under the Scanning Electron Microscope (SEM) after burst test was completed to confirm required crack depth was obtained in the specimen. Figure 7.4b shows how the samples were numbered and where they were located. Figure 7.5 shows SEM pictures taken from specimen SP1-X70-D4-A.
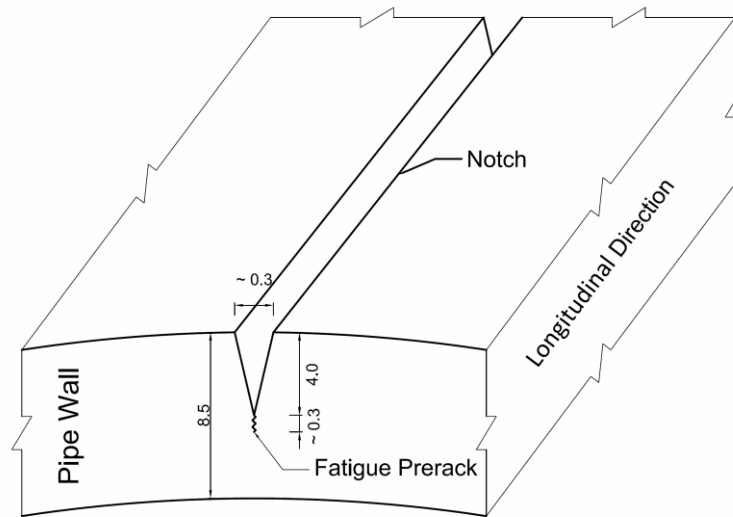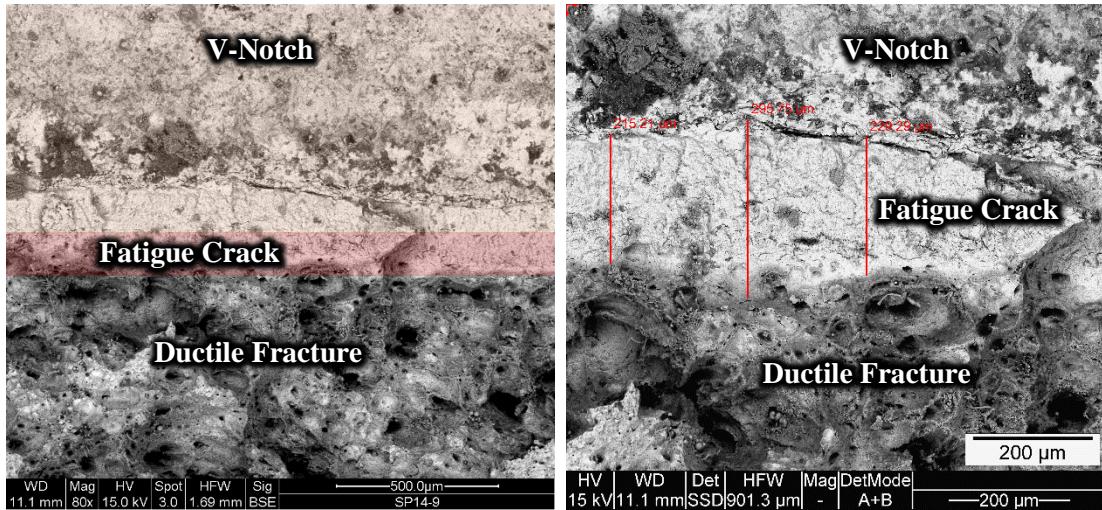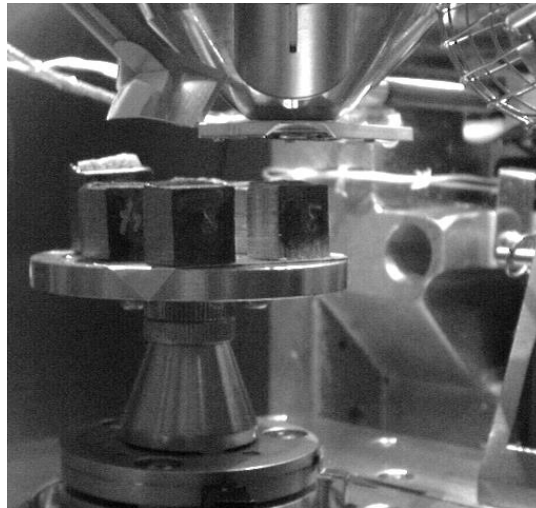
**a) Pipe wall section showing V- notch and crack**
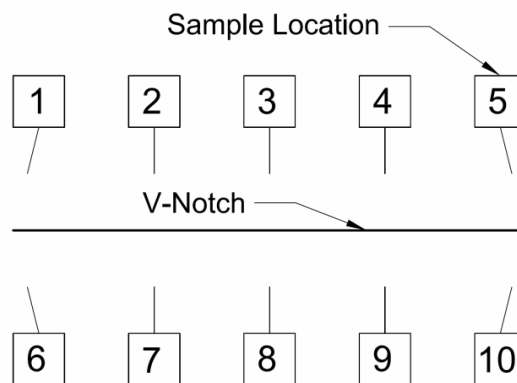


**b) Sample location on the V-notch**

**Figure 7.4: EDM cut V- notch on pipe wall**

**a) V-notch, fatigue crack, and ductile fracture area for location 9**



**b) Higher magnification of location 9**



**c) Sample's inside the SEM chamber**

**Figure 7.5: SEM picture at location 9 of the V-notch in SP1-X70-D4-A**

Figure 7.6 shows the schematic and a photo of fatigue load step. The test specimen located on three stiff steel supports. A steel roller and a steel pin were installed in between the pipe and the supports at two ends of the pipe specimen. A ±500 kN capacity fatigue loading actuator was used to apply the fatigue cycles with a load ratio of 0.5. A total of 50,000 of fatigue load cycles were applied on each pipe specimen to obtain a precrack depth of about 0.3 mm at the tip of the V-notch. Number of cycles required to reach 0.3

mm crack depth was predicted from the test data obtained from CT (compact tension) specimens completed in a previous research [19] and by verifying that data with several trial tests completed on full-scale pipe specimens.
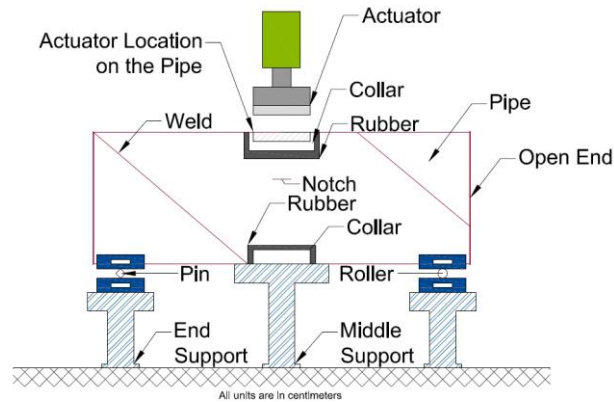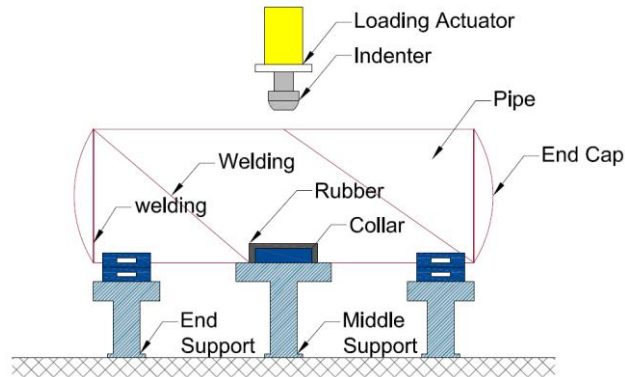


**a) Schematic**



**b) Photo**

**Figure 7.6: Schematic and photo of fatigue load test setup**

*Denting test*

Rectangular indenter was used to create the dent with the notch (Figure 7.1). Figure 7.7 shows a schematic and a photo of the test setup. The pipe specimen was placed on three stiff and rigid steel supports. The hydrostatic pump was used to apply and hold the internal pressure of 3.8 MPa (550 psi) (Table 7.2) when the dent load was applied on the pipe specimens. A universal loading actuator was used to apply denting load on the top surface

155

of the pipe wall. The denting load data was obtained from a load cell and the pressure data was acquired through a digital pressure transducer which were connected to the computerized data acquisition system.



**a) Schematic**



**b) Photo**

**Figure 7.7: Schematic and photo of denting test setup**

The total and plastic deformation (dent depth) of the pipe due to application of denting load was measured using two linear variable differential transformers (LVDTs). The LVDTs were located on the actuator to acquire downward displacement of the steel indenter. All specimens were instrumented with strain gauges to monitor circumferential strain distribution around the dent-crack defect. Figure 7.2 shows the strain gauges layout on top surface of SP1-X70-D4-A, SP3-X55-D4-A, and SP4-X55-D2-A around the dented

area and Figure 7.3 shows the strain gauges layout on SP2-X70-D4-C which had crack defect in the corner of the dent. These strains were later used to validate finite element (FE) model.
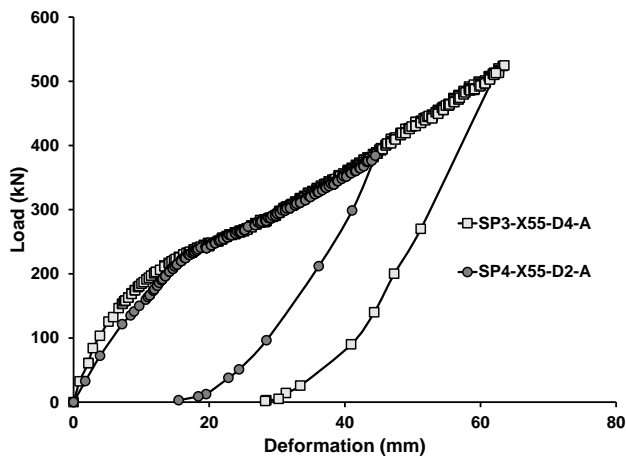
The load-deformation behaviours of these specimens are shown in Figures 7.8a, 7.8b, and 7.8c. The load in these figures represents the quasi-static load applied through the indenter during the indentation process and the deformation is the vertical downward movement of the steel indenter. It can be found from Figure 7.8a that specimens SP1-X70-D4-A and SP2-X70-D4-C exhibited almost same load-deformation behaviours. Also, after unloading these two specimens experienced almost same amount of plastic deformation (dent depth) of 28 mm. It is worth mentioning that these two specimens were identical except the location of crack. It can be observed from Figure 7.8b that specimens SP1-X70-D4-A and SP3-X55-D4-A exhibited very similar load-deformation behaviour and also same amount of permanent plastic deformation (dent depth) even though two grade pipes used. It is due to the fact that the global load and deformation during application of the dent load is more controlled by internal pressure than the pipe material properties. Figure 7.8c shows the load-deformation for specimens, SP3-X55-D4-A and SP4-X55-D2-A. From this figure it can be found that these two specimens experienced very similar of load-deformation behaviour. However, the permanent dent depth varied from 2% for specimen SP4-X55-D2-A to 4% for specimen SP3-X55-D4-A.
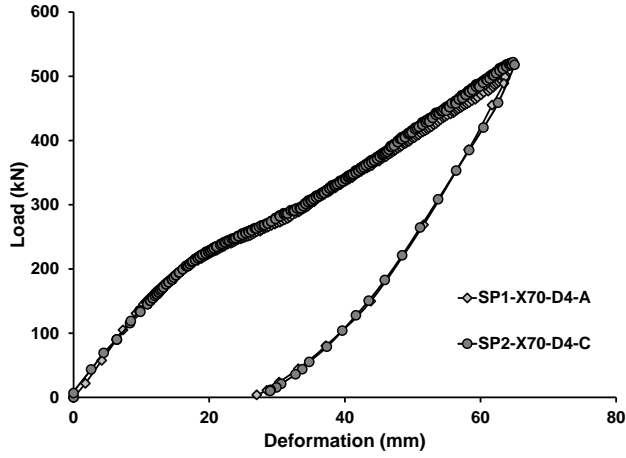
a): Specimens SP1-X70-D4-A and SP2-X70-D4-C
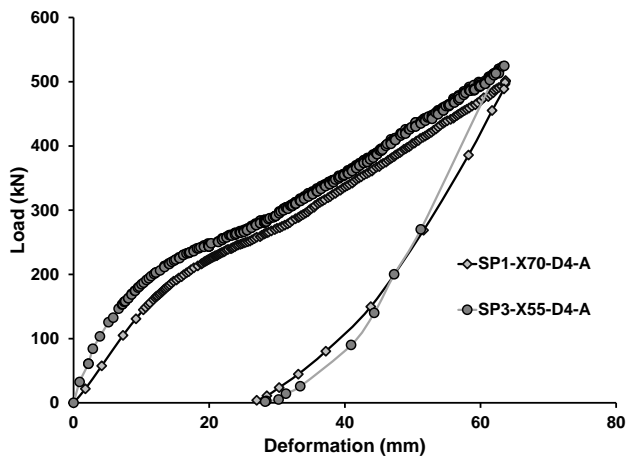
b): Specimens SP1-X70-D4-A and SP3-X55-D4-A

c): Specimens SP3-X55-D4-A and SP4-X55-D2-A

**Figure 7.8: Load-deformation behaviours**

*Burst pressure test*

The pipe specimen with dent-crack defect was then subjected to monotonically increasing water pressure until a leak or a rupture failure occurred in the dent-crack defect. The pipe specimen in this burst pressure load step was placed in a circular chamber (Figure 7.9). Pressure was monitored using an electronic pressure transducer and also through a mechanical pressure gauge. Both were mounted on one of the end caps. The pipe specimen was pressurized with a high capacity hydrostatic pressure pump to determine the burst strength of the pipe with dent-crack defect.



**Figure 7.9: Burst test setup**

## 7.3 TEST RESULTS

### 7.3.1 Burst Strength

Specimens SP1-X70-D4-A and SP2-X70-D4-C had same dent depth of 4% and crack depth of 4 mm; however, the location of the crack varied. The crack and the dent located along the length of the pipe specimen SP1-X70-D4-A whereas, the crack located at the corner of the dent in specimen SP2-X70-D4-C (Figures 7.2 and 7.3). The burst

pressure for specimen SP1-X70-D4-A was 9.4 MPa (1367 psi) which is $0.74p_y$ (Figure 7.10). The value of yield pressure ($p_y$) for X70 grade pipe specimens used in this study is 12.67 MPa (1837 psi). The burst pressure of SP2-X70-D4-C was 9.5 MPa (1382 psi) which is $0.75p_y$. Hence, experimental data of this study showed that the burst strength of pipes with dent-crack defect is not affected by the location of the crack with respect to the location of the dent as far as part of the crack is located inside the dent. Nonetheless, the burst pressure of both specimens (SP1-X70-D4-A and SP2-X70-D4-C) is less than the maximum allowable operating pressure (MAOP) of $0.8p_y$ (Figure 7.10). Hence, both specimens can pose a threat to the structural integrity of the linepipe if the pipeline is to be operated with a pressure above $0.75p_y$.
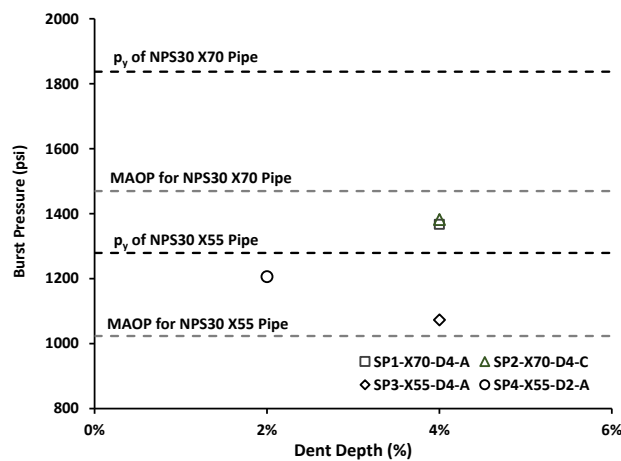


**Figure 7.10: Burst pressure of test specimens**

Specimens SP1-X70-D4-A and SP3-X55-D4-A experienced same load-displacement behaviour and had same total plastic deformation (dent depth). However, the material properties were varied in these two specimens which were made of X70 and X55 grad steels, respectively. Figure 7.10 shows, the burst pressure for these specimens was found to be 9.43 MPa (1367 psi), and 7.40 MPa (1073 psi), respectively. In other words, the burst strength of these specimens was found to be $0.74p_y$ for SP1-X70-D4-A, and

0.84p$_y$ for SP3-X55-D4-A. It is worth noting that the value of yield pressure (p$_y$) for X55 and X70 grade steel used in this study are 1279 (8.82 MPa) and 12.67 MPa (1837 psi). The burst pressures of specimens SP1-X70-D4-A is less than its MAOP; however, the burst strength of SP3-X55-D4-A is higher than its MOAP. It is therefore, found that the dent-crack defect causes more damaging effect on X70 grade steel pipe than the X55 grade steel pipe. It can be found from Figure 7.10 that X70 operating pressure of linepipe that has developed a dent-crack defect with dent depth of more than 4% and crack depth of 4 mm should be reduced.

For specimens SP3-X55-D4-A and SP4-X55-D2-A which had different dent depths of 2% and 4%, the burst strength varied by more than 0.9 MPa (130 psi). The values of burst pressure for these two specimens were found to be 7.40 MPa (1073 psi) and 8.3 MPa (1206 psi), respectively (Figure 7.10). In other words, it can be concluded that the burst strengths of these two specimens were found to be 0.84p$_y$ and 0.94p$_y$, respectively. Hence, the burst strength of SP4-X55-D2-A that had 2% dent depth was 13% higher than the same pipe with 4% dent depth (SP3-X55-D4-A). It is worth mentioning that the dent in these two specimens were formed with 3.8 MPa (0.3p$_y$) internal pressure. As it can be found from Figure 7.10, the burst pressures of specimens SP3-X55-D4-A and SP4-X55-D2-A are more than the maximum allowable operating pressure (MAOP) which is assumed to be 0.8p$_y$. Hence, The study found that the burst strength of this pipe with dent-crack defect is significantly affected by the dent depth and Figure 7.10 shows that X55 linepipe with dent-crack defect with dent depth above 5% is not able to sustain MAOP.

The MAOP in field linepipe is usually restricted to 0.8p$_y$. However, the linepipes are expected to subject to 1.05p$_y$ to 1.10p$_y$ during hydro test. Therefore, the test results of

this study found that these linepipe with dent-crack defect (crack depth of 4 mm and with dent depth of 2% or more) will pose a threat to the structural integrity of the pipeline while subjected to hydro test (Figure 7.10).

**7.3.2 Failure mode**

Figures 7.11a, 7.11b, 7.11c, and 11d show the opening at the dent-crack location due to burst pressure test for specimens SP1-X70-D4-A, SP2-X70-D4-C, SP3-X55-D4-A, and SP4-X55-D2-A, respectively. These figures show that in specimens SP1-X70-D4-A and SP2-X70-D4-C even though the crack location changes the amount of opening of the crack after failure did not change much. For specimen SP1-X70-D4-A it was at the mid-length of crack, however, location of crack opening for specimen SP2-X70-D4-C was at one end of the crack which was situated inside the dented area.

Further, it can be found from Figures 7.11a and 7.11c the pipe specimen SP3-X55-D4-A which was made of X55 grade steel exhibited much more ductile failure (leaking) in comparison with the pipe specimens SP1-X70-D4-A which was made of X70 grade steel. These two specimens exhibited a leaking failure at the mid-length of the crack; however, the failure (leak), in specimen SP3-X55-D4-A occurred in a smaller area than the pipe specimen SP1-X70-D4-A. It is worth noting that both pipe specimens experienced same load-displacement and dent depth of 4% and had same internal pressure of 3.8 MPa (0.3py) during denting. The only difference between these two specimens was the grade of steel.

Comparison of Figure 7.11c with Figure 7.11d shows that specimen SP4-X55-D2-A had more ductile failure than SP3-X55-D4-A. This is due to the fact that specimen SP4-X55-D2-A experienced less dent depth which means less permanent deformation than the specimen SP3-X55-D4-A. Nonetheless, both specimens exhibited failure due to leaking.

**a) Fracture area in SP1-X70-D4-A**



**b) Fracture area in SP2-X70-D4-C**



**c) Fracture area in SP3-X55-D4-A**



**d) Fracture area in SP4-X55-D2-A**

**Figure 7.11: Fracture area after burst test on pipe**

## 7.4 FINITE ELEMENT MODELING AND ANALYSIS

In this study, numerical modeling technique considering both material and geometric nonlinearities was used to simulate the behaviour of the test specimens. Commercially available general purpose finite element analysis code, ABAQUS/Standard version 6.13 distributed by SIMULIA [20] was used to model the pipe behaviour. The objective was to develop finite element model for predicting the burst strength of the NPS30 X70 grade pipe with a crack-dent defect. The effect of internal (operating) pressure

during indentation process and size and shape of the indenter were studied using the FE model.

A half-length FE model considering the symmetry with the axial length of about $3D_0$, was adopted to save computational time. However, comparison between this half-length FEA model and the full-length FEA model showed a good agreement between them. Appropriate boundary conditions were applied along the periphery of the half-length model and same geometry and loading steps as test specimen were used in FEA modeling (see Figures 7.6 and 7.12).

A 10-node quadratic (second order) tetrahedron solid element, C3D10, was used in and around the dent load application area where strain and stress concentrations were expected to be high. Around Crack tip where the J-integral counters were located, 20-node quadratic brick element with reduced integration was used. The rest of the pipe specimen was modeled with solid element, C3D8R (8-node linear brick), with reduced integration. Minimum of four elements were used through the wall thickness. The total number of node and elements were 122,358 and 101,066, respectively. Each node of these elements have three translation degrees of freedom: u1, u2, and u3. The directions 1, 2, and 3 correspond to x, y, and z axes as shown in Figure 7.12. The u1 represents translation degree-of-freedom in the x-direction. The reduced number of integration point increases computational efficiency and generally yield more accurate results than the corresponding fully integrated elements. Indenter was modelled as discrete rigid body using 4-node rigid quadrilateral elements, R3D4 to avoid any deformation in loading plate and supports. In the tests, the loading plates were at least 75 mm thick and hence, they were almost rigid if compared with the rigidity of the pipe wall. Mesh convergence studies were performed to obtain

optimum sizes of various elements used in the FEA model. Figure 7.12a shows a typical meshed pipe.

There were two contact areas which were modeled in the numerical simulations and these are; contact between rectangular indenter and the pipe wall and between the pipe wall and the end supports. A surface-to-node contact using a hard contact algorithm was assigned to these two regions during the application of denting load. The internal pressure was applied to the inner surface of the pipe wall and end caps. In the tests, thick hemispherical steel end caps were used at both ends of the pipe specimen to hold the water and to apply internal pressure. Hence, in the FEA model, these end caps were modeled as an elastic-plastic steel with modulus of elasticity of 204 GPa. An elastic-plastic material model using von-Mises yield criterion and isotropic hardening with associated plastic flow rule was used in the FE models. The Sharcnet clusters were used for parallel computing due to the complexity of the model and it was time consuming [21].

The critical J integral ($J_{1c}$) can be used to predict the crack initiation in a pipe with dent-crack defect. Also it can be assumed that a failure occurs when the maximum equivalent plastic (MEP) strain at any integration point reaches the maximum equivalent plastic strain at rupture obtained from material tensile tests. As a result, the rupture strain can be considered as unit [22]. In the FE model, five J-integral counters were requested around crack tip (Figure 7.12c) and it was assumed that a failure occurs when the J-integral (J) at any integration point around crack tip reaches the maximum value of 1.15 $J_{1c}$ which is equivalent to the equivalent plastic strain of unit. The $J_{1c}$ of X70 steel grade pipe obtained from fracture toughness tests according to ASME E1820 on five standard bend specimens cut out from the pipe materials and precracked according to the ASTM E1820 [23]. Figure

7.13 shows a typical bend specimen and its dimensions. The resistance curve procedure were followed to determine $J_{1c}$ for X70 pipe material and the critical J integral ($J_{1c}$) was found to be 136 N/mm.
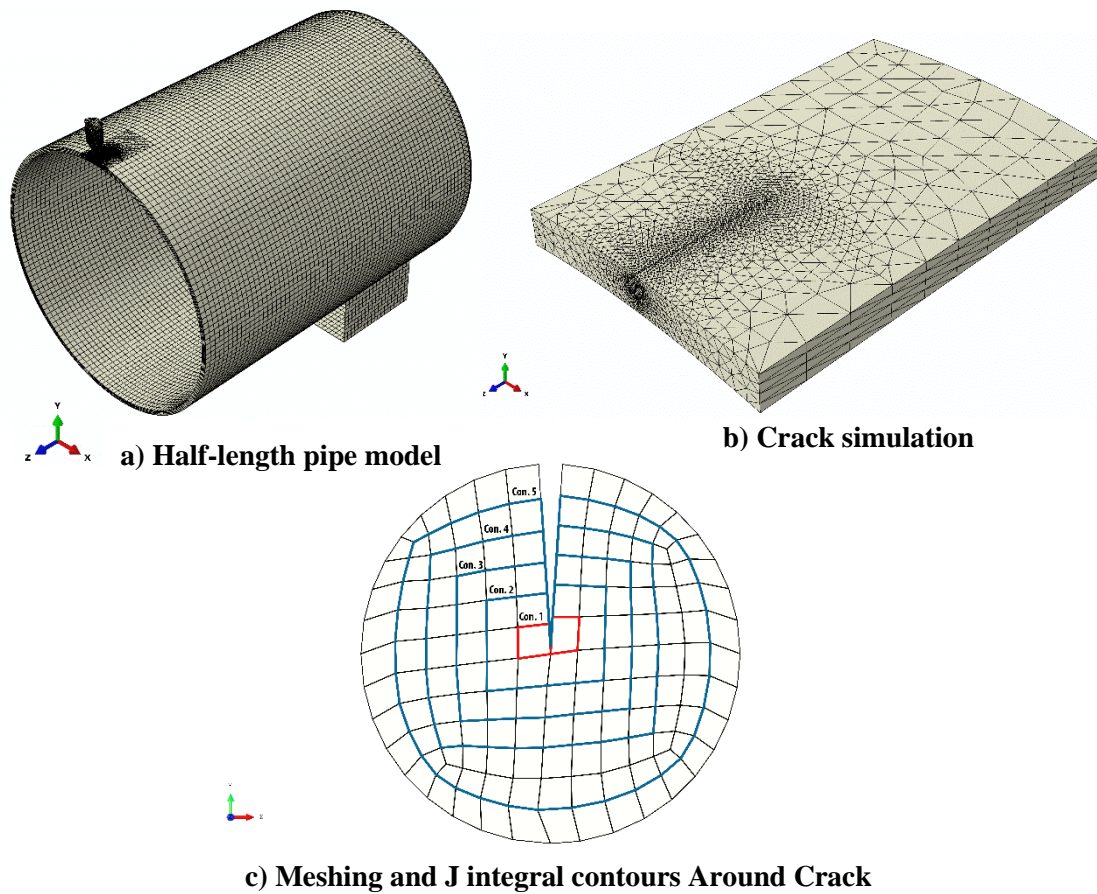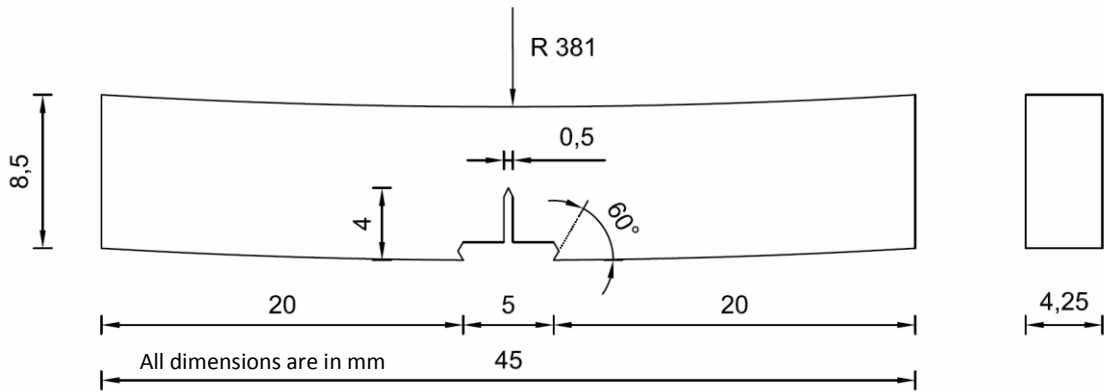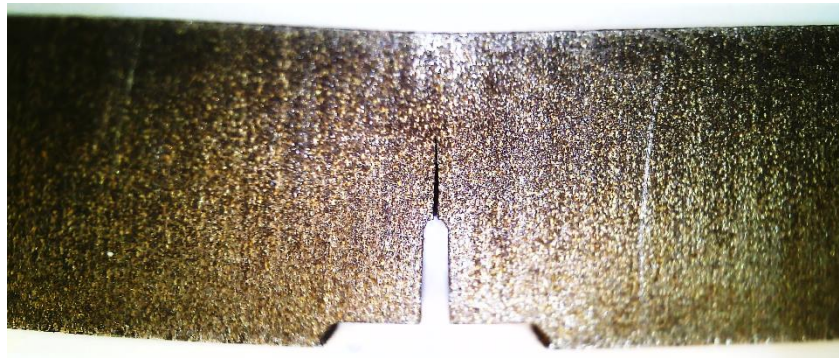


**a) Half-length pipe model**

**b) Crack simulation**

**c) Meshing and J integral contours Around Crack**

**Figure 7.12: Meshed pipe and notch area**

**a) standard bend specimen geometry**



**b) Standard bend specimen after fracture toughness test**

**Figure 7.13: Standard bend specimen [23]**

## 7.4.1 FEA model validation

The finite element (FE) model was validated using the load-deformation behaviour and strain data obtained from the full scale tests. The comparison for the load-deformation relationship for specimen SP1-X70-D4-A obtained from the test and the finite element analysis are shown in Figure 7.14. A good agreement between the test and numerical behaviours is observed. It is worth mentioning that all the four specimens had almost same loading-deformation behaviour (see Figure 7.8). The circumferential strain distributions in and around the dent for the same specimen, SP1-X70-D4-A, obtained from the test and the FEA are shown in Figure 7.15. The experimental strain data were acquired from the strain

gauges located on the circumferential line drawn through the centerline of the dent and hence, this line passes through the mid-length of the crack (Figure 7.3). In Figure 7.15, the distance on the x-axis was measured from the edge of the crack (Figure 7.3). These figure also shows a good agreement between the test and FEA. Similar correlation between test and FEA for circumferential strain distributions was also found for other specimens.
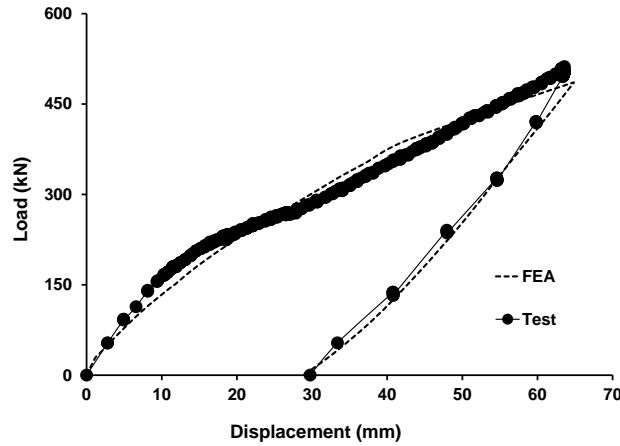


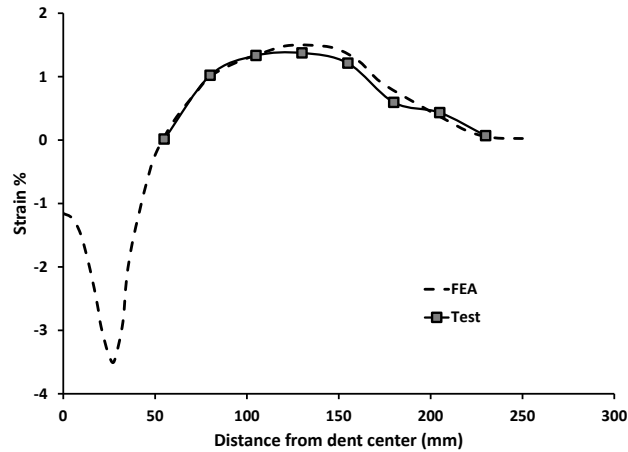**Figure 7.14: Comparison of load-deformation behaviour for SP1-X70-D4-A**



**Figure 7.15: Comparison of strain distribution for SP1-X70-D4-A**

The burst strength of the pipe specimens predicted using $J_{1c}$ obtained from fracture toughness tests. Crack initiation and burst strength of the specimen SP1-X70-D4-

A and same finite element model specimen but dented with spherical indenter is shown in Figure 7.16. Also, this figure shows the crack initiation and predicted burst strength for the same pipe specimen but dented with the spherical indenter.
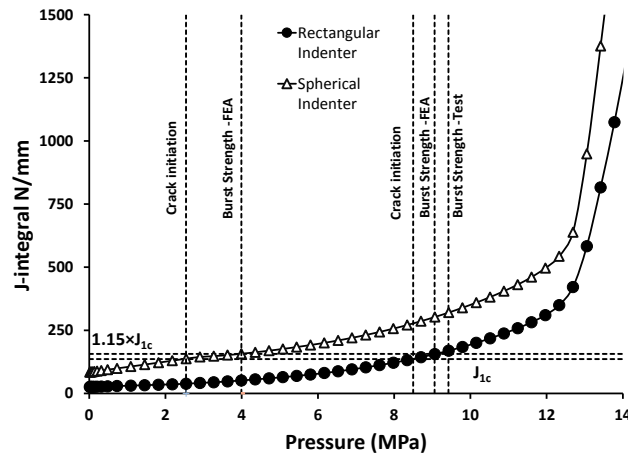


**Figure 7.16: J-integral-pressure curve**

### 7.4.2 Parametric study

Parametric study was completed to study the effect of the dent depth, operating (internal) pressure, and shape of the Indenter (rock) on the burst strength of NPS30 X70 grade oil and gas pipe with dent-crack defect (Table 7.3). The parameters chosen in the FEA based parametric study are: (1) dent depth which was varied from 1% to 11% of pipe outer diameter, (2) internal pressure applied during denting process (operating pressure of linepipe) which was varied from internal pressure ($0.3p_y$ to $0.8p_y$) and (3) Indenter shape. Two shapes of the indenter namely rectangular and spherical were used in the parametric study (Figures 7.17a and 7.17b). The spherical shaped indenter simulates a narrower rock tip whereas, the rectangular shaped indenter simulates a relatively wider rock tip.

**Table 7.3: Parameters and their ranges chosen**

| Parameters | Loading plate shape | | Dent depth | Internal pressure |
|---|---|---|---|---|
| Range | Rectangular | Sphere | 1% to 11% | $0.3p_y$, $0.5p_y$, $0.8p_y$ |
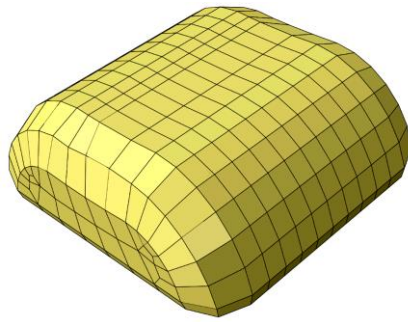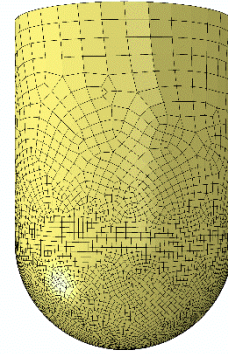


**a) Rectangular indenter**          **b) Spherical indenter**

**Figure 7.17: Indenter shapes used in parametric study**

Figure 7.18 shows the effect of two parameters: (i) level of internal (operating) pressure ($p/p_y$) and (ii) dent depth on the burst strength of NPS30 X70 steel pipe with a crack-dent defect when load is applied using rectangular and spherical indenters (Figure 7.17). As it can be found from Figure 7.18, the internal (operating) pressure (p) and the burst pressure are normalized by the yield pressure ($p_y$). The permanent dent depth is normalized by the outer diameter of the pipe.

From Figure 7.18, it is evident that the burst strength decreases as the dent depth increase for both rectangular and spherical indenters. This is due to the fact that as the dent depth increases, area around crack experienced more strain concentration and more plastic deformation occurs resulting in reduction in the burst pressure capacity. Figure 7.18 also shows that as the internal (operating) pressure increases the burst pressure decreases, though the effect of internal pressure is not that significant. Same behaviours were

observed for specimens dented with both rectangular and spherical indenters. As an example, for the pipes dented with rectangular indenter and dent depth of 7% of outer diameter (0.07D) and for various internal pressures the maximum difference between the burst strength is only 0.046py or 0.58 MPa. Same trend has been observed for the pipes dented with spherical indenter. The lowest burst strength was obtained at $0.19p_y$ when the internal pressure and the dent depth were maximum.
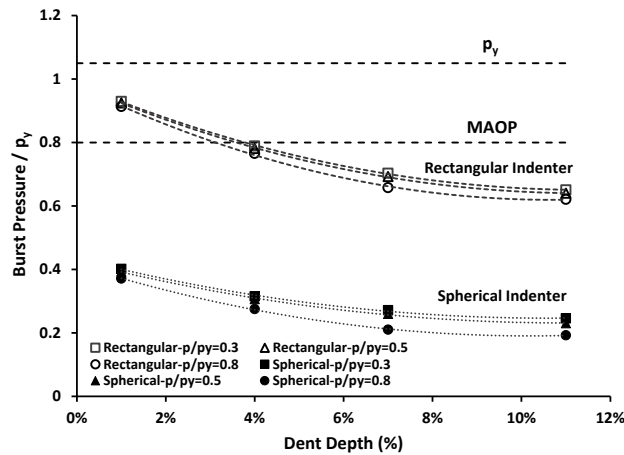


**Figure 7.18: Effect of dent depth and internal pressure on burst strength of X70 pipes**

The effect of dent shape and size on the burst strength was found to be significant and it varied in the range of 40% to 53%. In the other words, pipe specimens that were dented with spherical indenter showed much lower burst strength than those indented with rectangular indenter (Figure 7.18). This is due to the fact that the spherical indenter causes much higher stress and strain concentrations in and around dented area and also higher permanent plastic deformations. Figure 7.19 shows strain distributions and strain concentrations for specimens with same crack depth of 4 mm, crack length of 100mm, and dent depth 4% but dented by two different indenters.

The minimum value of the burst strength for these pipes dented with spherical indenter was obtained at $0.19p_y$ which is much smaller than the MAOP (Figure 7.18). As a result, burst pressure of pipe with 100 mm of crack length, 4 mm of crack depth, 1% of dent depth, and dented with spherical indenter is 53% less than the similar specimen with same crack and dent depth when dented with rectangular indenter.
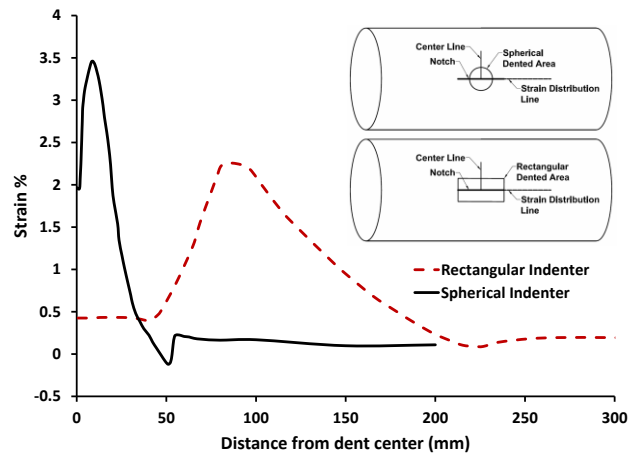


**Figure 7.19: Longitudinal strain distributions**

## 7.5 CONCLUSIONS

The conclusions made in this paper are based on full-scale tests and finite element analyses completed. Hence, these conclusions are limited to the pipe specimen, test method, and parametric study used in this research work.

1. The burst pressure or burst strength of this pipe with dent-crack defect is affected by material property, the dent depth, operating pressure, and the dent shape. However, the dent shape and size has much greater effect whereas; the operating pressure does not have much effect if the dent depth remains unchanged.

2. It was found from the test data that the burst strength of this pipe with dent-crack defect is not affected by the location of the crack formation as if the crack is located inside the dent.

3. This study found that the burst strength of X55 steel grade pipes with rectangular dent-crack defect with dent depth above 5% is not able to sustain MAOP.

4. X55 and X70 steel grade linepipe with rectangular dent-crack defect with dent depth above 5% and 4%, respectively and 4 mm crack depth is not able to sustain MAOP. However, the crack depth of 40% of the wall thickness (0.4t) and along with 4% of dent depth is a lot larger than allowable crack depth of 12.5% (associating with no dent) according ASME B31.4 [24].

5. The X55 steel grade pipe specimens showed much lower burst strength than X70 steel pipe. However, the burst strength of X55 steel pipes were higher than its MAOP while the burst strength of X70 steel test specimens were lower than its MAOP.

6. X70 or X55 steel linepipes with rectangular dent-crack defect with crack depth of 0.4t or larger and crack length of 100 mm or longer with dent depth of 4% can pose a threat to the structural integrity of the pipeline while subjected to hydro test.

7. Parametric study found, the burst strength of X70 steel grade linepipe with spherical dent-crack with 4 mm crack depth is always less than MAOP.

## 7.6 ACKNOWLEDGEMENTS

## 7.7 REFERENCES

[1] Cosham, A., and Hopkins, P., 2004, "The effect of dents in pipelines-guidance in the pipeline defect assessment manual," International Journal of Pressure Vessels and Piping, 81(2), pp. 127-139.

[2] Smith, R. B., and Gideon, D. N., 1979, "STATISTICAL ANALYSIS OF DOT-OPSO DATA," Proceedings, Annual Symposium - Society of Flight Test Engineers, pp. D. 1-D. 9.

[3] Wang, K. C., and Smith, E. D., 1982, The effect of mechanical damage on fracture initiation in line pipe, part I dents, Energy, Mines and Resources Canada, Canada Centre for Mineral and Energy Technology, [Ottawa].

[4] Zarea, M. F., Toumbas, D. N., Philibert, C. E., and Deo, I., "Numerical models for static denting and dynamic puncture of gas transmission linepipe and their validation," Proc. Proceedings of the 1996 1st International Pipeline Conference, IPC. Part 2 (of 2), June 9, 1996 - June 13, 1996, ASME, pp. 777-784.

[5] Lancaster, E. R., 1996, "Burst pressures of pipes containing dents and gouges," Proceedings of the Institution of Mechanical Engineers, Part E: Journal of Process Mechanical Engineering, 210(1), pp. 19-27.

[6] ASME, 2012, "B31.4: Pipeline Transportation Systems for Liquids and Slurries," ASME International, New York, NY, USA.

[7] CSA, 2007, "Z662-07: Oil and gas pipeline systems," Canadian Standard Association, Mississauga, ON, Canada.

[8] Staat, M., and Duc Khoi, V., 2013, "Limit analysis of flaws in pressurized pipes and cylindrical vessels. Part II: Circumferential defects," Engineering Fracture Mechanics, 97, pp. 314-333.

[9] ASME, 2004, "B31G-1991 (R2004): Manual for determining remaining strength of corroded pipelines: supplement to B31 code-pressure piping," ASME International, New York, NY, USA.

[10] DNV, 2012, "OS-F101: Submarine Pipeline Systems," Det Norske Veritas.

[11] Allouti, M., Schmitt, C., Pluvinage, G., Gilgert, J., and Hariri, S., 2012, "Study of the influence of dent depth on the critical pressure of pipeline," Engineering Failure Analysis, 21, pp. 40-51.

[12] Błachut, J., and Iflefel, I. B., 2007, "Collapse of pipes with plain or gouged dents by bending moment," International Journal of Pressure Vessels and Piping, 84(9), pp. 560-571.

[13] Pluvinage, G., Krasowsky, A. J., and Krassiko, V. W., 1992, "Dynamic fracture toughness at crack initiation, propagation and arrest for two pipe-line steels," Engineering Fracture Mechanics, 43(6), pp. 1063-1084.

[14] Alabi, J. A., and Sanders, J. L., Jr., 1985, "Circumferential crack at the fixed end of a pipe," Engineering Fracture Mechanics, 22(4), pp. 609-616.

[15] Allouti, M., Schmitt, C., and Pluvinage, G., 2014, "Assessment of a gouge and dent defect in a pipeline by a combined criterion," Engineering Failure Analysis, 36, pp. 1-13.

[16] API, 2012, "Spec 5L: Specification for Line Pipe," American Petroleum Institute, Washington, DC, USA.

[17] ASTM, 2011, "E8/E8M-11: Standard Test Methods for Tension Testing of Metallic Materials," ASTM International West Conshohocken, Pennsylvania, USA.

[18] Ghaednia, H., Silva, J., Kenno, S., Das, S., Wang, R., and Kania, R., 2013, "Pressure tests on 30-in diameter X65 grade pipes with dent-crack defects," The Journal of Pipeline Engineering, 12(1), p. 7.

[19] Silva, J., Ghaednia, H., and Das, S., "Fatigue life assessment for nps30 steel pipe," Proc. 2012 9th International Pipeline Conference, IPC 2012, September 24, 2012 - September 28, 2012, American Society of Mechanical Engineers, pp. 619-624.

[20] SIMULIA, 2011, Analysis User's Manuals, Dassault Systèmes Simulia Corp., Rising Sun Mills, Providence, RI, USA.

[21] Network, S. H. A. R. C., "https://www.sharcnet.ca/."

[22] Das, S., Cheng, J. J. R., and Murray, D. W., 2007, "Prediction of fracture in wrinkled energy pipelines subjected to cyclic deformations," International Journal of Offshore and Polar Engineering, 17(3), pp. 205-212.

[23] ASTM, 2013, "E1820-13: Standard Test Method for Measurement of Fracture Toughness," ASTM International, West Conshohocken, Pennsylvania, USA.

[24] ASME, 2012, "B31.4: Pipeline Transportation Systems for Liquids and Slurries," ASME International, New York, NY, USA.

# CHAPTER 8

# DEVELOPING EMPIRICAL EQUATION

## 8.1 INTRODUCTION

Mathematical software, Eureqa, was used to drive an empirical equation to predict burst strength of linepipe with the dent-crack defect. This mathematical software tool originally created by Cornell's Creative Machines Lab. The software uses symbolic regression to determine mathematical equations that describe sets of data in their simplest form [1].

Symbolic regression, or symbolic function identification, seeks to discover many symbolic expressions of functions that fit the given data set. In the other words, it searches the space of mathematical expressions to find the model that best fits a given dataset, both in terms of accuracy and simplicity. In this method, the start point is blindly chosen. Instead, initial expressions are formed by randomly combining mathematical building blocks such as mathematical operators, analytic functions, constants, and state variables. Usually, some of these primitives will be specified by the user operator, but that's not a requirement of the technique. As a results, symbolic regression isn't affected by human bias, or unknown gaps in domain knowledge. New equations are then formed by recombining previous equations, using genetic programming [2].

It attempts to find best fitted relationships of the dataset, by searching all the possible patterns in the data to find the appropriate models, rather than imposing a model structure that is deemed mathematically tractable from a human perspective. The fitness function that drives the evolution of the models takes into account not only error metrics

(to ensure the models accurately predict the data), but also special complexity measures, thus ensuring that the resulting models reveal the data's underlying structure in a way that's understandable from a human perspective [2].

## 8.2 EMPIRICAL EQUATION

An empirical equation developed using the symbolic regression, or symbolic function identification to calculate the burst strength of linepipe with dent-crack defect. The empirical equation developed in this study is as follows.

$$P_b = 1750 + 2 * 10^5 \left(\frac{d}{D}\right)^2 + 0.07 * \frac{C_l{}^2}{C_d} - 124.4 * \left(\frac{p}{p_y}\right) - 48.6 * \left(\frac{d}{D}\right) C_l * C_d - 7.8$$
$$* 10^5 \left(\frac{d}{D}\right)^3$$

The empirical equation was developed based on the full-scale tests and the parametric study using finite element method completed in this study. Hence, this equation is limited to the pipe specimen, test method, defect type, and parametric study of this research work.

Table 8.1 shows the sensitivity of this equation to each independent parameter. Figure 8.1, 8.2, and 8.3 show complexity-error, observed-predicted, and solution fit, respectively.

**Table 8.1: Variable sensitivity**

| Variable | sensitivity | % Positive | Positive magnitude | % Negative | Negative magnitude |
|----------|-------------|------------|--------------------|------------|--------------------|
| $C_l$ | 0.570 | 0 | 0 | 100 | 0.570 |
| d/D | 0.533 | 6 | 0.0047 | 94 | 0.566 |
| $C_d$ | 0.317 | 0 | 0 | 100 | 0.317 |
| $p/p_y$ | 0.080 | 0 | 0 | 100 | 0.080 |
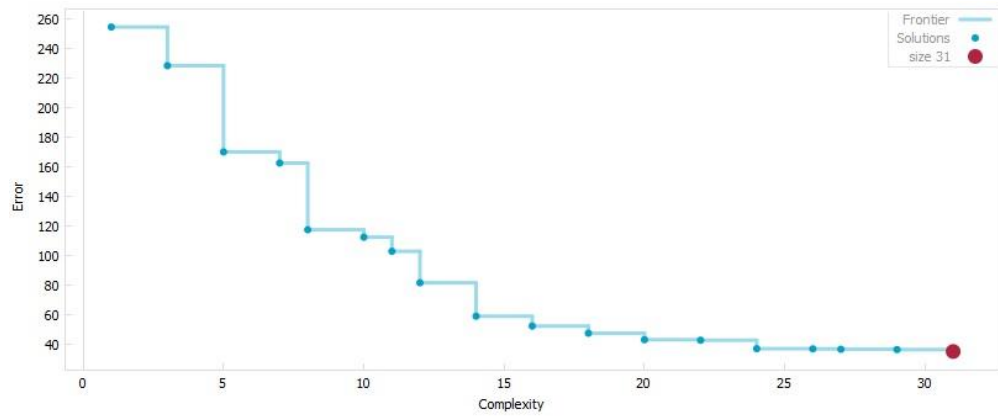


**Figure 8.1: Error vs complexity**
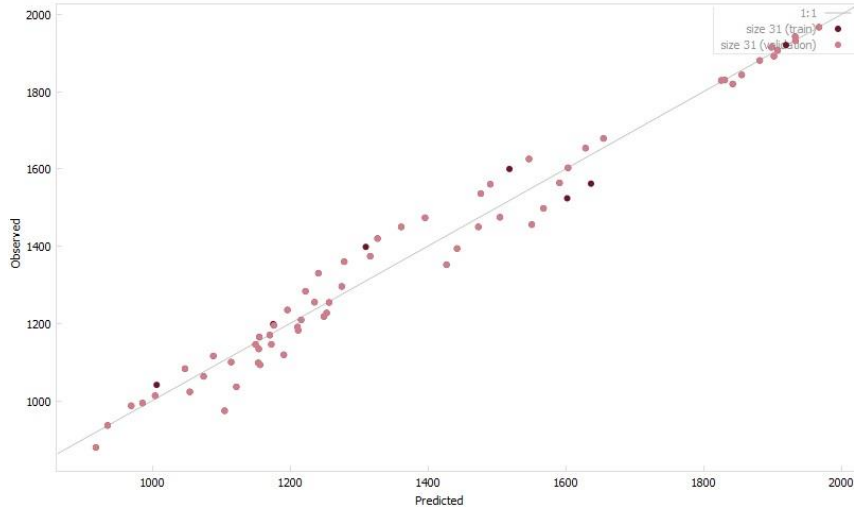
**Figure 8.2: Observed vs predicted**
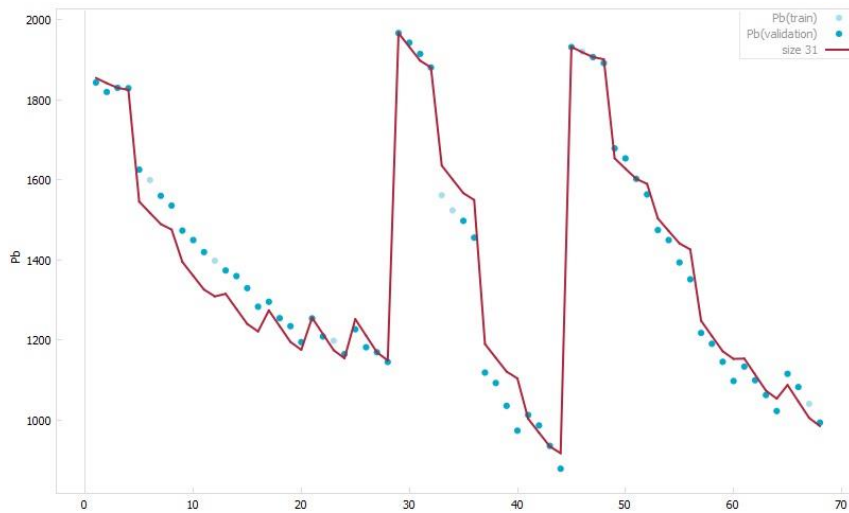


**Figure 8.3: Solution fit**

## 8.3 REFRENCES

[1] Eureqa, "http://creativemachines.cornell.edu/Eureqa."

[2] Vladislavleva, E. J., Smits, G. F., and den Hertog, D., 2009, "Order of nonlinearity as a complexity measure for models generated by symbolic regression via pareto genetic programming," IEEE Transactions on Evolutionary Computation, 13(2), pp. 333-349.

# CHAPTER 9

# GENERAL DISCUSSION AND CONCLUSION

The current study was conducted to investigate structural behaviour oil and gas pipe with dent-crack defect. The main objective was to determine the burst strength of full-scale steel pipe specimens when the dent-crack defect developed on their surfaces. In doing so, a combined experimental and numerical approach was adopted. This chapter concludes the main findings which discussed in detail in previous chapters and provides recommendations for future research.

## 9.1 CONCLUSIONS

The following conclusions are made based on the full-scale tests and detailed FEA based parametric study completed under the scope of this study. Hence, the conclusions are limited to the findings associated with specific test specimens and finite element analyses presented in previous chapters.

1. According to this study of the structural behaviour of a dent, all three parameters: level of dent depth, dent shape and size, and internal or operating pressure affect the maximum strain value and possibly its location as well. However, the effect of indenter shape and length chosen in experimental and numerical program is significant on the value and location of maximum strain, in comparison with the other parameters. Hence Evaluation of severity of a dented pipeline solely based on dent depth is not appropriate. Rather, critical strain values must be included in the dent assessment criteria.

2. It has been observed despite of using displacement or load control method, as the internal pressure increases the maximum ovalization decreases and this trend was found to be opposite for D/t. Moreover, this study found, the total deformation of 65 mm may not be a safety concern from dent evaluation criterion for some pipe specimens, but, it is a concern when ovalization limit criterion of 4% is considered.

3. Bursting pressure of pipe with dent-crack defect was not significantly affected by dent shape, internal (operating) pressure during indentation process when crack depth is less than 2 mm.

4. The dent depth drastically affect the burst pressure or burst strength of linepipes with dent-crack defect. In other words, this linepipe with crack depth of 4mm and with dent depth above 2.5% is not able to sustain MAOP. Parametric study shows that burst strength in this pipe can reduce by as much as 38% just by changing the dent depth from 0% to 12% and this could be a matter of serious concern for structural integrity of this linepipe.

5. The burst pressure of this linepipe with dent-crack defect is highly influenced by the crack depth, and the crack length. Parametric study shows that by changing the crack depth and crack length burst strength in this pipe can reduce by as much as 55% when a dent-crack defect develops in the pipe wall and this could be a matter of serious concern for structural integrity of this linepipe.

6. Linepipe with dent-crack defect with crack depth of 3.5 mm or larger and crack length of 80 mm or above can pose a threat to the structural integrity of the pipeline while subjected to hydro test. However, 3.5 mm is a lot larger than minimum allowable crack depth of 1 mm (recommended in ASME B31.4) for this thickness

of pipe. Hence, this study found that the ASME code is over conservative in specifying limitation on the crack depth.

7.  It was found from the test data that the burst strength of this linepipe with dent-crack defect is not affected by changing the location of the crack formation if the crack is still located inside the dented area.

8.  Parametric study found, when this pipe indented with a relatively sharp indenter the burst strength of X70 steel grade linepipe with dent-crack defect (with 4 mm crack depth) is always less than MAOP.

9.  This study found that the burst strength of X55 steel grade pipes with rectangular dent-crack defect with dent depth above 5% is not able to sustain MAOP when a dent-crack defect developed in its surface. However, the crack depth of 0.4t (3.5 mm) and along with 5% of dent depth is a lot larger than allowable crack depth of 1 mm (associating with no dent) according to ASME B31.4

10. The X55 steel grade pipe specimens showed much lower burst strength than X70 steel pipe. However, the burst strength of X55 steel pipes with dent-crack defect were higher than its MAOP while the burst strength of X70 steel test specimens with the same defect were lower than its MAOP.

11. FEA model developed in this study estimates the burst strength this linepipe using $J_{1c}$. the predicted burst strengths were really close to the data obtained from tests, however, they were slightly conservative.

12. The finite element model was used to predict the burst strength of the full-scale pipe specimen. Moreover, an empirical equation developed using the parametric

study data to calculate the burst strength of linepipe with dent-crack defect (Appendix A). The empirical equation developed in this study is as follows.

$$P_b = 1750 + 2*10^5 \left(\frac{d}{D}\right)^2 + 0.07 * \frac{{C_l}^2}{C_d} - 124.4 * \left(\frac{p}{p_y}\right) - 48.6 * \left(\frac{d}{D}\right) C_l * C_d - 7.8$$

$$* 10^5 \left(\frac{d}{D}\right)^3$$

## 9.2 RECOMMENDATIONS

The following recommendations are made regarding future research works.

1. It is recommended to conduct more full-scale specimen tests on pipe specimens with different diameter and steel grades to obtain a wider range in the test data pool. Objective is to obtain more data to validate the sensitivity of linepipe with dent-crack defect to deferent parameters.

2. The finite element model could possibly be implemented for wider range of parameters. Objective is to obtain better empirical equation for calculating the burst pressure. Also, this could aid in determining better coefficient for $J_{1c}$ in predicting the burst strength.

3. More fracture toughness tests using compact tension specimens or standard bend specimens are recommended to find $J_{1c}$ for deferent material. The objective is to assist in better prediction of burst strength.

4. Due to the small size of the bend specimens and the fine size of cracks, it is recommended to use a digital microscope that can focus at a higher magnification or use compact tension specimens to find $J_{1c}$.

5. It is recommended to develop a stress intensity factor solution for a wider range of cracks in pipes. Clearly this is a complex task, but it is worthwhile to improve current approaches.

# APPENDICES

## APPENDIX A

## PERMISSIONS

**University of Windsor**

---

## How are you John?
4 messages

---

**Sreekanta Das** <sdas@uwindsor.ca>                    Wed, Mar 4, 2015 at 12:24 PM
To: John Tiratsoo <jtiratsoo@gs-press.com>
Cc: ghaedni@uwingmail.uwindsor.ca

Good day John,

I hope that you are doing well.

My student, Hossein Ghaednia had a paper (as enclosed with this e-mail) published in Pipeline Engineering Journal, 1st Quarter 2013. This student has submitted his thesis for examination and he needs copy right permission from you to use content of the paper in his PhD thesis. I hope that this is fine with you. Please let me know if you are not fine with this.

Thanks.

Best regards,

Sreekant

Sreekanta Das, Ph.D.,P.Eng.(AB)
Professor, Department of Civil and Environmental Engineering
University of Windsor
401 Sunset Avenue
Windsor
Ontario N9B 3P4
Canada.

Tel: (1) (519) 253 3000 Ext. 2507
Fax: (1) (519) 971 3686

e-mail: sdas@uwindsor.ca

---

📄 **Printed paper-18 April 13.pdf**
7178K

---

**John Tiratsoo** <jtiratsoo@gs-press.com>                    Thu, Mar 5, 2015 at 4:16 AM
To: Sreekanta Das <sdas@uwindsor.ca>
Cc: "ghaedni@uwingmail.uwindsor.ca" <ghaedni@uwingmail.uwindsor.ca>

Dear Sreekant,


I am naturally very pleased to confirm that we assign joint copyright to Hossein, and I wish him good fortune with his endeavours.


Best regards,

John

_____

John Tiratsoo

Editor-in-chief

The Journal of Pipeline Engineering

PO Box 21, Beaconsfield HP9 1NS, UK

tel: +44 1494 675139

fax: +44 1494 670155

cell: +44 7771 641372

email: jtiratsoo@gs-press.com

web: www.j-pipe-eng.com

**From:** Sreekanta Das [mailto:sdas@uwindsor.ca]
**Sent:** Wednesday, March 4, 2015 5:25 PM
**To:** John Tiratsoo
**Cc:** ghaedni@uwingmail.uwindsor.ca
**Subject:** How are you John?

[Quoted text hidden]

This message was protected by Step FWD IT MailGuard: e-mail anti-virus, anti-spam, Archive & content filtering.
http://www.stepfwdit.com.au

---

**Sreekanta Das** <sdas@uwindsor.ca>                                          Thu, Mar 5, 2015 at 8:25 AM
To: ghaedni@uwingmail.uwindsor.ca

Sreekanta Das, Ph.D.,P.Eng.(AB)
Professor, Department of Civil and Environmental Engineering
University of Windsor
401 Sunset Avenue
Windsor
Ontario N9B 3P4
Canada.

Tel: (1) (519) 253 3000 Ext. 2507
Fax: (1) (519) 971 3686

e-mail: sdas@uwindsor.ca
—— Forwarded by Sreekanta Das/sdas/University of Windsor on 2015-03-05 08:25 AM ——

From:        John Tiratsoo <jtiratsoo@gs-press.com>

To:      Sreekanta Das <sdas@uwindsor.ca>
Cc:      "ghaedni@uwingmail.uwindsor.ca" <ghaedni@uwingmail.uwindsor.ca>
Date:    2015-03-05 04:20 AM
Subject:    RE: How are you John?

[Quoted text hidden]

---

**Hossein Ghaednia** <ghaedni@uwindsor.ca>                    Thu, Mar 5, 2015 at 8:51 AM
To: Sreekanta Das <sdas@uwindsor.ca>

Thank you

[Quoted text hidden]

# VITA AUCTORIS

| | |
|---|---|
| NAME: | Hossein Ghaednia |
| PLACE OF BIRTH: | Boushehr, IRAN |
| YEAR OF BIRTH: | 1982 |
| EDUCATION: | • University of Persian Gulf, B.Sc.-Civil Engineering, Boushehr, IRAN, 2005 |
| | • AmirKabir University of Technology, M.Sc.-Civil Engineering, Tehran, IRAN, 2008 |
| | • University of Windsor, Ph.D.-Civil Engineering, Windsor, ON, 2015 |